DOCTOR OF PHILOSOPHY

Identification and characterisation of phytophthora capsici CRN effector proteins and their targets in planta

Stam, Remco

Award date:
2013

DOCTOR OF PHILOSOPHY

Identification and characterisation of phytophthora capsici CRN effector proteins and their targets in planta

Remco Stam

2013

University of Dundee

Identification and Characterisation of *Phytophthora capsici* CRN effector proteins and their targets *in planta*

Remco Stam

Doctor of Philosophy

College of Life Sciences The University of Dundee

Cell and Molecular Sciences The James Hutton Institute

December 2013

Table of contents

List of illustrations

List of tables

List of abbreviations

ANOVA	Analysis of Variance
BiFC	Bimolecular Fluorescence Complementation
BLAST	Basic Local Alignment Search Tool
cDNA	coding DNA
CF	Culture Filtrate
CPRG	chlorophenolred-ß-D-galactopyranoside
DAMP	Damage Associated Molecular Pattern
DAPI	4',6-diamidino-2-phenylindole
DNA	Deoxyribonucleic acid
DPI	Days Post Infiltration/infection
DTT	Dithiothreitol
eGFP	form of GFP
EST	Expressed Sequence Tag
ETI	Effector Triggered Immunity
ETS	Effector Triggered Susceptibility
EV	Empty Vector
FDR	False Discovery Rate
FTMS	Fourier transform mass spectrometry
GFP	Green Fluorescent Protein
HMM	Hidden Markov Model
HR	Hypersensitive Response
HRP	Horse Radish Peroxidase
i.a.	inter allia (amongst others)
IP	ImmunoPrecipitation
JGI	Joint Genome Institute
LB	Lysogeny Broth
LOH	Loss of Heterozygosity
MAMP	Microbe Assicoated Molecular Pattern
Mb.	Mega base: one million bases.

MUSCLE	MUltiple Sequence Comparison by Log-Expectation
NCBI	National Centre for Biotechnology Information
NLS	Nuclear Localisation Signal
OD	Optical Density
OGG	Orthologous Gene Group
oNPG	ortho-Nitrophenyl-β-galactoside
ORF	Open Reading Frame
PAGE	Polyacrylamide Gel Electrophoresis
PAMP	Pathogen Associated Molecular Pattern
PB	Pea Broth
PCR	Polymerase Chain Reaction
PRR	Pattern Recognition Receptor
PTI	PAMP Triggered Immunity
PVDF	Polyvinylidene fluoride
q(RT)PCR	Quantitative (Real Time) PCR
RFP	Red Fluorescent Protein
RNA	Ribonucleic acid
RNAseq	(indirect) Next generation (short read) sequencing of RNA
RT-PCR	Reverse transcriptase PCR
SDS	Sodium Dodecyl Sulfate
SNP	Single Nucleotide Polymorphism
Spp.	Species (plural)
TAL	Transcription Activator Like
TBS	Tris Buffered Saline
TBSV	Tomato Bushy Stunt Virus
TCA	Trichloroacetic acid
TDS	Total Dissolved Solids
TF	Transcription Factor
TOF	Time of Flight
YFP	Yellow Fluorescent Protein

Acknowledgements

This thesis would not be here without the support of many people and I apologise in advance if you are not named in this section. We both know that you were also indispensible for the accomplishment of this thesis.

Let me start to thank Edgar for all his stimulating and motivating discussions. Edgar, it rarely happened that I didn't leave your office without loads of new ideas to work on. I hope I lived up to your expectations and also that you don’t regret telling me that it is a good thing if a student disagrees with its supervisor. I am very grateful for the opportunities you gave me and especially for giving me the freedom to follow up the experiments that I found interesting.

Second, Petra, for others you were probably not that visible as supervisor, but I think you played a crucial role in the whole process. Without your input on cell biology and feasibility of some crazy ideas, I don't think this thesis would look as nice as it does and it would certainly be riddled with Americanisms and spelling mistakes.

Then there are all the people in the lab. I would especially like to thank Jullietta for the microarray data, Andy for getting me started with the proteomics and Gaëtan for the discussions we had in the lab, the pub or at home. They might not always have been of the highest scientific standard, but they sure were good.

I also want to thank the rest of the lab for creating such a great atmosphere to work. Everybody’s positive attitude greatly motivated me and I could not have done without it. I would also like to thank you all again for all your input on Chapter 3, that chapter would surely not have been accepted for publication without help of the whole lab.

Then I would like to thank all the people that made my daily life in Dundee fun. Thanks for all the good times in the pub, all the parties and also all the hikes, climbs and bike rides. Without some good time off work, I would surely have ended up crying in a corner.

I, of course, would like to thank my parents, who supported me to chase this scientific career and pretending to be interested in the projects I work on. Lastly I want to thank Dorine: Thanks for coming with me to Dundee and for not going too far away when Dundee didn't have anything to offer. Thanks for sometimes pretending to be interested in my thesis and equally important for not talking about my thesis at other times. Thanks for sharing a lot of good times. I hope that we can be together wherever life takes us.

Declarations

The results presented here are of investigations conducted by myself. Work other than my own is clearly identified with references to relevant researchers and/or their publications. I hereby declare that the work presented here is my own and has not been submitted in any form for any degree at this or any other university.

Remco Stam

We certify that Remco Stam has fulfilled the relevant ordinance and regulations of the University Court and is qualified to submit this thesis for the degree of Doctor of Philosophy.

Dr. Petra Boevink, Cell and Molecular Sciences, James Hutton Institute

Dr. Edgar Huitema, College of Life Science, University of Dundee

Summary

Upon infection plant pathogens secrete a large amount of effector molecules into the host plant. These effectors are thought to aid the infection processes by fending off the plant's defence and modifying its transcriptional machinery to benefit the pathogen. This is true for *Phytophthora capsici* an oomycete pathogen of many important crops including tomato and cucumber.

We identified and characterised CRN effectors in *P. capsici.* With 84 putative effectors composed of 29 different effector domains, the CRNs form a large and diverse class. CRN domain expansion is likely to have occurred in the peronosporales lineage of oomycetes (to which *P. capsici* belongs), though CRNs can be identified in all oomycetes sequenced to date.

We show that CRN effectors are upregulated during infection and as expected by their diverse sequences, appear to have different dynamics. Even though all CRNs localise to the plant nucleus, suggesting involvement in key regulatory processes of the host, their subnuclear localisations differ.

We confirm that one CRN, CRN12_997 is targeting a tomato TCP transcription factor. This transcription factor plays crucial roles in development, but is also involved in defence responses. CRN12_997 alters TCP localisation by dissociating it from the chromatin-associated fraction of the cell and thus prevents it function.

Additionally we have identified putative targets for three other CRNs. Again these targets, including glyceraldehyde 3'phostphate dehydrogenase, Fibrillarin 2 and histone H4, indicate the potential involvement of CRNs in altering transcription machinery of the host plant; all targets can be linked to transcriptional complexes in plants.

We conclude that CRNs are likely to play an important role in the infection process. The study of CRN effectors will provide insight into infection mechanisms and may also help to unravel networks involved in plant regulation and development

Chapter 1 . General introduction into plants, pathogens and effectors

Figure 1.1 and Figure 1.2 have been published in Lamour *et al*. (2012b)

Figure 1.3 has been published in Jupe *et al.* (2013)

Figure 1.4 was taken from Jones and Dangl (2006)

Figure 1.5 was taken from Pritchard and Birch (2011)

Plant pathogens

Plant pathogens have played important roles in the history of humans, they have ruined harvests and thereby caused famines and forced people to change diets, or migrate. The bible mentions blight and mildew (E.g. I Kings 8:37) and Pliny the Elder dedicates multiple chapters of his Natural History to diseases of fruit bearing trees, wheat, other cereals, and other crops.

A well-known example of a devastating plant pathogen is *Phytophthora infestans*. It caused the Irish potato famine in the late 1840s and not only had effects on the Irish population; it caused famine all over Europe (Zadoks, 2008). Another example is *Fusarium oxysporum*. This disease caused the complete loss of banana plantations worldwide in the 1950s. All of these plantations consisted of the Gros Michel cultivar (Ploetz, 2000). By the late 1960s the disease had forced growers to switch to the resistant Cavendish cultivar.

Even when plant pathogens don't have a direct effect on agriculture, like Dutch elm blight (*Ophiostoma ulmi* and *O. nova-ulmi*) and chestnut blight (*Cryphonectria parasitica*), they can be devastating. These diseases decimated elm and chestnut populations in North America in the 1950s and 1970 and have had a long lasting effect on the landscape and ecosystems (Schlarbaum *et al.* 1997; Loo 2008).

Plant pathogenic fungi and oomycetes still pose significant threat on a worldwide scale. Virtually all plants are under attack by filamentous pathogens like oomycetes and fungi. Farmers do their utmost to keep the damage to a minimum. Nonetheless, the pressure on agricutural systems is likely to increase due to global climate change

and a growing and more mobile world population. In recent years a large number of plant disease epidemics have been reported (Fisher *et al.* 2012), including: rice blast fungus (*Magnaporthe oryzae*) a foliar disease that causes losses of 10-35% in 85 countries and Wheat stem rust (*Puccinia graminis*), an important disease on six continents with some strains, like Ug99 wiping out 100% of local wheat crops (Fisher *et al.* 2012) .

For many years researchers have tried to identify genetic sources of resistance to pathogens, first by regular cross-breeding, later using map based cloning and allele mining. For example, a resistance gene has been identified in a specific rice cultivar that confers resistance against *Xanthomonas oryzae* pv. *oryza* race 6 (Song *et al.* 1995) and in potato a number of resistance genes against *P. infestans* have been identified, each with specificity against certain strains. However some of these resistances have been rapidly overcome (Fry 2008; Vleeshouwers *et al.* 2011). To tackle this problem scientists are looking for genes with broader resistance spectra in wild relatives of crop plants (van der Vossen *et al.* 2003; Foster *et al.* 2009; Song *et al.* 2003) and are using strategies that involve stacking multiple resistance genes into one plant (Zhu *et al.* 2012).

The growing use of large scale monoculture plantations and the high rate of adaptability and evolution of plant pathogens in combination with the long distance dispersal of spores mean that plants are constantly attacked by changing pathogen populations (Brown and Hovmøller, 2002). This makes engineering durable resistance difficult. The study of the molecular mechanisms of plant pathogens will help understand essential processes and can aid towards designing disease resistant crops.

Oomycetes as plant diseases

Oomycetes form a diverse class of organisms. Their phylogeny remained largely unknown until the late 1990s, due to their high morphological resemblance with true fungi (Beakes *et al.* 2011). Like fungi they grow filamentous hyphae, form mycelia and use similar biological activities to invade and colonise their hosts. This is a clear case of convergent evolution as there are great differences in their

biochemistry and cell structure. For example, oomycete cell walls are made of cellulose whereas fungal cell walls are made of chitin (Latijnhouwers *et al.* 2003; Richards *et al.* 2006; Money *et al.* 2004). Small-subunit ribosomal RNA analyses revealed that oomycetes belong to the chromalveolata and are more related to dinoflagellates, diatoms and other single cellular algae (Simpson & Roger 2004; Gunderson *et al.* 1987).

Oomycetes can be found in marine, freshwater and terrestrial environments. Saprophytic oomycetes do exist but most have pathogenic lifestyles (Beakes *et al.* 2011). The current evolutionary theory is that oomycetes derived from marine ancestors. The most basal lineages consist of marine parasites of seaweeds and nematodes and the latter possibly moved to land with their nematode hosts. Plant pathogenicity is said to have evolved at least three independent times (Thines and Kamoun, 2010). Once in the more basal lineage of the saprolegniales where one can find legume pathogens like *Aphanomyces euteiches* (Diéguez-Uribeondo *et al.* 2009) and twice in the most studied peronosporalean lineage which contains the genera *Albugo*, *Pythium*, *Hyaloperonospora* and *Phytophthora* (Thines and Kamoun, 2010).

Albugo spp. have a characteristic biotrophic lifestyle and are predominantly pathogens with a narrow host range (Thines *et al.* 2009; Heller & Thines 2009). At the other extreme of the peronosporalean lineage are the *Phytophthora* spp; undoubtedly the best-known members of the oomycetes. *Phytophthora* infect an enormously wide range of plants (Erwin and Ribeiro, 1996). Over 100 of the identified *Phytophthora* species are very important pests and together they infect an extremely large number of hosts ranging from temperate trees (*P. ramorum, P. kernoviae*) and tropical trees (*P. palmivora*) to all major food crops (*P. infestans*, *P. sojae*, *P. capsici*). *P. cinnamomi* has been reported to infect over 3000 different plant species (Erwin and Ribeiro, 1996; Hardham, 2005; Blair *et al*., 2008). Costs incurred by losses and chemical control of *P. infestans* on potato alone are estimated to be €5.2 billion globally (Haverkort *et al*., 2009). These numbers highlight the urgency of studying *Phytophthora* species in a world with ever-increasing demands for food supplies.

Phytophthora capsici

The phylogenetic tree of *Phytophthora* spp has been divided into 10 clades; the finer resolution of the tree is still under discussion (Blair *et al*., 2008; Kroon *et al*., 2012; Seidl *et al*., 2012). *P. capsici* belongs to clade 2b of the *Phytophthora*, together with two closely related sister species *P. mexicana* and *P. tropicalis* (Figure 1.1). It was first identified on chilli pepper (*Solanum capsicum*) in New Mexico Agricultural Experiment Station in 1918 (Leonian, 1922). The disease was thought to be specific to infection of pepper, hence the name, but later it became evident that *P. capsici* can, in fact, be classified as a broad host range pathogen. It has been reported to infect numerous crop host plants including solanaceae like tomato, pepper and aubergine, and cucurbiceae like courgette squash, pumpkin and melon (Table 1.1) (Erwin and Ribeiro, 1996; Davidson *et al*., 2002; Granke *et al*., 2012).

The impact that *P. capsici* can have on agriculture is tremendous. Hausbeck and Lamour reviewed its impact in the United States and concluded that *P. capsici* has spread throughout the country. When the weather is favourable it is capable of destroying up to 25% of the value of cucurbit crops alone. Due to its life-style and ability to grow on foliage, root and fruits, it can not only cause premature plant death, but also fruit rot after harvest (Hausbeck and Lamour, 2004). *P. capsici* also poses a threat to crops in South America and large parts of Asia.

Table 1.1 Botanical Families susceptible to *Phytophthora capsici*

Families and example species susceptible under field conditions (adapted from Granke *et al.* (2012)).

Aloaceae: Aloa	Ericaceae: new year flower	Piperaceae: betel, black pepper
Apiaceae: carrot	Fabaceae: i.a. sweet pea, bean	Portulacaceae: purslane
Araceae: flamingo lily	Geraniaceae: carolina geranium	Proteaceae: i.a. macadamia nut
Asteraceae: cosmos, safflower	Lauraceae: avocado	Rosaceae: i.a. apple, pear
Brassicaceae: i.a. cauliflower	Liliaceae: onion	Rutaceae: citrus
Cactaceae: Indian fig	Linaceae: flax	Solanaceae: i.a. pepper, tomato
Caryophyllaceae: carnation	Malvaceae: i.a. okra, cotton	Sterculiacae: cocoa
Chenopodiaceae: i.a. beet,	Moraceae: fig	
Cucurbitaceae: i.a. cucumber	Orchidaceae: vanilla	
Ebenaceae: persimmon	Pinaceae: fraser fir	

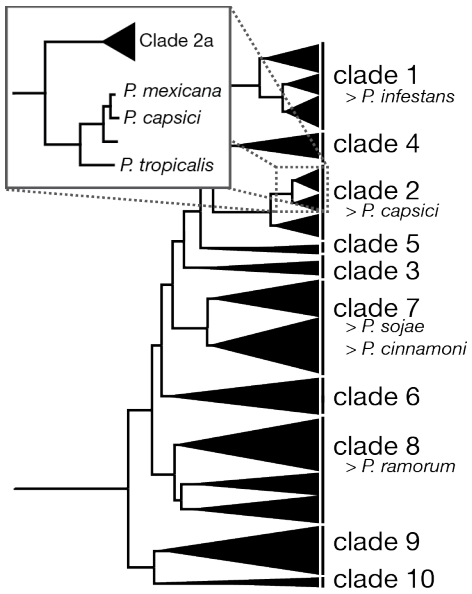

Figure 1.1 Phylogenetic tree of the *Phytophthora* clades

Phylogenetic tree redrawn and modified from Blair *et al* (Blair *et al*., 2008). *Phytophthora* species can be grouped into 10 clades. *Phytophthora capsici* falls within Clade 2b. Inset, *P. capsici* clusters with its related sister species *P. mexicana* and *P. tropicalis*. *Phytophthora* species that have or are being sequenced are listed beside the clades. From (Lamour *et al*., 2012b).

Like all *Phytophthora* species, *P. capsici* is a hemi-biotrophic pathogen. Encysted zoospores germinate on the host plant surface. Germ tubes are formed that, aided by the secretion of degradative enzymes, penetrate the plant cuticle and form an appressorium. *P. capsici* continues to colonise the host tissue in hyphal form in-between the host cells, without killing the host. After this biotrophic phase, which takes approximately 2-3 days depending on the host and tissue, *P. capsici* switches to a necrotrophic life style and infected tissue is killed (Figure 1.2). This causes severe damage to the foliage (in some cases complete defoliation) in leaf infections or severe root or fruit rot when infection established on roots or fruits respectively (Hausbeck and Lamour, 2004; Lamour *et al*., 2012b).

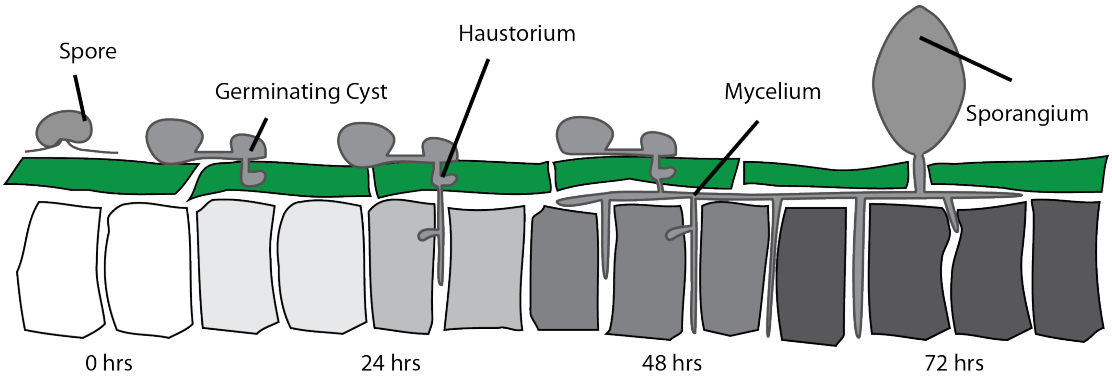

Figure 1.2 Schematic infection cycle of *P. capsici*

Infection features an initial biotrophic phase in which haustoria are observed in colonised tissues (white). On further ingress (18–42 h), *P. capsici* lesions become visible and affected tissues collapse. In the later (>66 h) time stages, sporulation ensues and tissue is fully macerated (dark grey). From (Lamour, Stam, *et al.* 2012).

During this necrotrophic phase *P. capsici* forms sporangia, which contain asexual zoospores. These sporangia can be dislodged by minute water droplets and are possibly dispersed by air, although dispersal solely by wind has not been observed (Granke *et al*., 2009). Sporangia can release 20-40 zoospores each. Enormous numbers of spores can thus be produced on a single fruit. Quantification of the number of spores on one squash in Michigan revealed the presence of at least 3 billion spores (Lamour *et al*., 2012b). Dispersed spores may end up on neighbouring crops, but can also travel longer distances. Viable spores have been detected in Michigan surface waters even when no host crops were present (Gevens *et al*., 2007). While optimal temperatures for spore germination are around 26 °C, infections are also established at 9 °C. Another experiment showed that the viability of zoospores lowers over time, but 5 day old spores remain capable of infection (Granke and Hausbeck, 2009).

P. capsici has two mating types. When these mating types are in close proximity, they sense opposite mating type factors and male and female gametangia are formed. After fertilisation, female gametangia grow to become thick-walled oospores that can survive in the soil for years and are resistant to harsh environmental conditions. Before oospores are able to produce progeny, they require a dormancy period. The exact length of this period is unknown, but it is

thought to be generally more than 8 weeks under field conditions. In the laboratory germination can be stimulated by chemical treatments (Bowers *et al*., 1990; Erwin and Ribeiro, 1996; Lamour and Hausbeck, 2003).

Interestingly, *P. capsici* has numerous clonal populations in South America: some populations in coastal Peru consist solely of mating type A2 (Hurtado-Gonzáles *et al*., 2008) and populations in Argentina solely consist of mating type A1 (Gobena *et al*., 2012). Though populations with both mating types did also occur in the Peruvian highlands (Hulvey *et al*., 2011). Populations in the United States and parts of Asia generally consist of both mating types (Sun *et al*., 2008; Truong *et al*., 2010).

In order to try to curb *P. capsici* infection, growers have used a number of fungicides, most notably metalaxyl and mefenoxam. However, already in 1981 it was shown that *P. capsici* is capable of adaptation to these fungicides and that under laboratory conditions insensitive strains were readily selected for using sub-lethal conditions (Bruin and Edgington, 1981). In the field, fungicide treatments have resulted in a significant percentage of isolates that developed full insensitivity. An insensitive isolate that was followed for three years in an environment without fungicides showed no reversion. Therefore other measures need to be applied to control *P. capsici*, including fumigation and implementation of genetic resistance. (Lamour and Hausbeck, 2003; Hausbeck and Lamour, 2004). Furthermore detailed understanding of the genes involved in infection is required to develop durable genetic resistance.

Plant pathogen genomics

Genome sequencing has greatly expanded our knowledge of the genetic make-up of different organisms. As of 2012, 12 years after the sequencing of *Arabidopsis thaliana*, over two dozen plant genomes have been sequenced and *Arabidopsis* has been resequenced 80 times (Cao *et al*., 2011; Hamilton and Buell, 2012). A large number of oomycete genomes have also been sequenced. These include *Saprolegnia parasitica*, a basal oomycete capable of infecting fish, the necrotrophic plant pathogen *Pythium ultimum* and mildews like *Pseudoperonospora cubensis*, *Albugo candida* and *Hyaloperonospora arabidopsidis*, the latter a pathogen of *Arabidopsis thaliana*, making it a pathosystem with well-studied host plant (Baxter *et al*., 2010;

Lévesque *et al*., 2010; Links *et al*., 2011; Savory *et al*., 2012b; Jiang *et al*., 2013).

Four main *Phytophthora* spp, including *P. capsici* have been sequenced (Lamour *et al*., 2012a). The others are *P. ramorum*, *P. sojae* (Tyler *et al*., 2006) and late blight pathogen *P. infestans* (Haas *et al*., 2009). In addition a 71 Mb draft assembly of the *P. parasitica* genome has been released [http://www.broadinstitute.org/annotation/genome/Phytophthora_parasitica].

Whereas *P. infestans* has by far the largest genome (240 Mb), with three quarters of its genome consisting of repetitive DNA (Haas *et al*., 2009), there is evidence that genomic expansion also happened in *P. capsici*. The *P. capsici* genome is 64 Mb long, a significant enlargement compared to the more distant oomycetes like *Pythium* (42.8 Mb) and more similar in size to *S. parasitica* (63 Mb) and *P. ramorum* (68 Mb), though not as large as *P. sojae* (80 Mb). The numbers of predicted protein coding genes, however, do not differ as much between the *Phytophthora* species and range from around 14.500 for *P. sojae* to 21.000 for *P. parasitica*, and 18.000 and 20.000 for *P.* infesans and *P. capsici* respectively.

It is likely that all Oomycete spp. originate from a common stramenopile ancestor with approximately 10,000 core genes. Studies of genome expansion in the *Phytophthora* genus show that gene duplications arose before speciation and the duplicated gene groups are strongly associated with pathogenicity (Seidl *et al*., 2012).

A great deal can be learned by looking at the genomes of other filamentous pathogens. Although it has been established that some parasites and bacterial symbionts have evolved to have smaller and more compact genomes than their free living counterparts (Opperman *et al*., 2008; Fournier *et al*., 2009; Raffaele and Kamoun, 2012), relatively large and extended genomes are a common feature in fungal plant pathogens (Spanu *et al*., 2010; Duplessis *et al*., 2011; Raffaele and Kamoun, 2012). Raffaelle and Kamoun (2012) reviewed genome expansion and diversity in all filamentous plant pathogens and concluded that genome architecture in these pathogens can be very different in appearance, but generally features large regions of non-coding DNA interspersed with coding regions: in some fungi one can

find clusters of secondary metabolite coding genes (Palmer and Keller, 2010). These clusters show little conservation between *Ustilago maydis* and *Sporisorium reilianum*, indicating that they rapidly evolved in these maize pathogens (Schirawski *et al*., 2010). The secondary metabolite clusters can in fact be found in subtelomeric regions, which tend to evolve faster (Palmer and Keller, 2010). Interestingly in *Magnaporthe oryzae,* the well-studied avirulence factor Avr-pita, which is recognised by some rice races, can be found in such regions. Avr-pita is linked to transposable element regions and frequent transfer of the gene between different chromosomes causes great differences in expression levels and the ability of the plant to recognise the pathogen (Chuma *et al*., 2011).

In *Leptosphaeria maculans* isochore-like regions have been found. These regions differ in GC content and contain almost no coding genes. The few genes that are located in these regions differ greatly between populations (Rouxel *et al*., 2011). In an interesting parallel with *Phytophthora* spp. Raffaele *et al* (2010) describe so called gene-dense- and gene-sparse-regions. Typically *Phytophthora* genomes consist of gene-dense blocks with conserved order and high levels of synteny between species. These blocks contain 90% of all core ortholog genes and are separated by gene-sparse regions. The gene sparse regions have no conserved order and contain predominantly pathogenicity-associated genes. These regions also have a higher non-synonymous over synonymous SNP rate, indicating that indeed these regions are more rapidly evolving than the rest of the genome. Interestingly, unlike the isochore-like regions the GC content of the gene-sparse regions is not different from the gene-dense regions. This phenomenon, where some regions of the genome are evolving faster than others, was dubbed the 'two-speed genome' and although it is less evident in *P. capsici* than it is in *P. infestans* and other members of clade 1, there is still evidence for rapid evolution of *P. capsici* pathogenicity-related genes (Lamour *et al*., 2012a). *P. capsici* shows a much larger SNP rate than any other oomycete, creating large variation in the population. Additionally, large stretches of the genome have been identified that show Loss of Heterozygosity (LOH). LOH has also been observed in *P. ramorum* and can possibly account for the rapid evolution and

high genomic diversity in *P. capsici* populations as beneficial mutations can be fixed rapidly in LOH stretches (Vercauteren *et al*., 2011; Lamour *et al*., 2012a).

Besides giving a basal understanding of pathogen evolution, studies of plant pathogen genomes will help in understanding the rise and fall of key factors involved in pathogenicity. Studies of previously uncharacterised genes revealed a large number of genes that play a role in pathogenicity, most importantly these studies revealed large numbers of effector genes; proteins that are translocated into the host and aid in pathogen virulence, which will be discussed in detail later in this chapter (Levesque *et al*., 2010; Oliva *et al*., 2010; Bozkurt *et al*., 2012; Goritschnig *et al*., 2012; Saunders *et al*., 2012b; Stassen *et al*., 2012; Jiang *et al*., 2013).

Gene expression patterns during infection

To elucidate the roles of specific gene classes and to determine their involvement in pathogenicity a number of expression studies have been performed for *Phytophthora* spp. Different methods exist to identify and follow genes that are expressed during infection. By creating a cDNA library from infected tissue Expressed Sequence Tags (ESTs) can be sequenced and a large number of potentially important pathogenicity related genes have been identified this way. These include the class of CRN effectors, the main subject of this thesis. Gaulin *et al* (2008) identified 7,977 unique sequences from over 18,000 ESTs generated from *Aphanomyces euteiches* a basal oomycete pathogen of pea and alfalfa. Their studies revealed that *A. euteiches* expresses amongst others a number of proteases and genes possibly involved in adhesion and a number of genes that suggest the presence of a defence mechanism against oxidative stress. In *Pythium ultimum* large scale EST sequencing revealed Kazal-like and cystatin-like protease inhibitors, and elicitins, in addition to a large number of translocated effector proteins (Cheung *et al*., 2008).

Microarrays can provide additional insight into the timing of gene expression. One study done on tissue of Soybean (*Glycine max*) infected with *P. sojae* showed strong up-regulation of genes encoding enzymes of phytoalexin biosynthesis and defence and pathogenesis-related proteins. *P. sojae* has a slightly shorter life cycle than *P.*

capsici and peak expression of these genes was generally observed at 24 hour after infection, coinciding with the pathogen's switch to necrotrophy (Moy *et al*., 2004).

Investigation of the expression of 15,650 genes shows that during its development from zoospore to sporangia-forming mycelium the transcriptome of *P. infestans* is very dynamic. 14% of genes are expressed in one specific stage only. Amongst the genes that are differentially expressed are cell regulatory protein like kinases (in zoospores), pathogenicity and necrosis related genes (in germinating cysts) and metabolism associated genes (in biotrophic hyphae) (Judelson *et al*., 2008). Similar findings have been reported in RNAseq studies of *P. phaseoli* on lima bean and *Pseudoperonospora cubensis* on cucumber, even though the latter features a largely biotrophic life-cycle (Kunjeti *et al*., 2012; Savory *et al*., 2012a).

Upon infection of tomato, *P. capsici* shows similar patterns. Using stage specific marker genes Jupe *et al.* (2013) show that genes co-regulated with biotrophy marker PcHmp1 are enriched for those involved in translation and metabolic processes, genes co-regulated with necrotrophy marker PcNPP1 show enrichment for catabolic processes and genes co-regulated with sporulation marker PcCdc14 are enriched for cell regulatory proteins (Figure 1.3). Subsets of effector genes and large classes of transcription factors are also differentially expressed during infection.

As reviewed by Judelson (2012) *Phytophthora* spp. have a unique transcriptional landscape. Coding genes are located close together on the genome and regularly share the same bidirectional promoter and, unlike in other eukaryotes, these adjacent genes on the genome often show differential expression patterns.

The host plant also undergoes transcriptional changes upon infection. After infection with *P. capsici* two drastic switches can be observed in tomato gene expression. One coincides with activation of early defence responses, whereas the second corresponds with the switch by the pathogen from biotrophy to necrotrophy (Jupe *et al*., 2013). Interestingly, the classes of upregulated genes differ from those observed in mutant tomato seedlings that show an induced hypersensitive response (HR), a cell death reaction thought to confer resistance to pathogens (Etalo *et al*., 2013). HR induced seedlings show upregulation of large numbers of genes involved

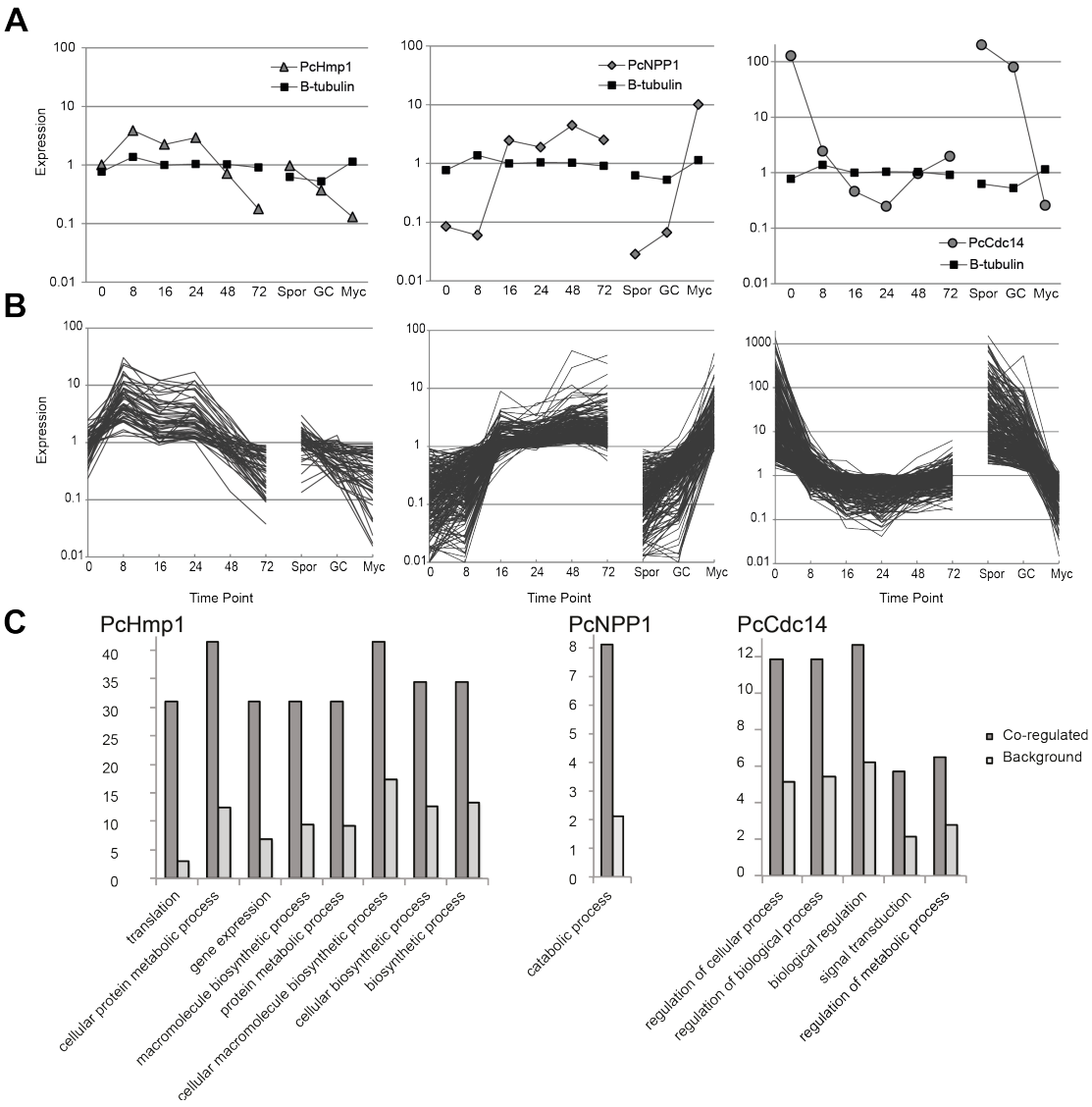

Figure 1.3 Genes co-expressed with *Phytophthora* marker genes

A) Expression of PcHmp1 (left panel), PcNpp1 (middle panel) and PcCdc14 (right panel) as determined by whole genome microarray analyses and compared to the constitutive control β-tubulin over a time course (0 – 72 hours post infection) and in Sporangia (Spor), Germinating Cysts (GC) and Mycelium (Myc). Marker genes were used in cluster analyses to identify genes that are co-regulated shown in B). Y-axis represents fold change expression values, determined by calculating fold changes over mean expression values across all treatments. C) Overview of significantly enriched ontologies present in marker co-regulated genes. Dark bar shows the percentage of genes in the co-regulated fraction compared to the fraction in background set in light grey. All ontologies shown are significantly enriched ($p<0.05$, FDR<0.05) (Jupe *et al.* 2013)

in secondary metabolite production and ubiquitin dependent protein degradation, suggesting *P. capsici* actively triggers differential regulation of host genes during the necrotrophic stage of infection.

Plant infection models: of PAMPS and effectors

As described above, a plethora of transcriptional changes is set in motion during plant-pathogen interactions, both in the pathogen and the host. Current plant-pathogen research however is focussed around a specific subset of molecules that are thought to have a direct effect on the plant-pathogen interaction and is centred around the so-called zig-zag model (Dangl and Jones, 2001; Jones and Dangl, 2006; Hein *et al*., 2009). This model describes how plants are capable of perceiving elicitins or PAMPS (Pathogen Associated Molecular Patterns) using Pattern Recognition Receptors (PRRs) (Nicaise *et al*., 2009). This recognition results in PAMP triggered immunity (PTI). In turn pathogens evolved effectors to dampen this immune response (Effector triggered susceptibility, ETS), however plants contain another set of receptors, coined resistance or R-genes, to detect effectors and initiate another layer of defence (Effector triggered immunity, ETI). This model has brought a better understanding of molecular mechanisms underlying plant pathogen interactions, however the limitations of the model are becoming evident.

PAMPS are generally thought to be small, essential molecules on the outer surface of the attacking pathogen. They are crucial for the pathogen but are thought to not necessarily play a role in pathogenicity. Classical examples of PAMPS are bacterial flagellin, fungal chitins and glucans from oomycetes (Ayers *et al*., 1976; Felix *et al*., 1993, 1999). The PAMP Flg22, a subunit from bacterial flagellin is recognised by the surface exposed PRR receptor FLS2. Upon recognition a FLS2-BAK1 complex is formed and the PTI associated signalling pathway is activated (Gomez-Gomez and Boller, 2002; Zipfel *et al*., 2004; Heese *et al*., 2007). Another bacterial PAMP is Elf18, a peptide formed by the N-acetylated first 18 amino acids of elongation factor EF-Tu (Kunze *et al*., 2004). Ef-Tu is predominantly an intracellular molecule, but is secreted by several bacteria to help adherence to the plant surface and can thus be recognised by PRRs on the plant surface (Zipfel *et al*., 2006). INF1 is a PAMP from *P. infestans* with unknown function. It is recognised in *N. benthamiana* by an receptor-like kinase NbSERK3 (Chaparro-Garcia *et al*., 2011). In tomato INF1 triggers jasmonic acid- and ethylene related defence signalling pathways (Kawamura *et al*., 2009).

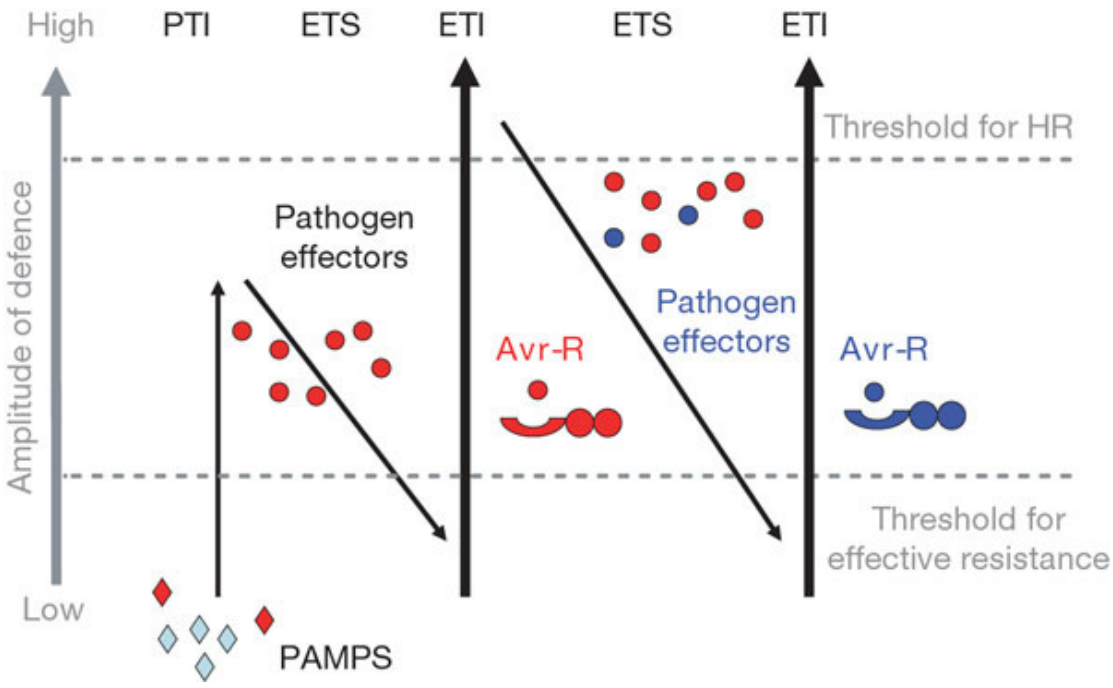

Figure 1.4 zig-zag-zig model

Taken from Jones and Dang (2006). In this scheme, the ultimate amplitude of disease resistance or susceptibility is proportional to [PTI – ETS + ETI]. In phase 1, plants detect microbial/pathogen-associated molecular patterns (MAMPs/PAMPs, red diamonds) via PRRs to trigger PAMP-triggered immunity (PTI). In phase 2, successful pathogens deliver effectors that interfere with PTI, or otherwise enable pathogen nutrition and dispersal, resulting in effector-triggered susceptibility (ETS). In phase 3, one effector (indicated in red) is recognized by an NB-LRR protein, activating effector-triggered immunity (ETI), an amplified version of PTI that often passes a threshold for induction of hypersensitive cell death (HR). In phase 4, pathogen isolates are selected that have lost the red effector, and perhaps gained new effectors through horizontal gene flow (in blue)—these can help pathogens to suppress ETI. Selection favours new plant NB-LRR alleles that can recognize one of the newly acquired effectors, resulting again in ETI.

The second step in the zig-zag model describes how specific small secreted proteins from the pathogen counteract PTI. These effector proteins have been the subjects of many studies (e.g. Hogenhout *et al.* 2009; Bozkurt *et al.* 2012; Oliva *et al.* 2010; Friesen *et al.* 2008; De Wit *et al.* 2009; Dodds *et al.* 2009). Classical examples of effectors that directly suppress PTI are AvrPto from *Pseudomonas syringae* that suppresses recognition of bacterial cell wall components (Hauck *et al.*, 2003) and AVR4 from *Cladosporium fulvum* which protects the fungal cell wall from hydrolysis

by host chitinases (van den Burg *et al*., 2006).

Recognition of effectors forms the last zig-zag in the model. The presence of R-genes and their direct interaction with pathogen genes was first coined by Harold Flor (Flor, 1942, 1971). It has now become evident that many R-genes belong to the class of NB-LRR (Nucleotide-binding site, Leucine-rich repeat) proteins. Large numbers of NB-LRR occur in plants, conferring resistance to many different pathogens. In potato, Jupe *et al.* (2012) identified 438 NB-LRR organised in 63 clusters and spread over all 12 chromosomes.

In order to evade recognition or to keep detecting effectors both effectors and R-genes need to be able to adapt. This leads to a perpetual evolutionary arms race between PRRs and effectors (Boller and He, 2009). A beautiful illustration of this is the high diversity found in *Arabidopsis* RPP13, which at the time of publication was the most diverse R-gene analysed. Only variants from certain accessions were able to recognise *H. arabidopsidis* ATR13, which in turn also shows high levels of polymorphism (Allen *et al*., 2004, 2008).

The zig-zag model, however does not fit all examples. Detailed studies have revealed a number of complexities in plant pathogen interactions. While gene-for-gene recognition of effectors by R-genes has been reported, examples of R-genes that work in pairs have become more common (Hein *et al*., 2009; Eitas and Dangl, 2010). Since direct Avr–R-gene interaction could rarely be observed, Van der Biezen and Jones (1998) developed the Guard hypothesis. In this, NB-LRRs monitor the state of key proteins in plants and when these are perturbed, initiate defence responses. Arabidopsis protein RIN4 forms a complex with NB-LRRs RPM1 and RPS2. *Pseudomonas* effector AvrRpt2 degrades RIN4 which in turn depresses RPS2 function, but phosphorylation of RIN4 by AvrB or AvrRPM1 leads to activation of RPM1 and subsequent defence signalling (Mackey *et al*., 2002; Axtell and Staskawicz, 2003). Additional layers have been proposed for the model to allow effectors that specifically overcome ETI and for plant genes to confer resistance to these effectors (Macho *et al*., 2010; Szczesny *et al*., 2010).

In the zig-zag model, PAMPS were originally defined as highly conserved elements

with no direct function in pathogenicity, whereas effectors, due to the need to evade recognition and suppress immunity are more diverse and are needed to fend off resistance. However, the division between PAMPs and effectors might not be as clear as previously suggested (Thomma *et al*., 2011): *Phytophthora* Nep1 proteins share characteristics with enzymes suggesting possible functions in pathogenicity (Gijzen and Nurnberger, 2006). Other PAMPS, like Pep-13, a surface exposed fragment of transglutamase in *Phytophthora*, cannot be found outside this family and therefore cannot be considered highly conserved (Brunner *et al*., 2002). Possible differentiation between pathogen associated molecular patterns, microbe associated molecular patterns (sometimes described as not being from pathogenic organisms) and endogenous damage associated molecular patterns (related to damage done by herbivores) adds to the complexity (Boller and Felix, 2009).

On the effector side of this debate, examples that complicate the model include the fact that the fungal effector Ecp6 from *Cladosporium fulvum*, which is required for chitin sequestering, is highly conserved amongst *C. fulvum* strains (Bolton *et al*., 2008; de Jonge *et al*., 2010). Additionally, some effectors are very small proteins that don't function as suppressors of NB-LRR-dependent resistance, but appear to actively modify host processes (Grant *et al*., 2006). Examples include apoplastic effectors discussed later and the class of transcription activator-like (TAL) effectors. These *Xanthomonas* effectors have specific DNA binding sites and function as transcription factors that induce expression of host genes that contribute to the development of disease symptoms (Kay *et al*., 2007; Kay and Bonas, 2009).

The previous paragraphs gave an overview of the complexity of the plant-pathogen research field. For clarity in this thesis we will use a broad definition for effector given in Hogenhout *et al.* (2009): "All pathogen proteins and small molecules that alter host-cell structure and function. These alterations either facilitate infection (virulence factors and toxins) or trigger defence responses (avirulence factors and elicitors) or both"

Effector redundancy and target hubs

Complications with fitting results into the zig-zag model are not the only challenges faced by molecular plant pathologists. As discussed above, RIN4 is targeted by at least three different effectors in relation to RMP1 mediated resistance and a fourth one, HopF2, can be added to that list (Wilton and Desveaux, 2010). In fact, redundancy in effectors seems to be a common theme; unrelated *P.* sygingae effectors AvrPto and AvrPtoB target BAK1 (Shan *et al*., 2008), *P. infestans* Avr2 has 10 gene family members of which five, like Avr2, target BSL1 and R2 (Saunders *et al*., 2012a).

Multiple effectors from unrelated species have the same targets, for example, *C. fulvum* Avr2 and *P. infestans* EPIC effectors both target tomato protease Rcr3 (Song *et al*., 2009). Mukhtar *et al* (Mukhtar *et al*., 2011) tested interactions within *A. thaliana* proteins with those of two of its pathogens *Ps. syringae* and *H. arabidopsidis*. A number of Arabidopsis proteins appeared to form highly connected hubs, with over 50 binding proteins within the plant (Hubs50). Both pathogens are separated by more than 2 billion years evolution, yet their effectors target overlapping *Arabidopsis* proteins. In fact, 7 of the 15 Hub50 proteins were targeted by both *Ps. syringae* and *H. arabidopsidis*.

This observation gave rise to the hypothesis that pathogens target essential hubs in plants. These hubs require modification for successful infection. This notion fits with the Guard Hypothesis, as R-genes can be deployed to guard limited number of hubs, which would have evolutionary advantages over deploying R-genes that need to be able to recognise each individual effector.

Given the problems in the zig-zag model highlighted in the previous paragraph and with a better understanding of complex network structures of plant-pathogen interactions, Pritchard and Birch (2011) suggested a systems biology approach to plant biology. They introduced a state based model in which there is a fine balance between healthy and unhealthy states. Perturbation of factors in the network, may lead to a transition from one state to the other.

In addition to putting effector-target interactions into the realm of large networks, this approach allows for incorporation of quantitative data (e.g. transcription levels) and could serve as a basis on which to develop a more comprehensive understanding of plant-pathogen interactions.

Apoplastic effectors in *Phytophthora*

Much can still be learned from studying individual effectors. In the oomycete community and for other filamentous pathogens, effectors are generally divided in two main classes; apoplastic and cytosolic effectors (Schornack *et al*., 2009).

Apoplastic effectors are generally small cysteine rich proteins, whereas cytosolic effectors vary greatly in size. The apoplastic effector Avr2 is secreted by *Cladosporium fulvum* upon infection and inhibits tomato cysteine proteases Rcr3 and PIP-1 that are under strong diversifying selection (Rooney *et al*., 2005; Shabab *et al*., 2008). The unrelated *P. infestans* effectors EPIC1 and EPIC2B (Extracellular Protease Inhibitors of Cysteine proteases) also target Rcr3 and PIP-1 (Tian *et al*., 2007). The interaction between Avr2 and Rcr3 triggers Cf2 mediated HR in tomato but the interaction between EPICs and the cysteine proteases does not (Song *et al*., 2009). In addition to Rcr3 and PIP-1 EPICs target another cysteine protease of potato and tomato, C14. This protein is also under diversifying selection in wild potato species (Kaschani *et al*., 2010). Interestingly, another unrelated effector from *P. infestans*, Avrblb2, targets C14 and prevents its secretion at the haustorial interface (Bozkurt *et al*., 2011).

Besides EPICs, *P. infestans* also secretes kazal-like serine protease inhibitors EPI1 and EPI10, which target a pathogenesis related protease in tomato: P69B (Tian *et al*., 2004, 2005) and *P. sojae* secretes GIP1, which inhibits endo-b-1-3-gucanase from soybean. Interestingly both effector and target appear to be under positive selection, which supports the idea of a continual arms race between host and pathogen (Rose *et al*., 2002; Bishop *et al*., 2004; Damasceno *et al*., 2008). These apoplastic effectors are dealing with the first layers of defence, however to establish itself a pathogen also needs to deal with intracellular defence mechanisms.

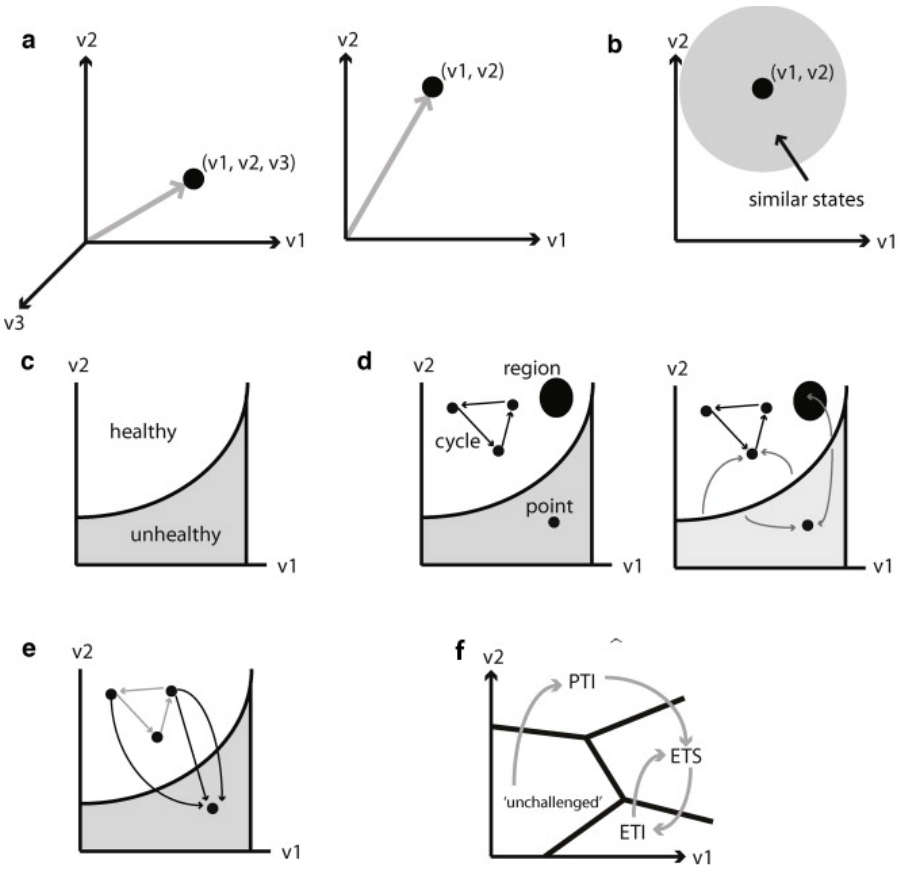

Figure 1.5 State based models of interaction

Taken from Pritchard and Birch (2011). The state of a biological system can be represented as a position in state space, which enables the visualisation of complex changes to the system. The state of a system described by n numerical values {v1, v2, ⋯, vn} can be considered as a point in n-dimensional state-space. A) A system described by three values (v1, v2, v3): states are points in three-dimensional space, and a system described by two values (v1, v2) for which states are points on the 2D plane. B) Points within a volume of state space describe similar states. C) States that correlate to a qualitative property or 'regime' of the system, such as 'healthy' or 'unhealthy, can correspond to volumes of state space that have complex surfaces and boundaries, and may be represented by a phase diagram. D) Complex systems can tend towards 'attractors' over time, which, in state space, may be single fixed point 'steady-states', repeating sequences of states in a cycle, or regions of state space. Regimes may be defined by the attractor(s) to which all points in the regime evolve. Grey arrows on the second set of axes represent transitions of a system from a starting state towards an attractor in the same regime E) Many parallel trajectories may be valid for transitions from one state or regime to another. A switch between qualitative properties of a complex system may correspond to any one of a number of possible trajectories. F) The conceptual phases of the Zig-Zag model can be represented as transitions of a system between attractors in state space.

Cytosolic RxLR effectors

Cytosolic or intracellular effectors are translocated into the host cell by a conserved translocation motif. In oomycetes two large subclasses can be defined. This thesis will focus on the CRN class, the other class is called RxLR and because these effectors have been subject to a large number of studies much can be learned from them about possible effector activities.

RxLR effectors are named after their conserved N-terminal RxLR motif (Arginine, any amino acid, Leucine, Arginine) (Whisson *et al*., 2007). Effectors with this motif have been identified in all *Phytophthora* spp. and some closely related oomyctes like *Hyaloperonospora* or *Pseudoperonopsora* (Tyler *et al*., 2006; Haas *et al*., 2009; Baxter *et al*., 2010; Savory *et al*., 2012b). Interestingly, the RxLR motif shows high similarity to the *Plasmodium* PEXEL motif (RxLxE/Q/D)(Bhattacharjee *et al*., 2006) and is even exchangeable, suggesting universal cell entry mechanisms (Grouffaud *et al*., 2008). The actual way in which RxLR effectors enter the plant cell remains a topic of much debate (Ellis *et al*., 2006; Ellis and Dodds, 2011). Kale *et al.* (Kale *et al*., 2010) suggest the involvement of P3P lipids and claimed that RxLR effectors are capable of entering the plant cell without the presence of the pathogen itself (Dou *et al*., 2008). However, these findings have been disputed by several other researchers as they could not be repeated independently (Yaeno *et al*., 2011; Wawra *et al*., 2013) and alternative pathways like tyrosine-O-sulfate–modified entry have been suggested (Wawra *et al*., 2012). Nonetheless the authors of the original article claim that multiple independent laboratories are able to reproduce their results (Tyler *et al*., 2013) and the question remains unresolved.

RxLR C-termini are thought to be the effector domains involved in pathogenicity. C-termini show larger sequence diversity than the N-termini, nonetheless conserved W, Y, and L domains can be identified in over half of 370 *P. sojae* and *P. ramorum* Ahv genes (RxLR homologous to known avirulence genes) (Jiang *et al*., 2008; Schornack *et al*., 2009). A comprehensive study of *H. arabidopsidis* RxLR localisation shows that upon entry different RxLR localise to distinct cellular compartments: 33% of the proteins localise to the nucleus, another 33% go to the nucleus and cytoplasm

and the remainder localise to a variety cellular membranes (Caillaud *et al*., 2012a). A large number of studies now show that RxLR effectors have a direct effect on *Phytophthora* virulence, either as cell death suppressors or as recognised HR inducers.

One study highlights examples of *P. infestans* RxLRs that show a phenotype when expressed *in planta*: PexRD8 and PexRD36 suppress INF1 induced cell death, whereas PexRD2 induced a delayed and weak cell death (Oh *et al*., 2009).

Similar antagonistic effects can be seen between P *sojae* effectors: Avr1b contributes to virulence and inhibition of cell death (Dou *et al*., 2008), Avr3b is a NADH and ADP-ribose, which also affects immunity (Dong *et al*., 2011) and the majority of tested *P. sojae* RxLR effectors are capable of repressing either BAX or INF1 induced cell death. Avh238 and Avh24, however are very potent and consistent cell death inducers themselves (Wang *et al*., 2011).

PscRXLR1 from Pseudoperonospora cubensis arises as a product of alternative splicing and induces a strong HR response (Savory *et al*., 2012b). Two homologous RxLR, one from P *sojae* (PsAvh163) and one from *H. arabidopsidis* HaRxL96 are induced early upon infection and are capable of suppressing immunity in soy bean. However, in *N. benthamiana* PsAvh163 induces HR, whereas HaRxLR96 still suppresses immunity (Anderson *et al*., 2012).

The key to proper understanding of RxLR function is identifying and confirming the proteins they target *in planta*. These targets have been elucidated for a small number of RxLR and already it is evident that, as their diverse localisations would suggest, RxLR are involved in many processes.

As mentioned, Avrbl2 targets a C14 protease on the haustorial membrane (Bozkurt *et al*., 2011). *P. infestans* Avr2 also localises around haustoria and to the plasma membrane, but targets BSL1 a protein involved in brassinosteroid-related defences (Saunders *et al*., 2012a). Interaction of Avr2 with BSL1 is required for association of BSL1 with R2, an R-gene that in turn is able to confer resistance. Strains of *P. infestans* that are virulent on potatoes that contain R2 genes, express an unrecognised homologue, A2L (Gilroy *et al*., 2011a).

Avr3a has two isoforms (Avr3aKI and Avr3aEM) that both suppress INF1 induced cell death through interaction with CMPG1 E3 ligase (Bos *et al*., 2006, 2009, 2010). However only Avr3aKI is recognised by resistance gene R3a (Armstrong *et al*., 2005). CMPG1 appears to be a key component in defence signalling, because it is involved in Cf-9/Avr9, Cf-4/Avr4, Pto/AvrPto and CBEL related defence responses (Gilroy *et al*., 2011b). R3a relocates from the cytoplasm to endosomal compartments only when coexpressed with AVR3aKI; not with AVR3aEM (Engelhardt *et al*., 2012).

Five crystal structures have been published for RxLR effectors. AVR3a4 and AVR3a11 from *P. capsici*, PexRD2 from *P. infestans* and ATR1 and ATR13 from *H. arabidopsidis* (Boutemy *et al*., 2011; Chou *et al*., 2011; Leonelli *et al*., 2011; Yaeno *et al*., 2011).

AVR3a homologues, PexRD2 and ATR1 share a conserved alpha-helical protein fold in the WY domain, which is a combination of previously defined W and Y domains, despite low sequence similarity. The WY domains occur in the proteins up to 11 times, and are abundant in RxLR effectors. 44% of *P. infestans* and 26% of *H. arabidopsidis* RxLR are predicted to contain at least one copy of the domain. ATR13 lacks WY domains (Jiang *et al*., 2008; Boutemy *et al*., 2011; Win *et al*., 2012).

ATR1 alleles are recognised by RPP1 variants RPP1-NdA and RPP1-WsB. Core residues required for recognition appeared to be differently spaced on the outer surface, whereas core residues for recognition of different alleles of ATR13 appeared to be all in one region (Chou *et al*., 2011; Leonelli *et al*., 2011). Comparison of Arv3a structures from *P. capsici* revealed two crucial residues for R3a recognition, although direct interaction has not been confirmed (Yaeno *et al*., 2011; Engelhardt *et al*., 2012).

The above paragraphs illustrate the diverse nature of effector functions for RxLR and begs the question if CRNs function in a similar fashion.

CRN effectors

CRN effectors were first identified in high throughput functional expression studies of ESTs from *P. infestans* (Torto *et al*., 2003). Using a Potato Virus X based vector and agrobacterium-mediated over-expression, two genes were identified that caused severe CRinkling and Necrosis of the infected plants, thus they were named Crn1 and

Crn2. It became evident that the *Crn* genes belong to a large family of putatively secreted proteins; both CRN1 and CRN2 have a predicted signal peptide and both proteins are constitutively expressed during infection of tomato.

CRN effectors share a conserved N-terminal domain with a highly conserved LQLFLAK (Leucine, Glutamine, Leucine, Phenylalanine, Leucine, Alanine, Lysine) motif within the first 60 amino acids after the putative signal peptide. (Haas *et al*., 2009; Schornack *et al*., 2010). Chimeric protein experiments show that the LFLAK motif is required for translocation of the effector in the host cell. CRN N-termini fused to known functional Avr3a effector domains were able to cause the expected HR response when the LFLAK motif was intact. With the LFLAK residues mutated to alanines however, the induction of HR was not observed (Schornack *et al*., 2010). While there is much debate about the mechanisms involved in RxLR cell entry, nothing is known about the mechanisms involved in plant cell entry of CRN effectors. An interesting feature is that unlike the RxLR, the CRN effectors that have been tested so far localise to the nucleus of the plant, an organelle that is believed to play an important role in plant-pathogen interactions (Deslandes and Rivas, 2011; Rivas, 2012)

The highly conserved CRN family is not only present in related oomycete species like *P. sojae* and *P. ramorum* (Tyler *et al*., 2006; Haas *et al*., 2009). CRNs are identified in other peronosporales like *Hyaloperonospora* and *Pseudoperonopsora* spp.(Baxter *et al*., 2010; Savory *et al*., 2012b) and in more distant species like *Pythium ultimum* (Lévesque *et al*., 2010) and *Albugo candida* (Links *et al*., 2011), one of the more ancestral oomycetes. This suggests that CRNs are an ancient class of effectors. RxLR effectors have only been identified in the peronosporales lineage (Schornack *et al*., 2010; Thines and Kamoun, 2010). Interestingly, *Hyaloperonospora arabidopsidis* contains a number of proteins with overlapping RXLR and LFLAK motifs (RXLRLFLAK)(Win *et al*., 2007). This suggests that as well as a similar delivery function, these motifs may share a common ancestor. Like RxLR effectors, CRNs are present on the genome in very large numbers. 61 CRNs have been identified in *P. ramorum* and as many as 451 have been identified in *P. infestans* (Haas *et al*., 2009).

The N-terminal region also contains a highly conserved HVLVVVP (Histidine, Valine, Leucine, 3xValine, Proline) domain which marks the end of the N-terminus and the start of the C-terminal effector domain. The C-terminal domains can be divided into many classes. These classes share little sequence similarity and with the exception of the D2 domain, have no predicted function (Haas *et al*., 2009). In *P. infestans* CRN8, the D2 domain has been reported to have serine/threonine RD kinase activity. This kind of enzymatic activity had been reported in animal pathogens, but was not found in plant pathogens before (Shao, 2008; van Damme *et al*., 2012). CRN8 is a functional RD kinase. It is capable of forming dimers or multimers, it is auto-phosphorylated and causes cell death when over-expressed *in planta*, but only when the kinase domain is intact (van Damme *et al*., 2012).

Two CRN effectors from *P. sojae* have been functionally characterised; PsCRN63 induces cell death when over-expressed in *N. benthamiana*, while PsCRN115 does not. PcCRN115 appears to be capable of suppressing cell death induced by PsojNIP; a potent elicitor from *P. sojae*. Silencing of both effectors decreases *P. sojae* virulence (Liu *et al*., 2011). Unfortunately, as for all CRNs to date, the *in planta* targets are unknown.

Outline of thesis

Most research on CRN effectors so far was conducted in *P. infestans*, with limited extension for comparative genomics to *P. sojae* and *P. ramorum* and only a small number of CRN effectors have been functionally characterised. In this thesis I will use a bioinformatics approach to identify CRN effectors in *P. capsici* and use a range of molecular biology techniques to confirm and characterise them. Furthermore I identify and confirm a number of plant molecules that are targeted by the CRNs.

In Chapter 2 I show the identification of *Crn* genes, using available gene models and data from other *Phytophthora* species and the draft genome sequence for *P. capsici*. I show how the *P. capsici Crn* gene models compare with other CRNs and identify commonalities and differences to try to get an evolutionary understanding of the *Crn* genes in general and a more thorough understanding of the structures and occurrence of *P. capsici Crn* genes in particular.

Secondly I show that predicted *Crn* gene models can be verified using reverse transcriptase PCR. If the predicted *Crn* genes can be amplified from infected plant material, they are likely to be correct models. I use the *Crn* gene models in a microarray study conducted by the lab. This study acts as a second confirmation for the CRN models and gives a detailed view of when CRN effectors are expressed during infection. The last part of Chapter 2 focuses on CRN function. Based on knowledge of *P. infestans* CRNs I expect large sequence variations in *P. capsici Crn* genes, however it is unknown if this variation also translates to CRN function. Over-expression and pathogenicity assays show that CRNs have an effect on the plant itself and that over expression of CRNs is sufficient to alter the virulence of *P. capsici* on model host plants like *N. benthamiana*.

In addition to this 'phenotypic' characterisation I make use of confocal microscopy to do basic localisation studies to show that all CRN localise to the nucleus.

In Chapter 3, I will expand on some of the observations made in Chapter 2. I show that three CRN effectors that have at first glance very similar characteristics are likely to perform very different functions in the plant. This finding not only helps in understanding CRN function, but may also aid towards understanding nuclear processes in the host during infection.

Chapter four focuses on an ancient CRN effector and the interaction with its target. I use several techniques including BiFC and Co-immunoprecipitation to confirm the interaction and show the effects the interaction has on *P. capsici* growth.

The final research chapter of this thesis describes de novo target identification, confirmation and characterisation. I use yeast-2-hybrid and mass spectrometry analysis of immunoprecipitated CRN effector domains to identify possible new interacting partners for the CRNs. These newly identified targets are tested in several assays to confirm their interactions, which reveals several new CRN target candidates.

In the last chapter I will discuss all findings and place them in the light of other contemporary effector research. I will highlight the important outcomes of this thesis and discuss their implementations for future research.

Chapter 2 . CRN effector identification and characterisation

This chapter has been published as:

R Stam, J Jupe, AJM Howden, JA Morris, PC Boevink, PE Hedley and E. Huitema. Identification and Characterisation of CRN Effectors in *Phytophthora capsici* Shows Modularity and Functional Diversity. PLoS ONE 8: e59517. Available: http://dx.doi.org/10.1371/journal.pone.0059517.

AJMH, JJ contributed plant materials; JJ, JAM and PEH contributed to the microarray experiments; PCB and EH contributed to data analysis.

Abstract

Phytophthora species secrete a large array of effectors during infection of their host plants. The *Crinkler* (CRN) gene family encodes a ubiquitous but understudied class of effectors with possible but as of yet unknown roles in infection. To appreciate CRN effector function in *Phytophthora*, we devised a simple *Crn* gene identification and annotation pipeline to improve effector prediction rates. We predicted 84 full-length CRN coding genes and assessed CRN effector domain diversity in sequenced Oomycete genomes. These analyses revealed evidence of CRN domain innovation in *Phytophthora* and expansion in the *Peronosporales*. We performed gene expression analyses to validate and define two classes of CRN effectors, each possibly contributing to infection at different stages. CRN localisation studies revealed that *P. capsici* CRN effector domains target the nucleus and accumulate in specific sub-nuclear compartments. Phenotypic analyses showed that few CRN domains induce necrosis when expressed *in planta* and that one cell death inducing effector enhances *P. capsici* virulence on *Nicotiana benthamiana*. These results suggest that the CRN protein family form an important class of intracellular effectors that target the host nucleus during infection. These results combined with domain expansion in hemi-biotrophic and necrotrophic pathogens, suggests specific contributions to pathogen lifestyles. This work will bolster CRN identification efforts in other sequenced oomycete species and set the stage for future functional studies towards understanding CRN effector functions.

Introduction

Plant pathogenic oomycetes continue to hamper crop production and damage ecosystems on a global scale. Perhaps the most notorious group of pathogens are found within the *Phytophthora* genus, where member species such as *Phytophthora infestans* and *Phytophthora sojae* wreak havoc on potato, tomato and soybean crops, whilst others such as *Phytophthora ramorum*, *Phytophthora kernoviae* and *Phytophthora lateralis* are rapidly emerging pathogens of trees, increasingly affecting forests and ecosystems. There is an urgent need to understand the mechanisms underpinning parasitism in this important group of eukaryotes, an undertaking that has sparked genome-sequencing efforts on a number of oomycete species (Bozkurt *et al*., 2012). With oomycete genome sequences available covering a broad spectrum of lineages and lifestyles, the challenge is to translate oomycete gene repertoires into the basic biology underpinning infection, virulence and pathogenic lifestyles.

Phytophthora spp are hemi-biotrophic pathogens that feature biotrophy early in infection and necrotrophy in the later stages of host tissue colonisation. Both sporangia and the motile spores they produce (zoospores) can germinate and produce hyphae that penetrate the plant epidermis and invade host tissue. Pathogen ingress is followed by formation of specialised structures (haustoria) that invaginate living host cells (biotrophy) and support further pathogen growth and colonisation of host tissues. Colonisation ultimately leads to cell death and tissue collapse (necrotrophy) and in those later stages of disease development, sporangia are formed to initiate the next disease cycle (Lamour *et al*., 2012b).

Plant pathogens secrete arsenals of proteins (effectors) that enable parasitic infection and reproduction (Birch *et al*., 2006; Kamoun, 2007; Oliva *et al*., 2010; Stassen and Van den Ackerveken, 2011). Plants perceive Pathogen Associated Molecular Patterns (PAMPs) upon which Pattern Triggered Immunity (PTI) is mounted. To counter PTI, successful pathogens have evolved large and diverse effector repertoires that can suppress PTI and trigger susceptibility (Effector-Triggered Susceptibility, ETS)(Jones and Dangl, 2006; Hein *et al*., 2009).

In addition to extracellular effectors that counter defence associated molecules in the host apoplast, *Phytophthora* species secrete and translocate effectors, termed RXLRs, across the haustorial host-pathogen interface where they target resident host proteins and cellular processes to enhance susceptibility. Translocation requires the presence of a signal peptide, followed by a conserved N-terminal RXLR motif (Morgan and Kamoun, 2007; Whisson *et al*., 2007; Birch *et al*., 2008), features which allow rapid identification of effector candidates from oomycete genome sequences. Consequently, RXLR effector repertoires have been easily identified in sequenced oomycete species, allowing rapid insights into their virulence functions [6]. Genome sequence and functional analyses have revealed that besides the RXLR effector class, *Phytophthora* genomes encode another class of host-translocated effectors. The Crinkler (CRN for CRinkling and Necrosis) protein family was identified and named after a characteristic leaf crinkling phenotype observed upon ectopic expression of *P. infestans* secreted proteins in plants (Torto *et al*., 2003). Critically, expressed mature CRN proteins retained cell death-inducing activity, suggesting functions targeting cytoplasmic host factors, a hypothesis that was confirmed when translocation activity of CRN N-termini, carrying an LXLFLAK motif, was demonstrated (Schornack *et al*., 2010).

Unlike RxLR effectors, CRNs are present in all plant pathogenic oomycete species sequenced to date (Tyler *et al*., 2006; Gaulin *et al*., 2008; Haas *et al*., 2009; Baxter *et al*., 2010; Lévesque *et al*., 2010; Schornack *et al*., 2010; Links *et al*., 2011; Lamour *et al*., 2012a). Over 196 full length CRN-genes and 255 pseudogenes have been predicted from the *P. infestans* genome (Haas *et al*., 2009). In other sequenced species, CRN predictions range from a total of 60 for *P. ramorum* to 202 for *P. sojae,* whereas much lower numbers (26) have been described in *Pythium ultimum* (Lévesque *et al*., 2010). All share a conserved N-terminal domain with a characteristic LXLFLAK motif, however this domain is slightly altered in *Albugo candida* to LYLAK (Links *et al*., 2011). Interestingly, the LXLFLAK motif in some *Hyaloperonospora parasitica* CRN proteins are fused with RXLR motifs, suggesting they share ancestors (Baxter *et al*., 2010). In contrast to CRN N-termini, CRN C-

terminal domains feature high levels of variation. Interrogation of the *P. infestans* genome sequence combined with analyses of other *Phytophthora* CRN effector complements, helped define and classify diverse C-terminal effector domains in *Phytophthora* species (Haas *et al*., 2009). Interestingly, transient expression of CRN C-termini in plants, cause cell death in some cases, suggesting effector-mediated perturbation of host cellular processes. Indeed, subsequent studies have demonstrated a role for some CRN C-termini towards *P. sojae* virulence on soybean (Liu *et al*., 2011). Although the exact functions have not been defined, recent studies demonstrated that at least one CRN effector domain in the *P. infestans* CRN8 C-terminus exhibits kinase activity, suggesting a role in modifying host signalling cascades during infection (van Damme *et al*., 2012).

Recently, the genome of the broad host range pathogen *Phytophthora capsici* was completed (Lamour *et al*., 2012a). Automated gene identification and subsequent annotation revealed the presence of a relatively small number of CRN coding genes. This observation, together with a limited understanding of CRN effector distribution and function in *Phytophthora* and other oomycete species, prompted us to identify, validate and study the full *P. capsici* CRN effector domain repertoire in more detail. We applied a simple but robust pipeline to identify 84 full-length CRN protein candidates in *P. capsici* and used this validated set of gene models to assess the occurrence of CRN domains in other sequenced oomycete species. Our results suggest dramatic expansion of effector domains in hemi-biotrophic oomycetes, suggesting CRN effector innovation for hemi-biotrophy. Despite CRN effector domain conservation across *Phytophthora* clades, we defined species-specific effector domains and combinations, providing evidence for recent evolution in this protein family. Consistent with the idea of CRN involvement in pathogenesis, we confirmed expression of most CRN coding genes during infection and defined two sub-classes of effectors based on contrasting gene expression patterns. Localisation studies showed that all tested eGFP-CRN fusion-proteins accumulate in the nucleus and some exhibited specific subnuclear localisation patterns. These results suggest that targeting of host nuclear and subnuclear factors is an important requirement for

infection. We substantiated these results with functional characterisations that indicate specific roles for CRN proteins towards *P. capsici* virulence. This work will bolster CRN identification efforts in other sequenced oomycete species and set the stage for future studies towards understanding CRN effector functions.

Methods

CRN identification and annotation

Databases: Phyca11 scaffolds, gene models and proteins, were obtained from the *Phytophthora capsici* sequencing consortium website (http://genome.jgi-psf.org/Phyca11/Phyca11.home.html). Databases for other oomycete species were obtained from their original sources: http://genome.jgi-psf.org for *P. ramorum* and *P. sojae*, genome.wustl.edu/ for *Hyalopernospora. arabidopsidis,* http://pythium.plantbiology.msu.edu/ for *Pythium ultimum,* http://www.polebio.scsv.ups-tlse.fr/aphano/ for *Aphanomyces euteiches. Albugo candida* sequences were obtained from Matthew Links (Agriculture and Agri-Food Canada). *Pseudoperonospora cubensis* genomic data are described by Savory *et al* (2012) and are, together with *Saprolegnia parasitica* data, available from NCBI. *P. infestans, P. sojae and P. ramorum* reference data and models were previously described. *Phaeodactylum tricornutum* (Bowler *et al*., 2008) and *Thalassiosira pseudonana* (Armbrust *et al*., 2004) genomes were obtained from JGI. *Arabidopsis thaliana* data was downloaded from TAIR, *Solanum lycopersicum* data from the SOL genomics consortium.

Annotations: ORFs were selected from Phyca11 scaffolds and basic sequence modifications were performed using EMBOSS (getorf –minsize 300) and bundled in a database (seqret). To identify CRN candidates we used BLAST (tblastp, –E 1e-4) (Altschul *et al*., 1990) with 16 PiCRN aa sequences and HMMer3.0 (hmmsearch, –E 1e-4) on extracted ORFs.

HMMer was used to investigate domain presence C-terminal domains and for analysis of domain orientation. Manual alignment in jalview (Waterhouse *et al*., 2009) was performed for curation of the final sequence and to see if identified CRNs

matched our full length criteria (full length sequences should contain domains LFLAK(DI)DWL and a match with a C-terminal domain for at least 80% of the length of the shortest known variant in *P. infestans, P. ramorum* or *P. sojae*). We used the domain nomenclature as previously (Haas *et al*., 2009). Sequences that did not match previously described domains were manually aligned and clustered to form new domains. Searches for specific functional domains and localisation domains were done using pFAM (Finn *et al*., 2008), NLStradamus (Nguyen Ba *et al*., 2009), PredictNLS (Cokol *et al*., 2000), Nod (Scott *et al*., 2010), SignalP3.0 (Dyrløv Bendtsen *et al*., 2004), TMHMM (Kahsay *et al*., 2004) and the results were stored in our CRN library (Table S01) and were uploaded to the *P. capsici* genome database (http://genome.jgi-psf.org/Phyca11). To analyse domain evolution we searched protein models (or translated transcripts) from the oomycte databases mentioned above using both existing and new CRN HMM profiles (hmmsearch -E 1e-5). The Sequence logo was made using weblogo (http://weblogo.berkeley.edu/logo.cgi) and Venn diagrams with Venny (http://bioinfogp.cnb.csic.es/tools/venny/index.html).

Microarray analysis

Microarray data was generated from a *Phytophthora capsici*-tomato time course infection experiment (Jupe *et al. ,* in prep). A custom Agilent 60-mer oligonucleotide microarray was designed from predicted *P. capsici* (LT1534 v11.0) and *Solanum lycopersicum* (ITAG 2.3) sequences using eArray software (https://earray.chem.agilent.com/earray/). The design is available at ArrayExpress (accession A-MEXP-2253; http://www.ebi.ac.uk/arrayexpress/) and represents 20,530 transcripts for *P. capsici* and 34,510 transcripts for *S. lycopersicum*. All RNA labeling and microarray hybridisation procedures were performed in the Genome Technology lab, James Hutton Institute, using standard operating procedures. Total RNA was extracted using a Qiagen RNA Plant extraction kit, quantified by a NanoDrop ND-100 spectrophotometer (NanoDrop Technologies, USA) and quality checked using a RNA 6000 Nano Kit on a Bioanalyzer (Agilent Technologies). Fluorescent one-colour labeling of the RNA was performed as recommended (Agilent One-Color Microarray-Based Gene Expression Analysis (Low Input Quick Amp

Labeling) v. 6.5) using 8x60k format slides. Following array scanning, images were first imported into Agilent Feature Extraction (FE v. 10.7.3.1) software, aligned and quality checked using a corresponding grid template file. The microarray experimental design, along with raw datasets is available at ArrayExpress (accession E-MTAB-1295). The extracted FE dataset was separated for each array into *P. capsici* and *S. lycopersicum* data to allow independent processing. Datasets were each independently quality filtered using flag values (present or marginal in 2/3 replicates) and then quantile normalised in Genomics Suite software (Partek), prior to loading into Genespring (Agilent v. 7.3) software for analysis. The *Crn* gene set was extracted from the dataset and filtered based on replicated minimum raw expression values (>50) and normalised values (>1) in more than two stages, with at least a 2log change between stages. Genes were clustered using k-means (100 iterations) and gene trees were constructed using Pearson correlation and single linkage (default settings).

PCR and cloning of CRNs

For gene confirmation, PCR primers were designed for a selection of predicted full length CRN coding genes. PCR reactions were performed on cDNA derived from RNA that was extracted from infected *Nicotiana benthamiana* leaves using Gotaq polymerase (Promega). Amplicons were purified and Sanger sequenced on ABI3730 using Big Dye labelling chemistry.

For gene expression *in planta*: PCR primers were designed to specifically amplify selected individual CRN C-termini (Table S04). For CRNs 1_719, 11_767, 20_624, 79_188 and 83_152 the primers were designed to contain restriction sites compatible with pENTR1A (Life Technologies). For cloning, PCR was done using Phusion proofreading polymerase (New England Biolabs) on cDNA samples described above. The purified PCR products were ligated after appropriate restriction digestion using T4 DNA ligase. The entry plasmids were transformed using electrotransformation into *E. coli* DH10B cells.

Primers for the additional CRNs were designed to contain a CACC sequence to allow for GATEWAY directional TOPO cloning in pENTR-D-TOPO (Life Technologies). We

cloned *Crn* genes following the manufacturer's instructions and transformed the entry plasmid into *E. coli* MACH1 cells (Life Technologies). Primers were designed to add a small strep-II tag (Schmidt *et al*., 1996) to the C-terminus of each CRN protein. Colonies carrying the correctly sized inserts were grown overnight in liquid LB medium and inserts were sequenced (Table S04). ENTRY vectors were recombined into pB7WGF2 (Karimi *et al*., 2002) using LR clonase II (Life Technologies) following the manufacturer's protocol and transformed into electrocompetent *E.coli* DH10B. Colony PCR was done using M13-Forward and one CRN specific primer to verify the presence of each insert.

Transient expression of CRNs

Transient expression: pB7WGF2 plasmids containing CRN inserts, were transformed into *Agrobacterium tumefaciens* strain AGL1. Transformants were grown on LB medium containing Rifampicin and Spectinomycin to maintain each plasmid. For each construct, a single colony was grown overnight and resuspended in infiltration buffer (10 mM MgCl, 150 uM Acetosyringone) to an OD of 0.1 for confocal microscopy, 1.0 for necrosis and 0.5 for growth assays. The buffer was mixed 1:1 with buffer containing *Agrobacterium* expression silencing suppressor P19 and infiltrated in *N. benthamiana* leaves. Plants were grown in a glasshouse under 16 hours light and set at 26 °C by day and 22 °C by night.

Phenotypic assays

For each CRN construct, three sites were infiltrated in different leaves and for each CRN the infiltration was repeated 3 times. The level of cell death was scored after 7 days using a 1-6 scale, with one indicating no symptoms and 6 signifying severe (black) necrotic lesions (Figure 2.7).

P. capsici growth assays were done on leaves that were fully infiltrated with *Agrobacterium* strains carrying CRN constructs. Two days after infiltration, leaves were drop inoculated with two 10 µL droplets of zoospore solution (500,000 spores per mL). Lesion diameters were measured 2 days post inoculation (DPI)

Confocal microscopy

All localisation studies were done on *N. benthamiana* leaves transiently expressing GFP-tagged CRN C-termini, two days after infiltration. To maintain cell structure after detachment, the leaves were infiltrated with water before mounting on a microscope slide. Subnuclear localisation was examined in stable transformants of *N. benthamiana* expressing RFP-Fibrillarin (Goodin *et al*., 2007). Leaf samples were imaged using a Leica SP2 confocal microscope. The excitation wavelengths used were 488 nm for GFP and 561 nm for RFP.

Western blots

Plant tissues were harvested at 3 dpi. Protein extractions were done using GTEN buffer (10% Glycerol, 25 mM Tris, 1 mM EDTA, 150 mM NaCl) supplemented with 2% PVPP, 10 mM DTT and 1X Complete protease inhibitor cocktail (Roche). Samples were pulled down using a GFP-trap (Chromotek) and run on 12% SDS PAGE gels before transfer to PVDF membranes. Blots were blocked for 30 minutes with 5% milk in TBS-T (0.1% tween), probed with StrepII-HRP antibody (Genscript) and washed 3 times in TBS-T for 5 minutes before incubation with Millipore Luminata Forte substrate or SuperSignal West Femto (Pierce). Images were collected on a Biorad Geldoc Imager

Results

A gene annotation pipeline improves CRN effector identification

We aimed to classify the full *P. capsici* CRN complement from the recently published *P. capsici* genome sequence. BLAST based searches of the publicly available Phyca11 gene model set, helped identify twenty-nine full length and seventy CRN-like pseudogenes (Lamour *et al*., 2012a). Given the high percentage of CRN pseudogenes in *P. capsici* (73%) compared to *P. infestans* (56%) or *P. sojae* (50%) and considering the relatively low abundance of CRN-like gene models compared to other *Phytophthora* sp. with similar genome size, we asked whether we could improve prediction rates for *P. capsici* CRN coding genes.

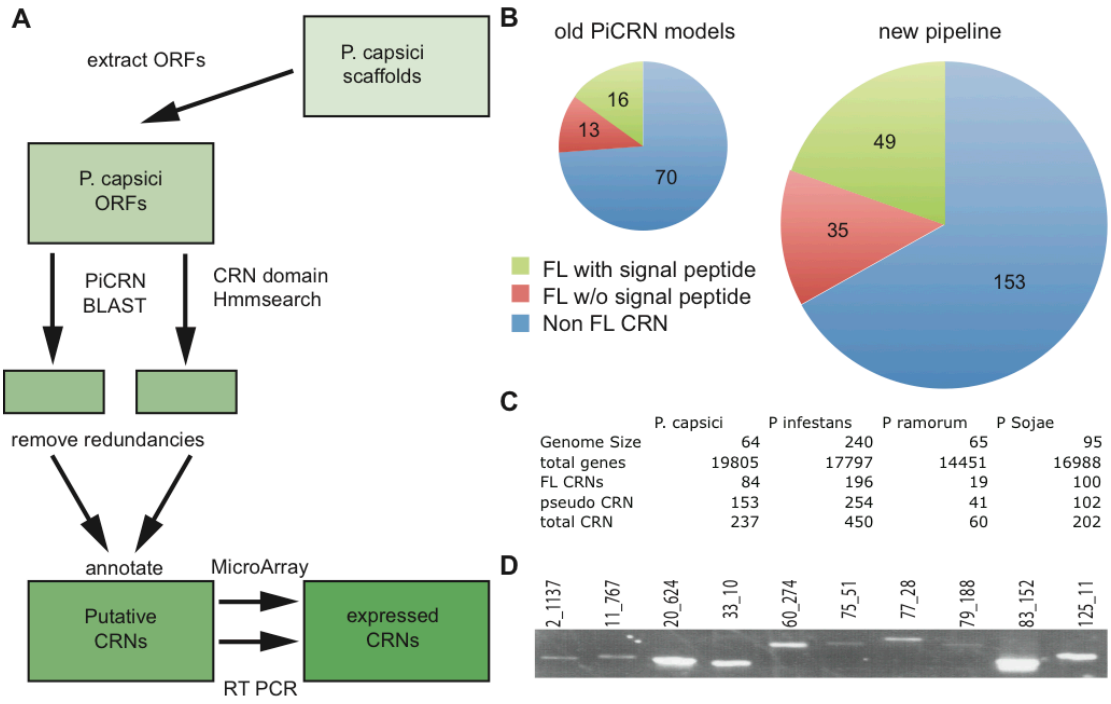

Figure 2.1 CRN identification pipeline

A) Pipeline used to re-annotate *P. capsici* CRN genes. ORFs were extracted from genome scaffolds. Known *P. infestans* CRNs and CRN HMM profiles were used to find putative CRNs. Candidates were filtered, annotated and verified via several methods. B) Visualisation of the different numbers of CRN-like genes identified using the predicted protein models of our new pipeline. Diameter of the circle represents the number of CRNs. C) Table showing gene size, gene number and number of (FL) CRNs for all sequenced *Phytophthora* spp. D) RT PCR on randomly selected *Crn* genes confirms presence on cDNA.

We devised a new pipeline for CRN identification and verification (Figure 2.1A). This pipeline was applied to raw genome sequence data and uses two separate search methods to identify putative CRN coding genes. We performed 6-frame translations of genome sequence scaffolds and extracted putative open reading frames (ORFs, >300 nt) from the *P. capsici* draft genome. BLAST searches with a set of verified *P. infestans* CRN coding genes (Win *et al.*, 2006) and HMMer searches employing models described previously (Haas *et al.*, 2009) were used to identify putative CRN domains. This yielded a set of 587 putative ORFs, each encoding a CRN-like sequence. Filtering out physical redundancies and subsequent semi-manual annotation resulted in a total set of 237 *Crn* gene models, a significant improvement over previous predictions (Figure 2.1B) and resembles the numbers of CRNs found in other *Phytophthora* species (Figure 2.1C). To test the robustness of our pipeline, we

analysed *Pythium ultimum* genome sequences and found 57 CRN-like ORFs in this species, including 16 CRN-like ORFs described during the original genome annotation. 10 other PuCRNs were not picked up by our pipeline. Closer examination revealed that these CRN-like ORFs were either too short (8) to be considered a *Crn* gene according to our parameters or lacked a proper LFLAK motif (2). To check for false positives we also applied the pipeline on the genomes of diatoms, *Phaeodactylum tricornutum* and *Thalassiosira pseudonana* and plants *Arabidopsis thaliana* and *Solanum lycopersicum* (tomato). One gene was flagged in tomato, as it shares similarity for the kinase domains, but lacks the characteristic LXLFLAK motif in the N-terminus. In all other control species *Crn* genes were not identified.

Analogous to other classes of intracellular effectors, CRNs are modular proteins that often carry a canonical secretion signal followed by a conserved N-terminal LXLFLAK motif, required for secretion and delivery of effectors into host cells(Schornack *et al*., 2009). In addition to the LXLFLAK motif, a highly conserved HVLVVVP motif, that defines the N-terminal DWL domain, marks a major recombination site that is followed by diverse C-termini that specify effector function (Figure 2A). We took advantage of this typical CRN architecture and defined full-length CRNs as proteins that carry the LXLFLAK motif within their first 66 N-terminal amino acids, feature the HVLVVVP motif and carry an additional effector domain. Manual inspection of all CRN-like candidates resulted in identification of 84 full-length CRN coding genes (35% of total). Prediction of signal peptides by means of SignalP indicates the presence of canonical secretion signals in 58% of the predicted full-length CRN proteins. It has previously been observed that *Crn* genes do not always contain canonical signal peptides. TMHMM searches failed to identify any transmembrane domains in the full-length effector set (cut-off e-value 1e-5).

To verify our predictions we performed semi-quantitative PCR on cDNA derived from RNA isolated from infected *N. benthamiana* leaf samples. We randomly selected 10 *Crn gene*s and designed primers to amplify the full-length genes (Figure 2.1D). RT-PCR analyses yielded amplification products with the expected size in each case, suggesting that our predicted gene models were accurate. Sequencing of each

amplicon confirmed amplification of the correct predicted gene and indicated the predicted sequences did not contain introns.

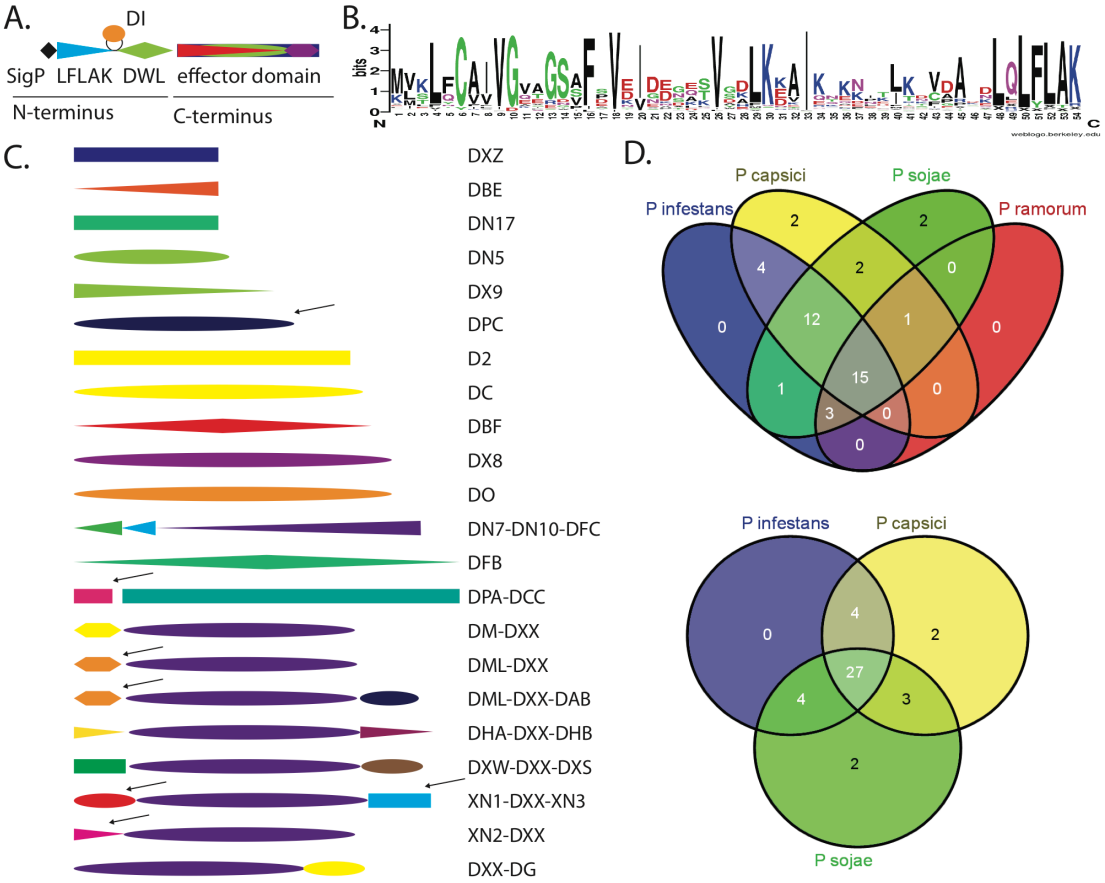

Figure 2.2 CRN domain organisation

A) Graphical representation of a CRN protein. A typical CRN has an N-terminus consisting of a Signal Peptide, LFLAK domain, containing the LxLFLAK-motif containing domain and DWL domain, containing the HVLVVVP-motif, in some cases a small DI domain is inserted between LFLAK and DWL domains. The C-terminus contains the effector domain and shows large variation in domain structure. B) Sequence logo representing *P. capsici* LFLAK domain. This LFLAK domain shows very close homology to the one from *P. infestans*. C) Variation of C-terminal domains found in full length CRNs of *P. capsici*. Arrows indicate domains that are unique in full length genes in *P. capsici*. D) Venn diagrams showing the distribution of CRN domains amongst different *Phytophthora* spp.

The *P. capsici* genome encodes both conserved and unique effector domains

CRNs are modular proteins consisting of a conserved N-terminus carrying the conserved LFLAK and DWL domains. CRN C-termini on the other hand are highly diverse and are thought to specify effector functions (Figure 2.2A). Indeed, alignments of N-terminal regions from our full length CRN set and subsequent

generation of sequence logos revealed that PcCRN N-termini share key features with those identified in other oomycete species (Figure 2.2B). As expected, both LXLFLAK and HVLVVVP motifs were found in the majority of N-termini and further sequence similarity was evident between *P. infestans* and *P. capsici* N-termini. These results are consistent with the observation that conserved N-terminal regions are required for secretion and delivery of CRN effectors inside host cells.

Previously, Haas *et al.* (2009) defined a domain structure for the *Phytophthora* CRN effector repertoire, based on sequence similarity. From these studies, 36 domains were defined after semi-automated alignment and analyses of conserved protein regions with unknown functions. 33 of these domains were found exclusively in C-terminal regions. We used these CRN domain models to assess their occurrence in *P. capsici*. HMM searches and subsequent manual assignment of CRN domains to our effector set showed that 30 C-terminal effector domains were present in the full *P. capsici* CRN complement. Of these 30 effector domains, 25 were present in at least one full length CRN, showing that collectively, *Phytophthora spp.* maintain a conserved but diverse effector domain repertoire.

We further investigated *P. capsici* effector domain composition in the predicted full length PcCRNs and identified 6 novel C-terminal domains in 7 combinations (Figure 2.2C). One CRN protein, for which we could not assign a known domain model, was found to carry a novel domain (we have called DPC) at its C-terminus. DPC is only present in full-length *P. capsici* CRN proteins, whereas in *P. sojae* and *Py. ultimum* this domain is only found in pseudogenes. In addition to the DPC domain, we identified DPA as a new domain that co-occurs with the C-terminal DCC domain in *P. capsici*, but cannot be found in other oomycetes. Similarly we found four additional domains that exclusively form full-length genes with the DXX domain (named XN1, XN2, XN3 & DML). Amongst these domains, XN2 appears unique to *P. capsici* whereas XN3 includes singleton SN4 from *P. infestans*. Figure 2D shows Venn diagrams indicating the number of domains that occur in the genomes of the sequenced *Phytophthora* spp. These analyses show that as many as 38 domains occur in the genomes of at least two species, and 27 domains occur in all three

closely related species, *P. capsici, P. infestans and P. sojae.*

These results indicate that although the CRN protein family forms an ancient and conserved protein family in the oomycetes, specific effector domains have emerged, reflecting on-going effector innovation underpinning host-pathogen co-evolution and pathogenesis.

CRN domain expansion may be linked to hemi-biotrophy and necrotrophy

We obtained evidence for this notion by super-imposing domain distributions onto a simplified phylogenetic tree describing relationships amongst sequenced oomycetes (Figure 2.3). Application of our HMM model set (Haas *et al*. , 2009 and this study) identified CRN domains present in publicly available genome sequences, covering a wide range of oomycete pathogens. Our searches identified previously annotated, as well as some previously un-annotated *Crn* genes.

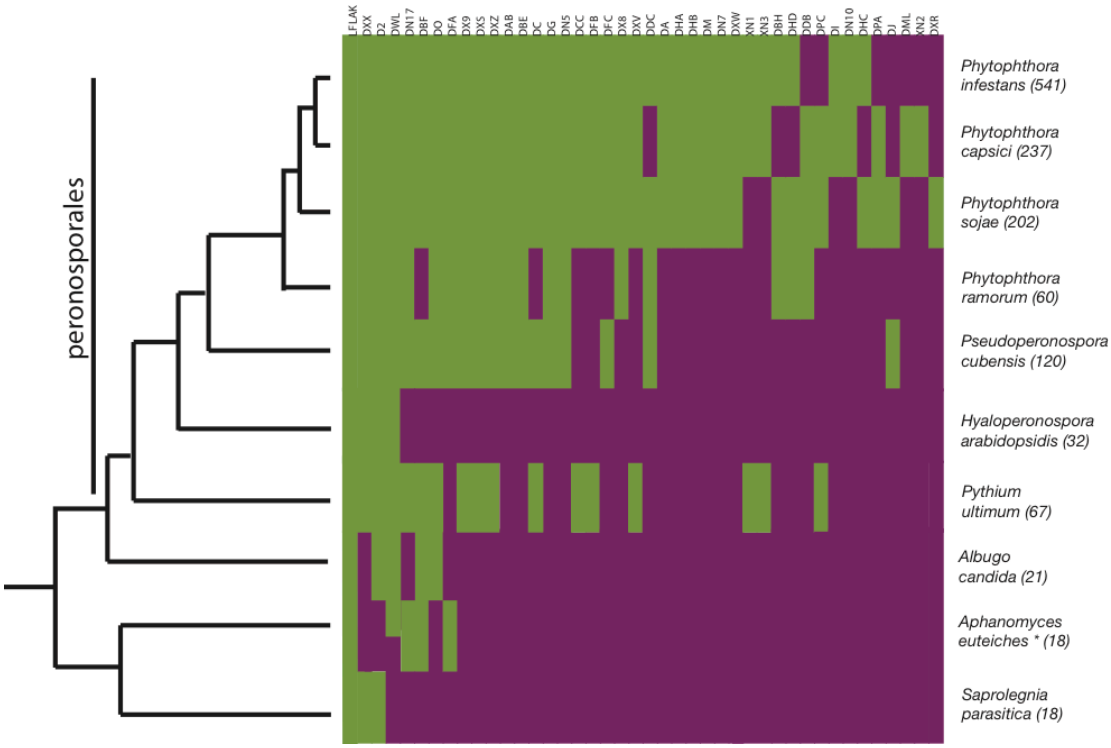

Figure 2.3 CRN expansion in Peronosporales

Occurrence of CRN domains in different oomycete species. Green = domain present, purple = domain absent. Total number of CRN-like genes is given between brackets. The tree left is adapted from Blair *et al.* (2008) and Thines and Kamoun (2010).

These analyses strongly suggest that the occurrence of described CRN domains

follows oomycete phylogenetic relationships with only a few ancient domains shared between all species and a large group of novel domains common between *Phytophthora* species (Figure 2.3).

To correct for a possible (evolutionary) bias caused by the use of *Phytophthora* derived CRN HMM models, we included distal LFLAK domain sequences from *P. ultimum* to remake HMM models. Subsequent searches revealed that the use of HMM model had no effect on overall *Crn* gene identification outcomes. Taken together, these results indicate that CRN domain expansion and diversification appears to have occurred after emergence of the *Peronosporales* lineage.

Interestingly, domain expansion appears to have occurred in pathogens that feature necrotrophy in their infection cycle. Domain expansion is evident in hemi-biotrophic *Phytophthora* spp. but does not occur in the biotrophic pathogen *Hyaloperonospora arabidopsis*. We also see expansion in *Pythium ultimum*, which is considered a necrotrophic species, although other *Pythium* species are hemi-biotrophs (Latijnhouwers *et al*., 2003; Lévesque *et al*., 2010). Thus there is evidence that CRN expansion may be correlated with an infection cycle that includes necrotrophy. Further genome sequencing from obligate biotrophs will confirm or refute this hypothesis.

Gene expression analyses defines two classes of CRN effectors

To investigate expression of our predicted *Crn* gene models, we performed reverse transcriptase PCR (RT-PCR) using cDNA samples derived from a *P. capsici* infection time course on tomato (*Solanum lycopersicum*). Samples were taken from a non-infected control and at 0, 8, 16, 24, 48 and 72 hours after infection and individual time course samples were used for PCRs.

We noted that our *Crn* coding genes show contrasting expression profiles (Figure 2.4A). One gene (77_28) appeared expressed at 0 hrs after infection, suggesting expression in zoospores and cysts, followed by a significant drop in subsequent biotrophic stages. Another gene however (20_624) did not show expression in the early time points but featured upregulation in the later stages of infection (Figure 2.4A). These results suggest the presence of distinct *Crn* gene expression patterns

during *P. capsici* infection and disease progression.

To substantiate and extend these results to the full *P. capsici Crn* gene repertoire, we assessed *Crn* transcriptional changes in microarray gene expression datasets generated from a *P. capsici*-tomato infection time series (Jupe *et al.*, 2013). We examined the expression profiles of *Crn* genes in the array dataset and found evidence of expression for 49 of our gene models (58% of full length *Crn* genes, using unique probes) as defined by detectable signal in biological replicates for at least two stages.

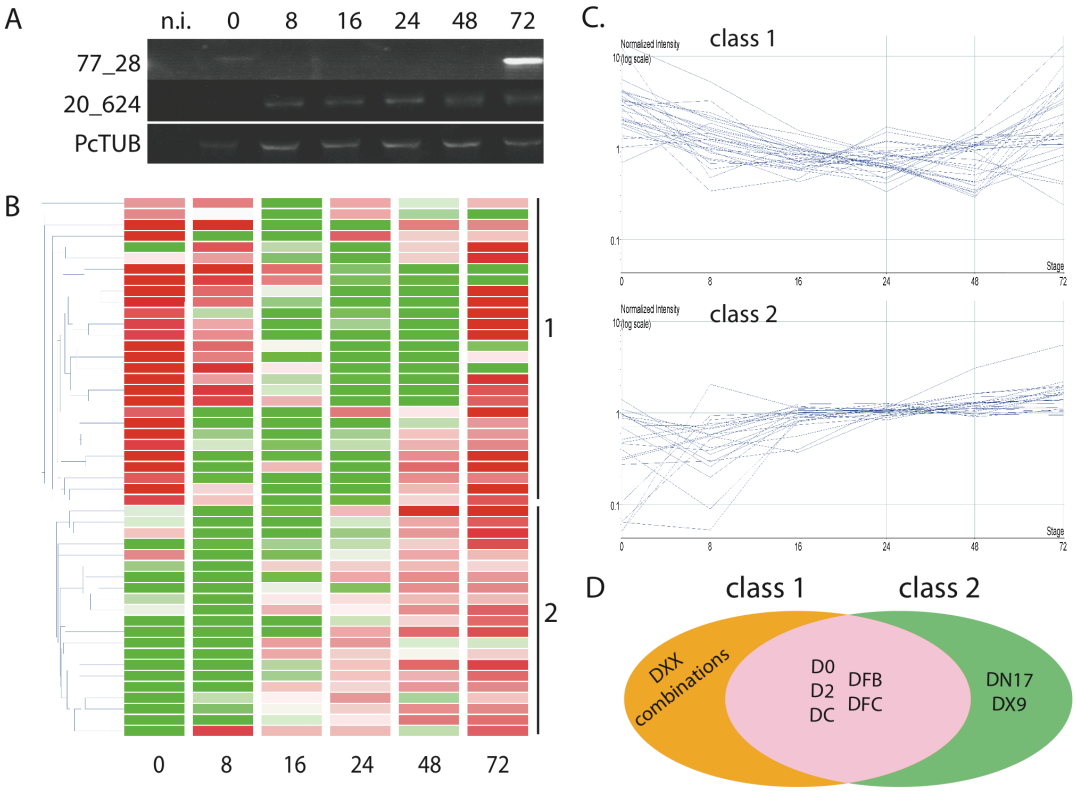

Figure 2.4 Crn gene expression during infection

A) RT-PCR on cDNA from tomato infected with *P. capsici*. Samples were collected at selected timepoints (hours post infection). B) Heat map showing expression pattern for full-length *P. capsici Crn* genes. Green is down regulated, Red is upregulated compared to the median of each sample. Gene classes are indicated on the right. Numbers at the bottom indicate the time after infection that the samples were taken. C) Expression profiles for *Crn* genes group in two different classes. Class 1 show genes that are upregulated compared to their mean expression values directly upon inoculation and after downregulation increase in expression in the later time points. Class 2 genes have upon inoculation expression values lower than their mean, but expression goes up during the course of infection, generally in the latest stages. D) Venn diagram showing the composition of both expression classes. Genes with DXX domain(combinations) all sit in class 1.

These results further validated our CRN identification and characterisation strategy and provided us with a robust set of genes suited to classifying gene expression patterns. We assessed *Crn* gene expression profiles and confirmed the presence of two classes of CRNs (Figure 2.4B, C). A total of 28 *Crn* genes fell into one class (1) featuring high levels of expression at the early time points, a drop during subsequent biotrophic stages and expression in the later stages (Figure 2.4B, C). A further 21 genes fell into another class (2), showing little or no detectable expression early in infection, but accumulation of transcripts in the late infection stages (Figure 2.4B and Figure 2.4C). We investigated if certain domains were specifically expressed in the two defined patterns. We assessed the expression of all C-terminal domains that were present more than once in the full length CRN set. This revealed that most domains were represented in both expression classes (Figure 2.4D). However, we found that all of the *Crn* genes encoding DXX domains were in class 1, whereas those containing DN17 and DX9 were in class 2 (Figure 2.4D, Table S02). These results suggest that the DXX domain in particular may have functions specific to early stages of infection.

P. capsici CRN proteins target the nucleus and sub-nuclear compartments

Previous studies established the CRN protein family as a class of nuclear effectors (Schornack et al., 2010). To assess whether the PcCRN proteins we identified feature Nuclear Localisation Signals (NLS), we applied NLStradamus, PredictNLS and NoD to the full length CRN set. Our analyses resulted in a combined set of 29 *P. capsici* FL CRN sequences with at least one localisation signal (Table S03), indicating that many of the *Crn* genes do not carry canonical NLS. Inspection of the predicted localisation signals in CRNs revealed few similarities between NLS motifs, consistent with the observation that CRN effector domains are divergent (Table S03).

We substantiated nuclear localisation of CRN effector domains from *P. capsici in planta*. We cloned 11 PcCRN C-terminal domains and fused them to GFP. Our selection included some very divergent domains (<10% sequence similarity) and CRNs with and without a predicted NLS. For some domains, we selected multiple representatives in order to assess domain-specific localisation. *Agrobacterium*

tumefaciens mediated expression of eGFP-CRN translational fusions in leaves showed specific nuclear accumulation (Figure 2.5). For all CRN domains tested, there was no or extremely weak GFP fluorescence in the cytosol whereas strong fluorescence emanated from plant nuclei. These observations contrasted with those observed in cells expressing eGFP only. Expression of eGFP consistently resulted in significant fluorescence in both the cytosol and nucleoplasm. Given that we sampled a comprehensive set of effectors covering the domain diversity in *P. capsici*, our results suggest that all CRNs target the host nucleus.

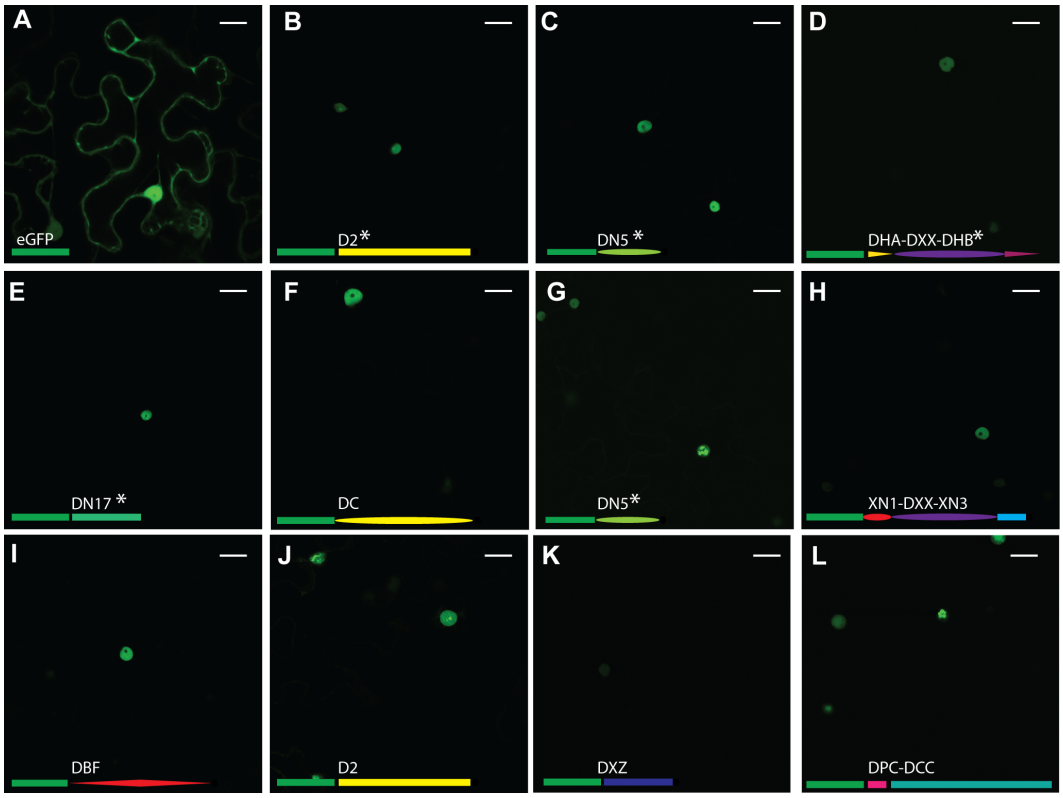

Figure 2.5 Nuclear localisation of CRN effectors

Localisation of GFP-tagged CRN C-termini. A) shows localisation of free GFP. B-L) show a diverse range of GFP-tagged CRN C-termini. B= 1_719, C= 11_767, D= 12_997, E= 20_624, F=32_283, G=33_10, H=36_259, I= 60_274, J= 79_188, K=83_152, L=105_26. All tested CRN fusions localise to the nucleus of the cell. Different subnuclear localisations can be observed for some CRNs (B, G, J, L). The domain organisations of the C-termini are represented as fused to GFP (green rectangle) for each image. NLS are predicted to be present in the genes marked with *. Scale bar = 25 µm.

Interestingly, we observed different subnuclear localisations for some effector

domains. Whereas most domains localised to the nucleoplasm and did not enter the nucleolus, some appeared aggregate in subnuclear bodies (Figure 2.5B,G,J,L). We selected two of these constructs (CRN1_719 (5B) and CRN79_188 (5J)) and CRN20_624 (5E) to represent the other CRNs and co-expressed them with RFP-tagged Fibrillarin, a marker of the plant nucleolus (Goodin *et al.*, 2007). We confirmed that the typical CRN localisation, as seen for CRN20_624, involved CRNs entering the nucleus, but not the nucleolus (Figure 2.6A-C). Two effectors containing the D2 domain, however, have different subnuclear localisations. CRN79_188 mainly localised to unknown nuclear bodies (Figure 2.6D-F) and was also seen to localise around the nucleolus, whereas CRN1_719 localised in the nucleolus (Figure 2.6G-I).

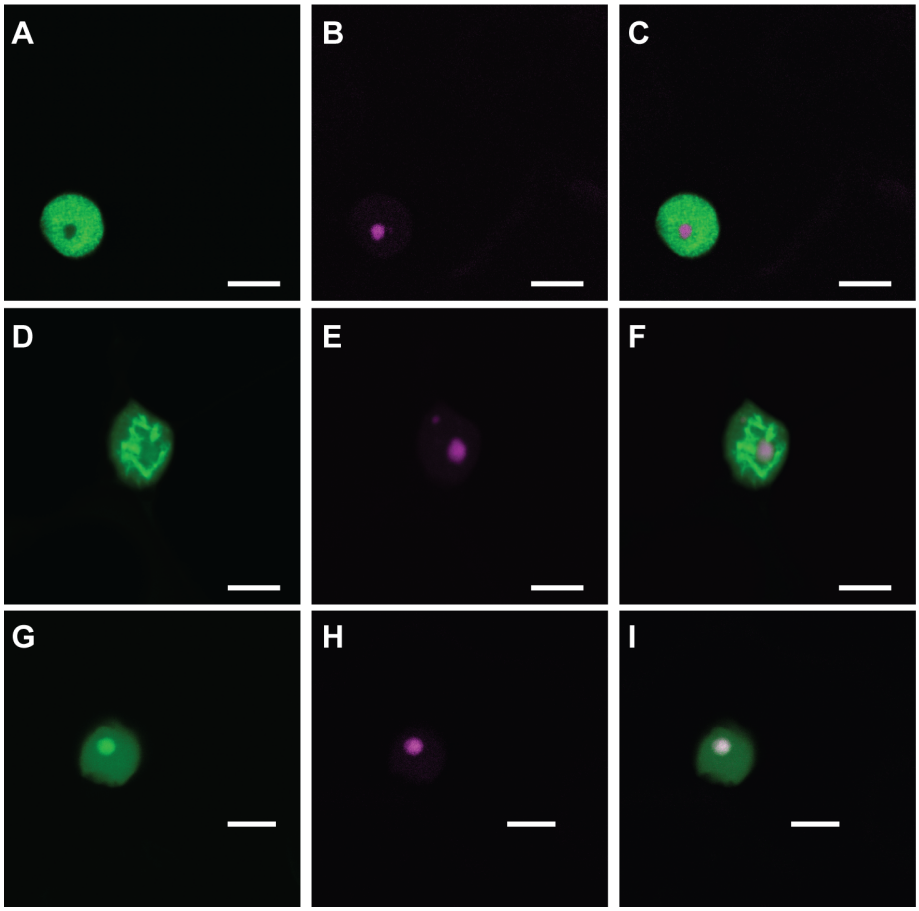

Figure 2.6 Differential subnuclear localisation for some CRNs

Different subnuclear localisations can be observed for CRN C-termini. First column shows GFP-tagged CRNs, second column shows RFP-tagged fibrillarin in the nucleolus and cajal body (Panel E). Third column shows overlay image. Scale bar = 10 µm

One CRN domain enhances virulence

The CRNs were named after a leaf crinkling and necrosis phenotype observed upon ectopic expression in plants (Torto *et al*., 2003). Recent studies however, show that this is not a universal feature of CRN proteins. Over-expression of PiCRN domains only induced necrosis in a few cases (Haas *et al*., 2009). To test whether *P. capsici* CRN domains were also variable in induction of cell death, we characterised 11 CRN domains *in planta* (Figure 2.7). We infiltrated three leaves for each of three independent replications and scored phenotypic effects on a range from 1 (no symptoms visible) to 6 (severely necrotic, black tissue). Only 3 of the 11 domains showed a strong necrosis phenotype after 7 days (Figure 2.7A). For other domains, ectopic expression occasionally resulted in chlorosis (yellowing), but this was not consistent across replicates. Protein expression levels were established by western blot. The results were similar for each repetition. Figure 2.8 shows a representative blot with some variation in protein levels between constructs, however these could not be linked to phenotypic observations.

To test whether CRNs have an effect on the growth rate of *P. capsici* during infection, we performed a simple drop inoculation assay on leaves transiently expressing CRN proteins. None of the CRNs had a direct positive effect on the growth rate of *P capsici*, except for CRN83_152 (Figure 2.7B). Interestingly this was only one of the three CRNs that showed a necrotic phenotype. The infiltration sites for CRN83_152 were swiftly colonised by *P. capsici*, leaving wet, infected tissue, whereas leaves for CRN20_624, which also causes necrosis after several days, remained uninfected (Figure 2.7C). This further indicates that the CRNs are a diverse group of effectors with a wide array of functions, some of which directly affect *P. capsici* virulence.

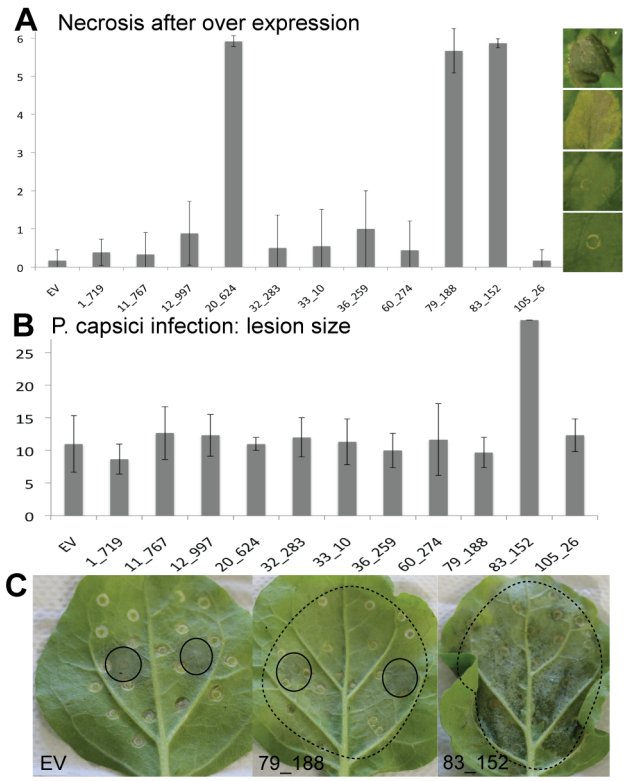

Figure 2.7 Phenotypic and functional analyses of CRN effector domains

A) Only three CRNs caused necrosis after over-expression in plants. Bars show average values for at least three independent infiltration events with four or more infiltration sites per construct per event. B) One CRN had a direct effect on virulence of *P. capsici*. Lesion size for all other CRNs was similar to that of the empty vector (EV) control. Error bars show standard deviations within the samples. Lesion size was measured during three independent infection events using four infection sites per construct. C) Onset of necrosis was not responsible for increased virulence. Panel 2 shows necrosis onset (dotted circles) for 79_188, but no increase in *P. capsici* lesion size (full circles) as seen for 83_152 (Panel 3). Panel A, X-axis: necrosis score as defined by picture panels on the right, Panel B X-Axis, Lesion size in mm.

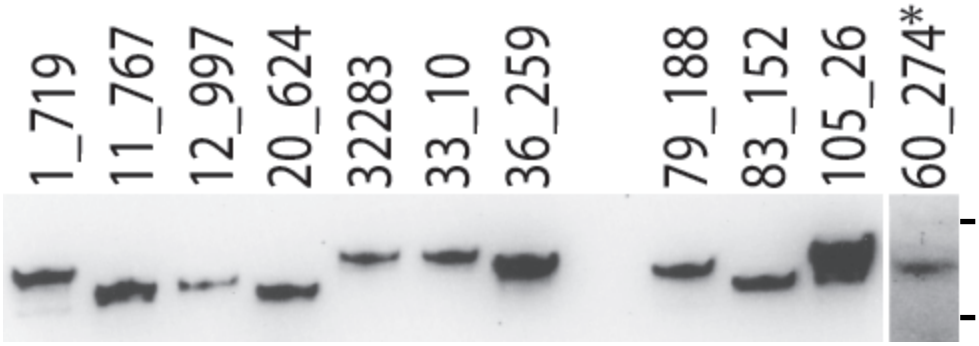

Figure 2.8 Stable expression of CRN proteins

Western blot showing stable expressed CRN C-termini fused to eGFP as shown in figure 5. *CRN60_274 has lower steady state protein levels compared to all others and could only be detected using stronger chemiluminescence substrates. Black lines right indicate approximately 70 and 50 kDa.

Discussion

The *P. capsici* CRN effector repertoire

The CRN protein family forms a class of oomycete effectors that are chronically understudied. The inability to reliably identify and classify CRN protein complements from a given pathogen has hampered functional studies in different oomycetes. Here, we applied a simple pipeline that employed 6-frame dynamic translation of raw genome sequences, followed by CRN prediction and verification studies. This approach enhanced CRN identification rates significantly for both full length genes and pseudogenes, compared to previously published results (Lamour *et al*., 2012a), thus providing a robust platform from which CRN evolution and virulence function can be further investigated. We identified 237 gene models with CRN features of which 84 were full-length. Existing descriptions of CRN domain composition and structure, allowed us to identify conserved domains, but also define novel C-terminal domains and domain configurations that may have specific roles in *P. capsici* virulence. The number of CRN coding (and pseudo) genes is similar to those found in other *Phytophthora* spp but exceed CRN repertoire size in other oomycetes such as *Saprolegnia parasitica* (18) *H. parasitica* (32) or *Py. ultimum* (67) (

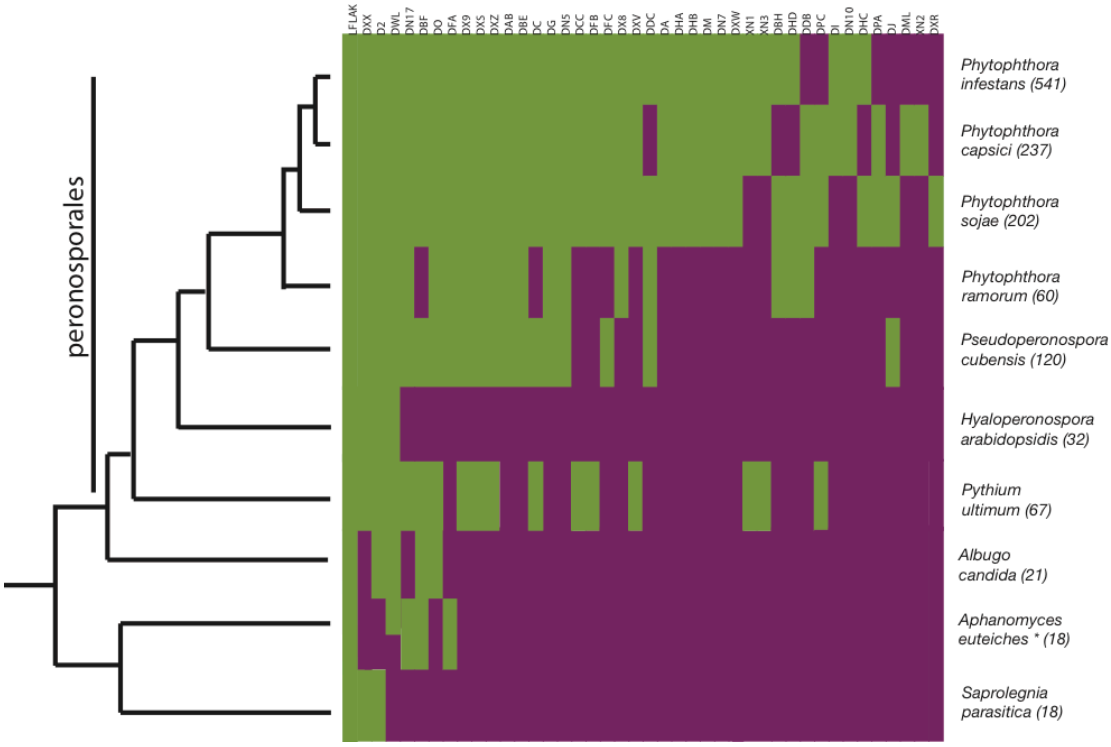

Figure 2.3). A subset of full-length genes was validated by PCR and subsequent amplicon sequencing. In addition, we obtained further support for our predictions as the majority of our predicted full-length genes were found to be expressed during infection in a *P. capsici*-tomato microarray experiment (Figure 2.4).

Occurrence and evolution of CRN domains in *P. capsici*

We assessed the *Crn* gene model complement encoded by the *P. capsici* genome. Detailed gene model annotations and comparative analyses show significant CRN domain variation and organisation within *P. capsici* and other *Phytophthora* CRN effector domains. Novel domain configurations and the presence of previously undescribed domains were found in CRN C-terminal regions. We provide evidence of dramatic expansion of the *Crn* gene family, suggesting possible roles in infection. Our analyses suggested that CRN domain innovation may be a feature of the Peronosporales lineage and pathogens that feature necrotrophy in their disease lifestyles. Further sequencing of biotrophic and necrotrophic oomycetes is required to confirm this hypothesis.

We show that the DXX and D2 domain are amongst the most widespread C-terminal CRN domains in the oomycetes. The DXX domain appears to have emerged early in oomycete evolution, yet it is part of an expanding complex. We found various effector domain configurations featuring DXX in *P. capsici*. Importantly, these included two new domains linked to DXX, suggesting that domain evolution and diversification in *P. capsici* is recent. The *P. infestans* CRN8 protein features a conserved D2 domain and has been found to carry kinase activity *in planta* which contributes to *P. infestans* virulence (van Damme *et al*., 2012). These results support the notion that CRN proteins play significant roles in oomycete parasitism and virulence. Future studies to identify isolate-specific domain configurations whilst assessing function in more detail will help build a better understanding of CRN evolution and function in *Phytophthora*.

P. capsici Crn genes group in two distinct expression classes

We investigated *Crn* gene expression and observed two different expression

patterns. Class 1 contains genes that are upregulated upon infection (e.g. in spores), drop down in biotrophy and show increased expression again in later stages, when sporulation is initiated. Class 2 shows no detectable expression in the very early stages, but increase after infection is established. Closer examination revealed that the DXX coding *Crn* genes exclusively exhibit class 1 expression patterns. We therefore hypothesise that the ancient DXX domain containing gene products play specific roles in establishing infection, whereas other domains support subsequent stages of the *P. capsici* life cycle. With the DN17 and DX9 domain encoding genes specifically falling into class 2, these domains may have specific roles in the late infection stages. The observation that both these domains are absent in biotrophic pathogens suggests a link to necrotrophy. Based on these observations, studies aimed at understanding pathogen lifestyles should include a detailed functional assessment of DN17 and DX9 domains.

CRNs localise and target nuclear compartments

Previously, studies on *P. infestans* CRN proteins revealed localisation to the host nucleus, suggesting that the CRN protein family form a class of nuclear effectors (Schornack *et al*., 2010). CRNs used in that study contained 4 different domains and all contained a predicted NLS, or slightly modified form (single aa changes). Our work extends these results by demonstrating that all tested, highly divergent *P. capsici* CRN domains localise to the nuclear compartment, regardless the presence of predicted nuclear localisation signals. Our results contrast with studies on other effector families that collectively target various subcellular compartments. Although increasing numbers of nuclear effectors are being described (Deslandes and Rivas, 2011), only the TAL class of effectors target the nucleus.

Besides the TAL effectors, pathogenic bacteria secrete a wide array of nucleo-modulins that manipulate a variety of animal host cell processes (Bierne and Cossart, 2012). In plants, there is increasing evidence that important processes take place in the plant nucleus that affect virulence and immunity. The wide variety of defence related proteins, ranging from NB-LRR R proteins to cysteine proteases, found to localise in or re-localise to the nucleus, only strengthens this notion (Deslandes and

Rivas, 2011). These observations lend support to the hypothesis that the host nucleus is a crucial compartment where plant-oomycete interaction outcomes are decided.

Detailed assessment of CRN localisation patterns revealed that in addition to nuclear accumulation, some CRN domains exhibited sub-nuclear localisation patterns. The majority of CRN domains tested localised to the nucleoplasm, whereas two D2 domain-containing effectors were found to accumulate in or around the nucleolus or in subnuclear bodies. These results suggest that the CRN protein family targets distinct sub-nuclear compartments and thus may perturb different components or processes in the host nucleus. There may be domain-specific sub-nuclear localisation patterns though more CRNs with D2 domains will have to be tested before this can be demonstrated.

Although all CRN proteins tested accumulate in the nucleus, Nuclear Localisation Signal (NLS) prediction exercises only identified NLS motifs in 26% of the PcCRN sequences tested. This indicates that either CRN proteins carry alternative NLS signals, not detectable by prediction software, or accumulate in the host nucleus by other means. The availability of large suites of CRN effector domains from a diverse group of pathogens, may allow application of computational strategies to identify novel sequence motifs that signal nuclear targeting.

CRNs are ancient proteins with diverse roles in pathology

Even though CRNs were named for their crinkling and necrosis phenotype upon their discovery, our assays show that only a small fraction of CRN domains induce necrosis in a short time frame. The observation that most CRNs do not show a necrosis phenotype after over-expression is consistent with previous findings (Haas *et al.*, 2009). Our results suggest that cell death induction is not a virulence function but rather a phenotypic manifestation reporting on effector activity.

Consistent with other studies, CRN domain classification may not distinguish between functions. We expressed two D2 domain-containing genes in leaves (CRN 1_719 and CRN 79_188) and only found evidence of cell death induction with one of them. Western blot analyses showed that both proteins were stable upon ectopic

expression suggesting that domain sequence variations may specify function. These results agree with observations made by Liu *et al.* (2011), who showed that two closely related PsCRN proteins have antagonistic functions when expressed in plants. The mechanisms by which small sequence variations within domains specify diverse phenotypic outcomes remain unclear. Regardless, these observations provide an ideal basis for structure-function studies in plants.

Only one CRN in our screen had a positive effect on *P. capsici* virulence. CRN83_152 enhances lesion growth rates in ectopic assays. However, this phenotype was unrelated to the cell death observed upon prolonged over expression of CRN83_152, as other cell death inducing CRNs do not have an enhancing effect on virulence. Although it remains unclear how virulence is boosted by CRN83_152 in these experiments, identification of its host targets may reveal processes that affect *P. capsici* disease progression.

Based on our results, we suggest that the CRNs have a subtler role in plant-pathogen interactions than perhaps assumed after their discovery. Identification of CRN host targets may therefore not only help implicate the processes that are targeted in host nuclei, but could also lead to a better understanding of the infection process. The characterisation of CRN targets may help delineate other requirements for infection. This is particularly significant considering that CRN domains are found in all plant pathogenic oomycetes, appear to have expanded in hemi-biotrophs and necrotrophs, pre-date the RxLRs and are specifically regulated during infection. We suggest that studies aimed at further understanding the role of CRN effectors *in vivo* during infection, will reveal novel effector functions and host targets that underpin pathogen lifestyles.

Acknowledgements

The authors would like to thank all members of the Dundee effector consortium for their support and advice, including Dr. Peter Cock and Dr. Leighton Pritchard for technical assistance and advice on bioinformatics analyses. We thank Prof. Paul Birch for helpful comments and suggestions. We also thank Connor Bowen for his help with phenotypic assays and Matthew Links for providing *A. candida* genome data.

Supplementary data:

Supplementary tables can be found on the CD-ROM attached to this thesis, or accessed online via

http://www.plosone.org/article/info%3Adoi%2F10.1371%2Fjournal.pone.0059517

Table S01
Overview of all CRN coding ORFs identified in *P. capsici*
Table S02
Microarray classification data for all Crn genes that had unique probes on our array.
Table S03
Overview of NLS in CRNs, identified with different prediction software
Table S04
Primers used in this study

Chapter 3 . Additional characterisation of three necrosis inducing CRN effectors

This chapter has been published as:

Stam R, AJM Howden, MC Delgado Cerezo M, TMMM Amarro, GB Motion, J Pham and E Huitema (2013) Characterisation of cell death inducing *Phytophthora capsici* CRN effectors suggests diverse activities in the host nucleus. Frontiers in Plant-Microbe Interactions 2013 (4) 387

AJMH contributed additional confocal microscopy for figure 5; performed infiltrations for figure 4; MDC performed confocal microscopy for figure 6; TMMMA performed experiments for figure 4, made cDNA for qPCR experiments; GBM performed western blots for figure 3; JP contributed qPCR experiments; EH contributed to data analysis

Abstract

Plant-Microbe interactions are complex associations that feature recognition of Pathogen Associated Molecular Patterns by the plant immune system and dampening of subsequent responses by pathogen encoded secreted effectors. With large effector repertoires now identified in a range of sequenced microbial genomes, much attention centres on understanding their roles in immunity or disease. These studies not only allow identification of pathogen virulence factors and strategies, they also provide an important molecular toolset suited for studying immunity in plants. The *Phytophthora* intracellular effector repertoire encodes a large class of proteins that translocate into host cells and exclusively target the host nucleus. Recent functional studies have implicated the CRN protein family as an important class of diverse effectors that target distinct subnuclear compartments and modify host cell signalling.

Here, we characterised three necrosis inducing CRNs and show that there are differences in the levels of cell death. We show that only expression of CRN20_624

has an additive effect on PAMP induced cell death but not AVR3a induced ETI. Given their distinctive phenotypes, we assessed localisation of each CRN with a set of nuclear markers and found clear differences in CRN subnuclear distribution patterns. These assays also revealed that expression of CRN83_152 leads to a distinct change in nuclear chromatin organisation, suggesting a distinct series of events that leads to cell death upon over-expression. Taken together, our results suggest diverse functions carried by CRN C-termini, which can be exploited to identify novel processes that take place in the host nucleus and are required for immunity or susceptibility.

Introduction

Within the natural environment, plants are continuously challenged by a diverse array of microbes that can cause disease, including bacteria, fungi and oomycetes. In order to counteract infection, plants have evolved the ability to recognise Microbe or Pathogen Associated Molecular Patterns (MAMPs or PAMPs, respectively) through Pattern Recognition Receptors (PRRs) localised in the host cell membrane. This recognition of PAMPs in turn activates PAMP-Triggered Immunity (PTI), preventing establishment of disease (Zipfel, 2008; Monaghan and Zipfel, 2012). In a select few cases, pathogens successfully infect plants by either limiting PAMP perception or perturbing PTI by interfering with signal transduction or associated cellular processes required for effective host immune responses (Jones and Dangl, 2006; Zipfel, 2008). This implies that pathogens have evolved molecular strategies to evade or circumvent host immunity. Consequently, host-pathogen interactions are considered dynamic associations featuring specialised pathogen machineries that aim to suppress (inducible) immune responses.

The key to understanding the mechanisms by which pathogens evade or suppress plant immune responses has been the identification of secreted proteins, termed effectors, which have been found in virtually all pathogen genomes studied to date (Hogenhout *et al*., 2009; Stergiopoulos and de Wit, 2009; Hann *et al*., 2010; Oliva *et al*., 2010). In some cases, effector activities towards virulence have been demonstrated and linked to host susceptibility, supporting the notion that effectors

can trigger susceptibility on their hosts (Effector Triggered Susceptibility (ETS)) (Bos *et al*., 2010; Yeam *et al*., 2010). Consequently, models have now emerged which describe secreted effector proteins that upon delivery to host cellular compartments, modify their targets and trigger susceptibility (Howden and Huitema, 2012). Besides PRR mediated responses, plants have acquired another layer of immunity. Most plants carry another class of receptors (termed Nucleotide Binding-Leucine Rich Repeat proteins or NB-LRRs), which reside inside host cells and upon recognition of cytoplasmic effectors, trigger immunity (Effector Triggered Immunity, ETI). With an increasing number of PRRs, PAMPs, effectors and NB-LRRs identified and characterised, observations suggest that both secreted pathogen proteins together with host receptors and signalling protein repertoires, determine interaction outcomes at the early stages of infection.

In recent years, a body of evidence has emerged which implicates the nucleus as a key cellular compartment in which the fate of host-pathogen interactions is determined (Liu and Coaker, 2008; Deslandes and Rivas, 2011; Rivas, 2012). In agreement with this, host protein classes with diverse functions have been shown to function in the nucleus towards immunity. These include plant disease resistance proteins, mitogen-associated protein (MAP) kinase signalling components, and transcription factors that collectively operate to regulate defence response genes following pathogen perception (Kinkema *et al*., 2000; Pandey and Somssich, 2009; Deslandes and Rivas, 2011; Park and Ronald, 2012; Rasmussen *et al*., 2012). In some cases, the mechanisms of activation are known and a major emerging theme is the exchange of key regulators and cellular signals between the cytosol and host nucleus (Shen and Schulze-Lefert, 2007). These processes generally result in the activation of defence responses and initiation of transcriptional programmes that elevate resistance. Given the role of the nucleus in plant defences and the ability of pathogens to suppress immunity, the view has emerged that perturbation of nuclear signalling by means of secreted pathogen effectors, may form an important virulence strategy to achieve disease.

Plant pathogenic oomycetes form a distinct lineage of eukaryotes that cause devastating diseases on a wide range of plants important to agriculture, forestry and natural ecosystems. For example, *Phytophthora infestans*, the causal agent of late blight on potato and tomato continues to cause hardship throughout the world with multi-billion dollar losses each year (Lamour *et al*., 2007). Other economically devastating pathogens include *P. sojae* and *P. capsici*, the major disease-causing agents on soybean and pepper, respectively. The shear economic impact that this group of pathogens incites has been, and continues to be, a driving force in our quest to understand *Phytophthora* parasitism.

Plant pathogenic oomycetes harbour a diverse class of effectors, termed the Crinklers (CRNs). All CRN proteins feature a conserved N-terminal domain specifying translocation and diverse C-terminal regions carrying distinct effector functions (Schornack *et al*., 2010). Crucially, a considerable number of CRN proteins have been identified in the genomes of all plant pathogenic oomycetes examined to date (Tyler *et al*., 2006; Gaulin *et al*., 2008; Haas *et al*., 2009; Lévesque *et al*., 2010; Schornack *et al*., 2010; Links *et al*., 2011; Lamour *et al*., 2012a; Stam *et al*., 2013b), suggesting that they have important roles in oomycete pathogenesis on plants.

Localisation studies on diverse sets of CRN effectors from divergent oomycete species revealed that they all accumulate in the host nucleus upon ectopic expression in plants (Schornack *et al*., 2010; Stam *et al*., 2013b). These observations combined with the identification of (cytoplasmic) RXLR effector proteins that target the nucleus (Dou *et al*., 2008; Caillaud *et al*., 2012a; Qiao *et al*., 2013) suggest that plant nuclear processes must present an important target for filamentous pathogens to achieve virulence (Birch *et al*., 2006; Morgan and Kamoun, 2007; Schornack *et al*., 2009). If true, nuclear effectors would carry the activities that allow modification of nuclear signalling networks and suppression of plant defences, providing useful tools for understanding the role of the plant nucleus during immunity.

CRN proteins were initially identified through their ability to cause crinkling and necrosis upon expression in plant tissue, and consequently this protein family is generally considered as a class of cell death inducing effectors (Torto *et al*., 2003). Recent studies however, show that this is not a universal feature of either CRN proteins or their C-terminal effector domains. Expression of CRN effector domains leads to cell death in only a select few cases, suggesting diverse activities underpinning effector function (Haas *et al*., 2009; Schornack *et al*., 2010; Stam *et al*., 2013b). Importantly, despite inducing cell death upon ectopic expression, infection assays revealed that only one CRN effector promotes virulence. Localisation studies revealed distinct subnuclear localisation patterns, further suggesting diverse functions in plants leading to cell death (Stam *et al*., 2013b). In this paper, we expand on our work on CRN effectors and provide evidence suggesting diverse molecular events leading to cell death in plants. Comparative analyses between three necrosis inducing CRN effector domains (DN17, D2, DXZ) revealed differences in the timing and occurrence of cell death in *N. benthamiana*. Consistent with diverse effector activities, we show that expression of only one CRN domain has an additive effect on PAMP-induced cell death, suggestive of distinct effector induced perturbations affecting different nuclear processes. Confocal and OMX 3D-SIM microscopy on living cells substantiated these observations by showing distinct subnuclear localisation patterns for each cell death inducing effector and crucially, specific effector induced changes in nuclear morphology, possibly leading to cell death. Taken together, our results suggest diverse functions carried out by CRN C-termini in the host nucleus that lead to cell death. We conclude that although cell death induction may not be a direct virulence function, it may represent an important phenotypic outcome, suited to study effector and target functions. A firm understanding of the molecular basis of CRN-induced changes to plant cells and nuclei in particular, will not only help understand CRN effector function, but also unveil novel nuclear processes that impact on cell death and immunity. We anticipate that ultimately, the study of nuclear effectors is pivotal to appreciate the nuclear processes that help determine infection outcomes.

Methods

Bacterial culture growth, Culture filtrate preparation procedures, Plant growth conditions and Phenotype scoring

For all experiments, *Agrobacterium tumefaciens* strain AGL1 was used as recipient strain for all constructs. AGL1 strains carrying respective constructs were grown in liquid cultures at 28 ^{o}C (shaking at 225 rpm) until mid-log phase. Optical Density (OD) was measured (at 600 nm) and cells adjusted to relevant densities using infiltration media (described below). *P. capsici* culture filtrates were prepared by inoculating liquid pea broth with mycelial plugs of strain LT1534. Cultures were incubated at 25 ^{o}C in the dark without agitation for 5 days. Culture filtrate (CF) was prepared by removing the mycelial mat after which the resulting liquid culture was filter sterilised. Pea broth used as negative controls was prepared simultaneously and sterilised before use in PTI assays. *Nicotiana benthamiana* plants were grown in a greenhouse under 16 hours of light and maintained at a temperature of approximately 25 °C/ 22 °C (day/night). For all experiments, 5-week old plants were used and kept under these conditions during the course of the experiment, unless otherwise stated. The level of cell death observed in plants during experiments was visually scored using a scale of 0 to 6, with a score of 0 indicating no symptoms, and a score of 6 indicating severe black necrotic lesions. This scale was used as described previously (Stam *et al.* 2013).

Preparation of fusion constructs

For construction of a GFP fusion construct containing the CRN N-terminus, corresponding gene fragments were amplified using primers 168080-F_BHI (5'-aaaaaggatccccGTGAAAGTGGACGAAGGCGC-3') and 168080_R_EcoRI (5'-aaaacgaattctaCGGAACCACCACCAGCACGTG-3'). For cloning of the mature gene coding fragment, primers 168080-F_BHI together with 20_624-R (5'-AAAAAGGCGCGCCTTATTGCAGCATCGCGTAAATTTTCCC-3') and ASC-I-STREPII-TAG (5'-aaaaagcggccGCTCACTTCTCGAACTGCGGGTGCGACCACCGGCGCGCC-3') were used.

*Bam*HI/*Eco*RI and *Bam*HI/*Asc*I digestions were performed for CRN-N terminal and mature protein constructs before ligation into pre-digested pENTR1a vector. Preparation of CRN C-terminal constructs has been described in Stam *et al.* (2013). pENTR1A-CRN constructs were sequence verified and used for recombination into the binary vector pB7WGF2 (Karimi *et al*., 2002), carrying a 35S promoter element and N-terminal GFP-fusion, using Gateway LR reactions (Life Technologies). Constructs were sequence verified before transformation into *A. tumefaciens* strain AGL1.

CRN induced cell death assays

All GFP-CRN effector domain fusion and control constructs were generated previously and prepared for infiltration as described in Stam *et al.* (2013). For cell death assays with CRN20_624 N-terminus, C-terminus and mature fusion proteins, all relevant cultures were adjusted to an OD of 1.0. Cultures were then mixed 1:1 with *A. tumefaciens* AGL1 cells carrying the silencing suppressor P19 at an OD of 1.0, giving a final OD of 0.5 for each CRN and 0.5 for P19. For experiments aimed to compare the kinetics of cell death induction upon ectopic expression of CRN20_624 (DN17), CRN83_152 (DXZ) and CRN79_188 (D2), ODs were adjusted to 0.5 for each culture and mixed with P19 in a 1:1 ratio (giving a final OD of 0.25). This OD proved to be optimal for monitoring cell death simultaneously for all of the CRNs. Plants were infiltrated with the bacterial suspensions and the level of cell death scored up to 7 days post-infiltration (dpi) as described above. Ten to twenty-five individual spot infiltrations were used per construct and all experiments were repeated at least three times. Means for the three CRN constructs were compared for each time point using one-way ANOVA with SPSS Statistics 21. Graphs show average values for one representative experiment. In a complementary experiment, ion leakage measurements were taken during the time course. For each measurement, 8 leaf disks were harvested from *N. benthamiana* plants infiltrated as described above, and placed together in 10 ml of Milli Q H_2O and shaken at room temperature at 75 rpm for 2 hours. After this time, total dissolved solids (TDS) were measured in the solution using a Primo pocket TDS tester (Hanna Instruments). For each time point

and treatment, 6 individual measurements were taken from plants grown in 2 separate greenhouses.

PTI assays

A. tumefaciens AGL1 cells carrying EGFP-CRN fusion constructs were prepared and used for infiltrations as described above using a final OD of 0.25 for each effector. After 48 hours, leaf panels were infiltrated with either culture filtrate generated from *P. capsici* liquid cultures or a control solution of pea broth media prepared as described above. Development of symptoms was recorded and the level of cell death was scored 48 hours after CF treatment. We infiltrated and scored ten leaves for each construct as described above. The experiment was conducted three times. Statistical analysis was done using SPSS Statistics 21. Equality of the means was tested for each relevant pair of treatments, using the t-test with independent samples.

PTI marker gene expression analyses

For qRT-PCR analyses, leaf panels expressing EGFP prepared as above, were treated with culture filtrate or a control solution of pea broth. After this second infiltration, 3 leaf discs (around 75 mg of tissue) were collected from individual plants at three different time points (1, 3 and 12 hours post CF/PB infiltration). Tissues were then used for RNA extraction using the RNeasy plant mini kit (Qiagen). RNA was treated using the DNA-free kit (Ambion) following the manufacturers protocol. cDNA was synthesised using superscript III reverse transcriptase kit (Invitrogen). qPCR was performed using the Power SYBR Green kit (Applied Biosystems) following manufacturer's instructions. The primer pairs used are described in Nguyen *et al.* (2010) and have previously been used successfully for *P. infestans* CF (Mclellan *et al*., 2013): NbEF1α-F TGGACACAGGGACTTCATCA and NbEF1α-R CAAGGGTGAAAGCAAGCAAT, NbPti5-F CCTCCAAGTTTGAGCTCGGATAGT and NbPti5-R CCAAGAAATTCTCCATGCACTCTGTC, NbAcre31-F AATTCGGCCATCGTGATCTTGGTC and NbAcre31-R GAGAAACTGGGATTGCCTGAAGGA, and NbGras2-F TACCTAGCACCAAGCAGATGCAGA and NbGras2-R TCATGAGGCGTTACTCGGAGCATT.

The following cycle conditions were used for all primers: initial denaturation at 95 °C for 15 minutes, followed by 40 cycles at 95 °C for 15 seconds and 60 °C for one minute, with a plate read after each cycle. Melt curve reads were performed every 1 °C between 60 and 95 °C and held for five seconds. Expression levels of each gene induced by CF were calculated relative to expression in leaves mock-infiltrated with pea broth. Expression of marker genes was normalised to the *NbEF1α* endogenous control gene.

ETI assays

A. tumefaciens AGL1 cells carrying GFP-CRN fusion constructs, empty vector, dexamethasone-inducible Avr3a^{KI} (in pBAV105), R3a and the silencing suppressor P19 were prepared for infiltration as described above. Cultures carrying CRN, empty vector and P19 constructs were diluted to a final OD of 0.25, and those harbouring Avr3a^{KI} and R3a were adjusted to a final OD of 0.1 before infiltration of plants. An OD of 0.1 was chosen for Avr3a^{KI} and R3a since higher ODs prevented an accurate comparison of the level of cell death between the three CRNs. For conditional expression of Avr3a^{KI}, 30mM dexamethasone (DEX) in 0.1% Tween 20 was infiltrated into leaves 48 h after initial *Agrobacterium* infection as described by Engelhardt *et al* (2012). As a negative control, we co-expressed R3a with the allelic variant Avr3a^{EM}, which is not recognised by R3a (Bos *et al*., 2009). Development of Avr3a^{KI}-R3a dependent cell death on CRN expressing leaves was assessed 24 hours after DEX treatment, scored and tested for significance as described above.

Western Blotting

Plant tissue was harvested 2, 3 and 4 dpi from infiltrated sites and frozen in liquid nitrogen. Protein extractions were performed on ground tissue using GTEN buffer (10% Glycerol, 25 mM Tris, 1 mM EDTA, 150 mM NaCl) supplemented with 2% PVPP, 10 mM DTT and 1X Complete protease inhibitor cocktail (Thermo Scientific). Samples were run on Biorad TGX gels before transfer to PVDF membranes using the Biorad Trans Blot Turbo Transfer System. Blots were blocked for 30 minutes with 5% milk in TBS-T (0.1% Tween 20), probed with StrepII-HRP antibody (1:5000) (Genscript) to

detect CRNs, and then washed three times in TBS-T for 5 minutes before incubation with Millipore Luminata Forte substrate. Images were collected on a Syngene GBox TX4 Imager. Blots were then re-probed with GFP antibody (Cambio) followed by anti Mouse-HRP antibodies (Santa Cruz) (1:20000), to detect free EGFP, and washed three times in TBS-T for 5 minutes before being imaged as before.

Confocal imaging

For confocal microscopy, *A. tumefaciens* cells were resuspended in infiltration buffer (25 mM MgCl2 and 150 µM acetosyringone) to a final OD of 0.05 - 0.1 enabling CRN visualisation while reducing the risk of observing over-expression artefacts. Control localisations with free EGFP were carried out using plants infiltrated with empty vector (EV). For nucleolar imaging, *A. tumefaciens* GFP-CRN suspensions were combined 1:1 with *A. tumefaciens* cells carrying a RFP-Fibrillarin expression construct (Goodin *et al*., 2007) to give a final OD of 0.05 for the CRN and 0.05 for RFP-Fibrillarin. Confocal imaging was carried out 48 hours post-infiltration. For DAPI staining, leaves were infiltrated with 4',6-Diamidino-2-Phenylindole dilactate (Invitrogen) at a final concentration of 5 µg/ml. Subnuclear localisation was examined on a Zeiss LSM 710 confocal microscope with a W Plan-Apochromat 40x/1.0 DIC M27 water dipping lens and using the following settings: GFP (488 nm excitation and 495-534 nm emission), mRFP (561 nm excitation and 592-631 nm emission) and DAPI (405 nm excitation and 415-481 nm emission). Cell viability was monitored during CRN localisation using transmitted light detection. Confocal imaging for localisation of the N- and C-terminus and mature protein was carried out using *A. tumefaciens* at an OD of 0.1 and using a Leica SP2 with HCX APO L U-V-I 63.0x water dipping lens with 488 nm excitation wave length.

OMX 3D-SIM imaging

For OMX imaging, *A. tumefaciens* AGL1 cells transformed with GFP-CRN fusion constructs (CRN20_624, CRN83_152 and CRN79_188) were grown and prepared as described above to a final OD of 0.05. The bacterial suspensions were infiltrated into leaves of 5 week old *N. benthamiana* H2B-RFP transgenic plants (Martin *et al*., 2009)

and *N. tabacum* plants grown and kept in the greenhouse as described above. OMX imaging was carried out 48 hours post-infiltration. Epidermal peels were harvested from infiltrated leaf panels and placed immediately into an agarose pad (*N. benthamiana*) or in 70% glycerol (for *N. tabacum*) for imaging. OMX 3D-SIM was performed as described in Posch *et al.* (2010).

Results

Cell death and localisation only requires the C-terminal domain

CRN effectors are modular proteins harbouring a conserved N-terminus required for translocation and C-terminal regions carrying effector activities (Haas *et al.* , 2009; Schornack *et al.* , 2010; Liu *et al.* , 2010; Stam *et al.* , 2013). Given their modularity and a possible impact of CRN N-termini on effector function, we assessed whether the N-terminus of CRN20_624 alters localisation or cell death inducing activity. To assess and compare localisation of the CRN20_624 N-terminus, the C-terminal effector domain as well as the mature protein were fused to EGFP, expressed in *N. benthamiana* leaves and localised by confocal microscopy in epidermal cells (Figure 3.1). Both mature protein and the C-terminal domain exclusively localised to the nucleus, suggesting that the CRN C-terminus drives nuclear localisation of mature CRN protein (Figure 3.1A). Consistent with this, expression of the EGFP-tagged N-terminal domain contrasted specific nuclear accumulation as this domain was found distributed throughout the cell, resembling distribution of free EGFP in the cytosol.

We used Western blot analysis to confirm that all EGFP-CRN domain fusions were expressed to similar levels *in planta*. Besides protein levels, these analyses revealed that resultant proteins were largely stable in plant cells as only low levels of EGFP cleavage was observed (Figure 3.1B). To test whether the presence of the N-terminus affects CRN induced cell death, we infiltrated *N. benthamiana* leaves with all CRN20_624 fusion constructs and the empty vector control.

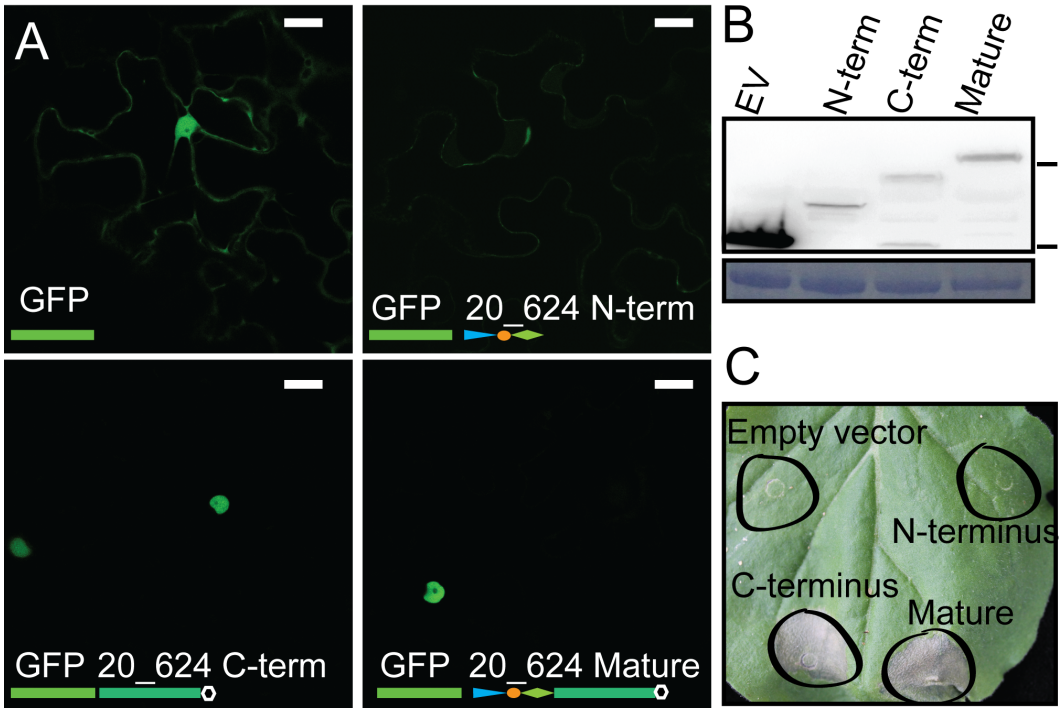

Figure 3.1 CRN C-terminus is the effector domain

A) Localisation of ectopically expressed CRN-GFP fusion products. The panels show the localisation for free eGFP, CRN20_624 N-terminus, CRN20_624 C-terminus, and mature CRN20_624 protein, 2 days post infiltration at OD 0.1 Scale bar = 25 µm. B) Immunoblot analysis of CRN20_624 upon over-expression in plant tissue. The blot was probed with anti-GFP antibody. 70 and 25 kDa markers are indicated on the right hand side. Lower panel shows coomassie brilliant blue staining loading control. C) Cell death inducing activity of CRN-GFP fusion products 7 days after infiltration at an OD of 1.0.

These experiments showed that both the mature protein and the C-terminus of CRN20_624 induce cell death (Figure 3.1C) at similar levels. Consistent with our localisation experiments, expression of the CRN N-terminus and GFP control only resulted in mild chlorosis. These data confirm that the CRN C-terminus is sufficient for nuclear accumulation and cell death inducing activity. Furthermore, these results suggest that the CRN N-terminus does not contribute to or impede effector activity once inside host cells.

Ectopic expression of CRN effector domains leads to different levels of cell death

Previously, we have shown that CRN20_624, CRN79_188 and CRN83_152 C-termini, classified as DN17, D2 and DXZ domains respectively, induce cell death upon ectopic over-expression in *N. benthamiana* (Stam *et al.* 2013). Given that these three CRNs

induce cell death but differentially affect *P. capsici* virulence in infection assays (Stam *et al.* , 2013) we elected to compare and contrast CRN induced cell death phenotypes in more detail. To assess whether there are differences in cell death inducing activity, we expressed each CRN effector domain in *N. benthamiana* and scored for cell death across different time points (Figure 3.2). Assessment of cell death occurring from 1-7 days showed significant differences in the timing and level of cell death between the CRNs from day 2 to day 7 (ANOVA $p < 0.01$) (Figure 3.2A). Expression of CRN83_152 led to a fast cell death response, reaching maximum levels (6) within 4 days of agro-infiltration, whereas CRN79_188 only induced marginal levels of cell death in the course of this experiment. Compared to CRN83_152 and CRN79_188, CRN20_624 exhibited an intermediate phenotype in these assays. Post-hoc Bonferroni tests show that cell death scores for all three CRN proteins were significantly different ($p<0.05$) on almost all days except for day 2, when CRN20_624 and CRN79_188 show no activity yet and day 7, where CRN20_624 and CRN83_152 both reached maximum cell death scores. We excluded the possibility of variation between leaves by expressing all CRNs and the empty vector on the same leaf (Figure 3.2C) and using multiple leaves in multiple experiments. To independently verify the levels of CRN induced cell death, we repeated these experiments and measured levels of ion leakage at 3 and 5 days (Figure 3.2B). Levels of ion leakage in infiltrated leaves differed significantly between CRN and empty vector constructs at both days and was consistent with macroscopic evaluation of CRN induced cell death (Figure 3.2A). CRN83_152 caused the greatest level of ion leakage determined by measuring total dissolved solids (TDS), while CRN79_188 caused ion leakage at levels just above those for the empty vector control. CRN20_624 expression led to ion leakage at levels between those seen for CRN83_152 and 79_188. Beyond 5 days it was not possible to measure ion leakage accurately, due to the advanced state of tissue necrosis.

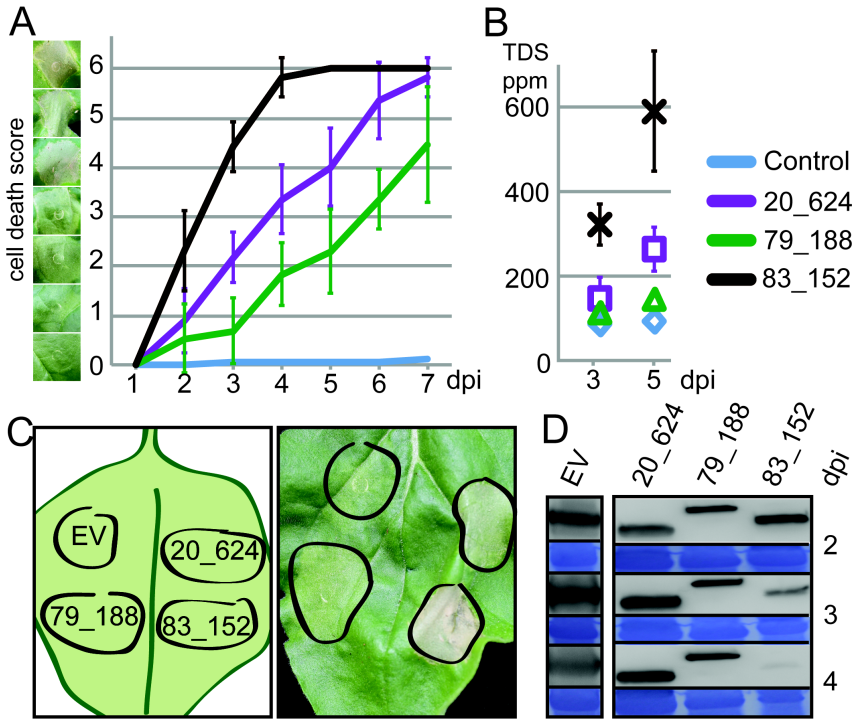

Figure 3.2 Necrosis inducing CRNs show distinct cell death dynamics

A) Progression of cell death in *N. benthamiana* leaves infiltrated with CRNs. Cell death was scored every 24 hours on a scale of 0-6. Example lesions for each score are shown on the left. The graph shows average values ± standard deviation for one representative experiment. B) Ion leakage measurements confirming differences in cell death response. Each data point is an average of 6 measurements ± standard deviation. TDS ppm: total dissolved solids in parts per million. C) Graphical representation of the experimental set-up (left) and a typical leaf 4 days post inoculations. D) Western blots and loading control for CRNs and control samples showing protein levels up to 4dpi. EV: GFP antibodies, CRNs: strepII antibodies. EV runs dat 25 kDa, CRNs around 60 kDa

Given the possibility that differences in cell death induction are due to levels of CRN proteins, we measured and compared EGFP-CRN levels in a typical experiment at day 2, 3 and 4. Western blots (Figure 3.2D) showed slight variation in expression levels between CRN constructs, which was not correlated to cell death levels. Given the differences in levels of cell death induction and the similar levels of EGFP-CRN found accumulating in our experiments, we conclude that CRN induced cell death phenotypes are distinct and may reflect different effector activities.

CRN20_624 expression has an additive effect on PTI,- but not ETI-related cell death

Given their proposed roles as virulence factors and the distinct differences in CRN sequence, cell death induction and subnuclear localisation, we asked whether CRN effector activity leads to perturbation of host PTI or ETI signalling pathways. To test for effects on PAMP induced cell death, *N. benthamiana* leaf panels expressing EGFP-CRN fusion proteins and EGFP were infiltrated with *P. capsici* derived culture filtrates (CF) and pea broth (PB) as negative control (Figure 3.3). Treatment of agro-infiltrated leaf panels with CF leads to PTI induction as qRT-PCR analyses on cDNA derived from EGFP-expressing leaf panels, treated with PB or CF, showed significant induction of PTI marker genes *NbPti5*, *NbAcre31* and *NbGras2* when compared to expression in PB treated tissues at 1 and 12 hours respectively (Figure 3.3A). Moreover, leaf panels expressing EGFP showed a specific cell death response to CF since infiltration of PB did not result in visible cell death (Figure 3.3B, D). Control experiments in which leaf panels expressing the *P. infestans* effector AVR3a were treated with CF, led to reduced cell death, suggesting suppression of CF induced response to PAMPs (data not shown). Interestingly, expression of CRN20_624 was found to have an additive effect on cell death induced by CF treatments in our experiments (Figure 3.3B). Direct comparisons of cell death between empty vector and CRN20_624 expressing leaf panels showed a significant increase of cell death ($p<0.01$), which contrasted results obtained with CRN79_188. Although CRN79_188 induced some cell death without CF treatment, the combination of CRN79_188 with CF did not result in a stronger cell death responses when compared to the EV control ($p=0.8$).

In these assays, we were not able to assess the effect of CRN83_152 on PTI since we could not find significant differences in the levels of cell death between CF treatment and the PB control (t-test for equality of means, $p=1$) (Figure 3.3B). These results indicate that the CRN effector activities leading to cell death are distinct and in the case of CRN20_624, intersect with other cell death pathways in plants.

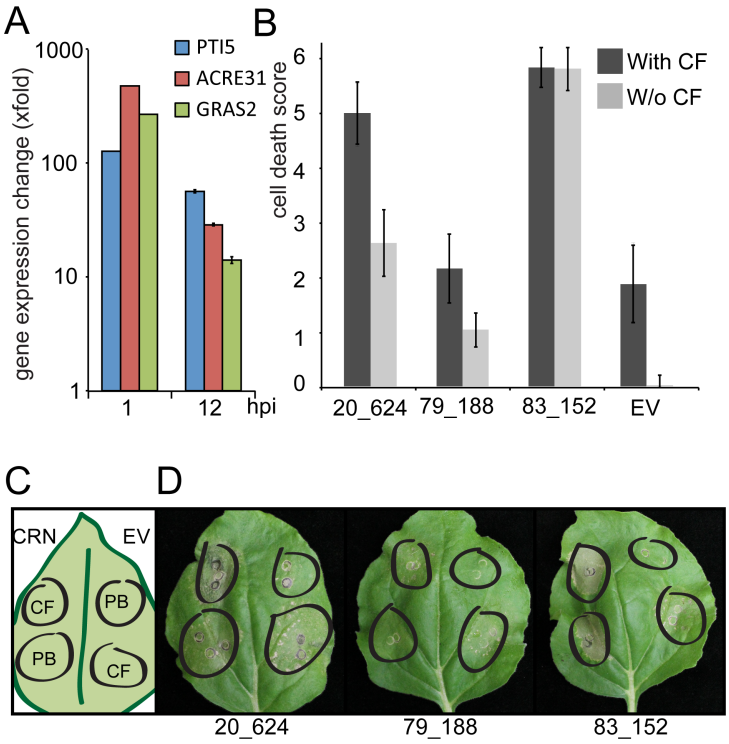

Figure 3.3 CRN20_624 causes altered PAMP responses within the plant.

A) qRT-PCR analyses on cDNA derived from leaf panels transiently expressing EGFP and treated with PB and CF. Each bar represents the fold change in gene expression upon CF treatment relative to PB ± standard deviation. Expression was examined for known PTI marker genes NbPti5, NbAcre31, and NbGras2 at 1 and 12 h post infiltration (hpi). B) Graph showing average necrosis scores ± standard deviation for three independent experiments. C) Graphical representation of the experimental set-up. CRN-GFP fusion constructs were infiltrated into N. benthamiana plants and after 48 h, leaves were infiltrated with either a PAMP cocktail (Phytophthora capsici culture filtrate) or a control solution of pea broth. Cell death was scored on a scale of 0–6, 48 h after CF treatment. D) Examples of representative leaves for each treatment on day of scoring.

Given that CRN20_624 has an additive effect on cell death upon CF treatment, we asked whether any of our effectors affect ETI mediated cell death (Figure 3.4). To test this, we over-expressed CRN20_624, CRN83_152 and CRN79_188 in *N. benthamiana* leaves with R3a whilst also introducing *P. infestans* Avr3a^{KI} and Avr3a^{EM} coding genes under a DEX inducible promoter. In these assays, Avr3a^{EM} served as a negative control, as it is not recognised by R3a (Bos *et al.* , 2009). Co-infiltration of CRN fusion proteins and EGFP in combination with R3a and AVR3a constructs, allowed us to express CRN fusion proteins with R3a first before activating Avr3a^{KI} induced ETI, with DEX treatment. Phenotypic assessment of leaf panels 24

hours after DEX induction revealed robust HR development. In these assays, there was no evidence of either enhanced or reduced ETI responses in CRN expressing leaves based on direct comparisons to our EV controls (ANOVA, p=1).

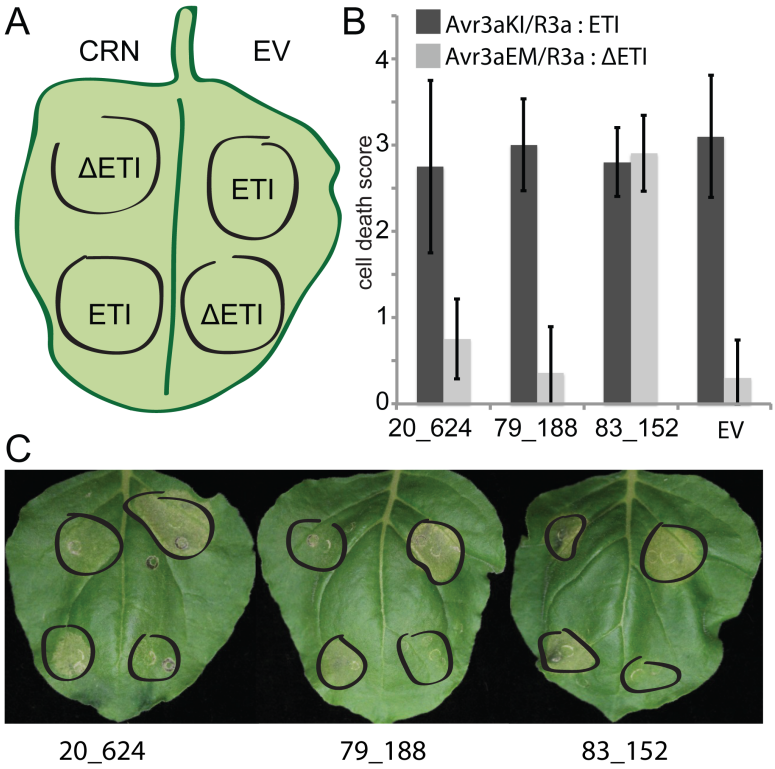

Figure 3.4 Necrosis inducing CRNs do not cause altered ETI responses

A) Graphical representation of the experimental set-up. CRN-GFP fusion and EV constructs were co-infiltrated into *N. benthamiana* leaves with Avr3aKI and R3a (ETI), and Avr3aEM and R3a (ΔETI) to monitor ETI responses. After 48 hours, leaves were infiltrated with dexamethasone and incubated for a further 24 hours for induction of Avr3a expression. B) Cell death in response to CRNs in ETI and non-ETI induced leaves scored on a scale of 0-6. Graph shows average necrosis scores ± standard deviation for one representative experiment. C) Examples of representative leaves for each treatment on day of scoring.

These results suggest that the presence of these CRN effectors does not affect ETI induced cell death. As expected, induction of AVR3a^{EM} expression in the presence of R3a did not lead to HR demonstrating that the observed cell death was due to specific recognition of AVR3a^{KI}. From these results, we conclude that CRN20_624 specifically promotes PAMP induced cell death. We suggest that the contrasting observations between CRN proteins reflect differences in effector functions, each of which leads to cell death upon ectopic expression.

CRN over-expression results in distinct changes to host nuclear morphology

We have presented evidence suggesting that CRN83_152, CRN20_624 and CRN79_188 feature distinct cell death phenotypes and differentially affect other cell death pathways. Given their distinct localisation patterns upon over-expression (Stam *et al.* 2013) we asked whether localisation of nuclear markers during CRN expression would allow further insights into the onset of cell death in plants. Confocal microscopy was used to determine the nuclear localisation of EGFP-CRN proteins as well as the nucleolar marker Fibrillarin and nuclear DNA. CRN20_624 showed a punctate distribution pattern confined to the nucleoplasm that contrasted localisation of CRN79_188. Expression of CRN79_188 consistently led to the detection of filament-like structures in the nucleus. In contrast, CRN83_152 was present in patches within the nucleus, with clear areas of nuclear space in which EGFP-CRN83_152 protein appeared absent (Figure 3.5). These patterns were observed in living cells as cytoplasmic streaming was evident in cells expressing all EGFP-CRN fusions (Supplementary videos 1-4). Interestingly, distribution of DAPI stained nuclear DNA appeared altered in cells expressing CRN83_152 (Figure 3.5A), suggesting re-localisation of host chromatin.

To confirm this observation, we expressed EGFP-CRN83_152 in transgenic *N. benthamiana* plants carrying histone-RFP (Figure 3.5B). These experiments revealed that consistent with our observation on DAPI stained DNA, over-expression of CRN83_152 caused Histone 2B-RFP labelled DNA to accumulate in distinct patches within the nucleus. In these assays, CRN83_152 was found to accumulate in areas in the nucleus from which DNA had been excluded.

Consequently, CRN83_152 and DAPI/ Histone 2B-RFP signal did not co-localise in neither of our experiments (Figure 3.5A,B). In contrast to CRN83_152, over-expression of CRN20_624 and CRN79_188 did not alter the distribution of DNA. DAPI and histone-RFP signal were detected evenly within the nuclear space, with only some small patches where DNA was absent, similar to the pattern observed for cells

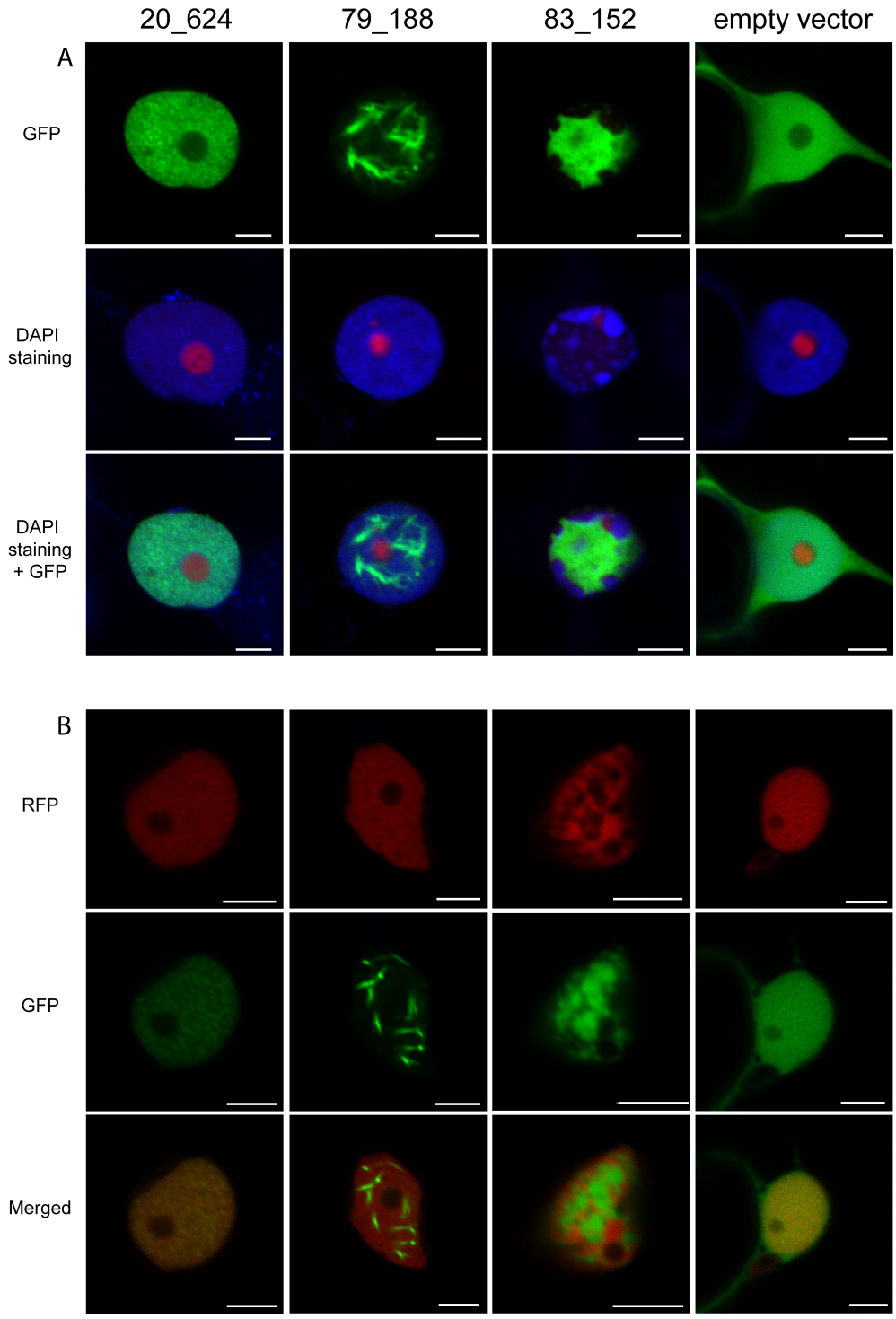

Figure 3.5 CRN 83_152 causes re-localisation of DNA

CRN-GFP fusion constructs were over-expressed in *N. benthamiana* plants and imaged by confocal microscopy 48 hours post-infiltration. A) Leaves were co-infiltrated with RFP-fibrillarin and were DAPI stained by infiltrating with 4',6-Diamidino-2-Phenylindole dilactate at a final concentration of 5 µg/ml. B) *N. benthamiana* plants stably expressing histone RFP were infiltrated with CRN-GFP fusion constructs as described above. Scale bars = 5 µm.

expressing free GFP. To exclude the possibility of changes in nuclear morphology after cell death, we repeated these assays whilst confirming cell viability by assessing cytoplasmic streaming and vesicle movement within the cytoplasm during CRN and EGFP expression. In these experiments, nuclear re-organisation caused by expression of CRN83_152 did not appear to affect cell viability within the time scale of these experiments (Supplementary video 3).

3D-SIM imagining of CRN effectors reveals distinct localisation within the nucleus.

Using confocal microscopy, we observed distinct subnuclear localisation and structures upon expression of the three CRN effectors characterised in this study. To gain a better understanding of these results, we used super-resolution 3D structured illumination microscopy (3D-SIM) to visualise the possible structures CRN proteins form or interact with at the subnuclear level (Figure 3.6). 3D-SIM imaging of *N. benthamiana* leaves expressing Histone 2B-RFP and EGFP-CRN fusions confirmed localisation patterns observed in our confocal microscopy experiments for CRN20_152 and CRN79_188 (Figure 3.5). CRN20_624 was found distributed in punctate patterns throughout the nucleoplasm in close proximity to Histone 2B-RFP labelled chromatin (Figure 3.6A). CRN79_188 was found to form regular and evenly distributed fibril-like structures interspersed with chromatin (Figure 3.6B). In both cases, distribution of chromatin in the nucleus is not impaired. High-resolution images, however, shines a different light on CRN83_152 localisation. Whereas confocal images suggest that CRN83_152 localises in a uniform manner in patches within the nucleoplasm, OMX microscopy reveals that these patches consist of long and undulating strands, surrounding areas of re-localised chromatin. This is particularly evident in single plane images (Figure 3.6B) and could not be observed with confocal microscopy.

Although the mechanism of chromatin exclusion or degradation in the presence of CRN83_152 is yet elusive, our results suggest that one mechanism of cell death induction could rely on the modification of chromatin affecting its integrity and consequently, disrupting important host cell processes.

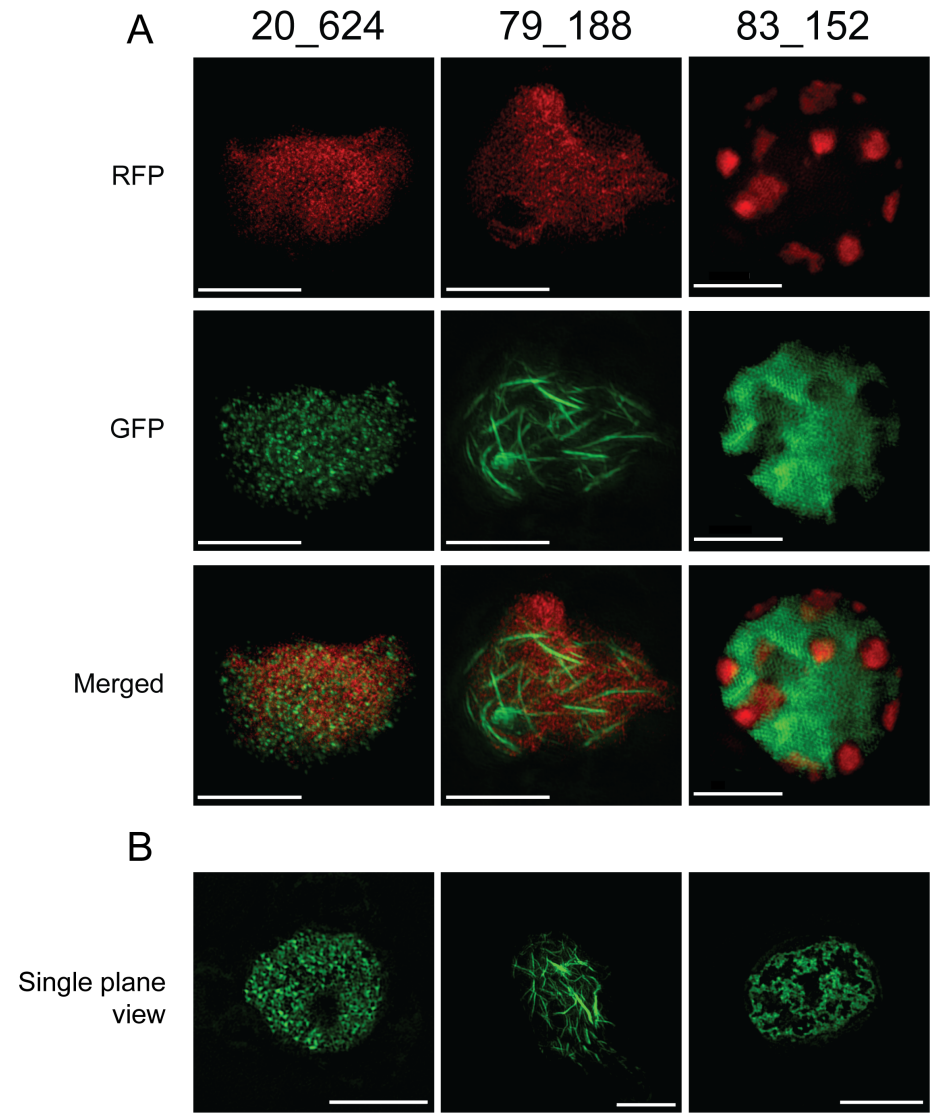

Figure 3.6 3D-SIM imaging reveals strand like pattern for CRN83_152

A) Projection view of 3D-SIM images on epidermal peels of *N. benthamiana* H2B-RFP transgenic lines infiltrated with CRN-GFP fusion constructs. Histone 2B distribution is shown in RFP channel whereas CRN protein distribution is in the GFP channel. Merged channel confirms impairment of chromatin distribution in CRN83_152 expressing cells. B) Single plane views of 3D-SIM images on epidermal peels of N. tabacum infiltrated with CRN-GFP fusion constructs show distinct nuclear distribution patterns for CRN effector proteins. All images were taken 48 hours after infiltration. Scale bars = 5 µm.

Discussion

CRN effectors are considered a diverse and ubiquitous class of effectors found in all plant pathogenic oomycetes sequenced to date. Consequently, various studies have hinted at a role in virulence, suppression of PTI and more recently, ETI (Liu *et al.*, 2011; van Damme *et al.*, 2012; Shen *et al.*, 2013; Stam *et al.*, 2013b). Here we

provide further evidence of functional diversity amongst *P. capsici* CRN proteins by studying the activity of three necrosis-inducing effectors. Consistent with previous studies, we show that for CRN20_624, the N-terminal region does not affect cell death induction or localisation, suggesting that only the C-terminal effector domain is required for function in the nucleus. Although only shown for CRN20_624, this work further supports the observation that nuclear localisation is required for cell death induction as shown for *P. infestans* CRN8 (van Damme *et al*., 2012) and that CRN C-termini carry the cell death inducing activity (Torto *et al*., 2003; Haas *et al*., 2009). We demonstrate that based on timing and intensity of cell death as well as their effects on CF triggered cell death, CRN20_624, CRN79_188 and CRN83_152 have distinct activities *in planta*.

Macroscopic evaluation of cell death as well as ion leakage measurements upon CRN expression revealed that CRN83_152 expression causes rapid cell death and tissue collapse, whereas CRN79_188 causes delayed cell death and CRN20_624 features an intermediate phenotype. Western blot analyses revealed that all EGFP-CRN fusions accumulated to similar levels, suggesting that differences in cell death reflect distinct activities rather than effector abundance. This observation is further illustrated by the diverse CRN localisation patterns as well as distinct changes in nuclear morphology and DNA distribution upon CRN83_152 accumulation.

Besides cell death induction, we have presented evidence that CRN20_624, but not CRN83_152 and CRN79_188 has an additive effect on PAMP induced cell death. Treatment of CRN expressing leaves with either pea broth (PB) or culture filtrates (CF) showed a marked increase in cell death on CF treated panels, suggesting modification of PAMP induced cell death signalling. These results contrasted with cell death induced by recognition of the *P. infestans* effector AVR3a by R3a. Importantly, these results could suggest that CRN20_624 activity induces specific cell cell death pathways, excluding those associated with ETI. If true, this would mean that CRN proteins could be used to classify and study PAMP triggered nuclear signalling pathways. CRN20_624 mediated promotion of PTI is counter-intuitive as

effectors are generally thought of as suppressors of PTI. It is possible however that PTI stimulation represents a virulence function in the late stages of a hemi-biotrophic lifecycle, when cell death and tissue collapse is apparent (Jupe *et al*., 2013). Interestingly, CRN20_624, which contains the DN17 C-terminal domain, is expressed at later stages during infection, coinciding with the switch of *P. capsici* from a biotrophic to a necrotrophic lifestyle (Stam *et al.* , 2013). This adds additional weight to a model in which *P. capsici* deploys effectors to co-opt host PTI signalling pathways and promote cell death. If true, the identification and engineering of CRN20_624 host targets may allow reduction of cell death during *P. capsici* infection and slow disease progression.

Consistent with diverse functions, we reveal distinct subnuclear localisation patterns for the CRN effectors studied here. Detailed co-localisation studies of CRN83_152, CRN20_624 and CRN79_188 together with DAPI staining as well as nucleolar and chromatin markers, not only confirmed the organisation of EGFP-CRN proteins in distinct patterns, but unveiled unexpected changes in the organisation of nuclear chromatin upon expression of CRN83_152. Multiple localisation experiments showed that CRN83_152 occupies the nuclear space around DAPI and H2B-RFP labelled patches of DNA. 3D-SIM high resolution microscopy not only confirmed these observations but added additional detail, showing organisation of CRN83_152 in intricately organised convoluted structures, wrapping around or in close proximity to nuclear chromatin. At this stage, we do not know the molecular basis or function of CRN83_152. Although we have previously shown that CRN83_152 enhances *P. capsici* virulence, we do not know the relevance of chromatin re-organisation towards immunity or susceptibility. Studies currently on the way in our group will aim to identify the principal targets for CRN83_152 and study their role in immunity. It is likely that these studies will help unveil novel processes underpinning *Phytophthora* virulence.

In contrast to CRN83_152, microscopy revealed that CRN79_188 is distributed in long thin filamentous strands. Importantly, we found that these filaments are

uniform and evenly distributed throughout the nucleoplasm. These results suggest that CRN79_188 either forms these structures by itself or interacts with yet unknown structures in the nucleus. In this regard, the recent identification of F-actin containing structures in plant cells containing the Turnip Vein Clearing Virus movement protein MP-TVCV (Levy *et al*., 2013), raises this possibility.

Based on our results, we question as to whether cell death induction is a direct virulence function or rather, is a feature that is an indirect consequence of (distinct) effector activities. Ectopic expression in plant cells led to rapid accumulation of CRN proteins in *N. benthamiana* cells to levels that are unlikely to occur *in vivo* during infection. We also cannot exclude that perception of bacterial PAMPs has an impact on our results in the case of our cell death assays. However, leaf panels expressing EGFP remained healthy, showing low levels of ion leakage and were responsive to CF treatment as evidenced by induction of PTI marker genes and occurrence of CF-specific cell death in our experiments. Whether priming of defence responses affect levels of cell death or not, the differences in cell death kinetics for the CRN effectors tested were consistent and significant across our experiments. Because of the necessity for both an epitope tag and fluorescent reporter, we have used EGFP-CRN protein fusions for this work. We can therefore not formally exclude the possibility that the presence of N-terminal EGFP affects CRN function or activity levels. Given the observations that CRN proteins are modular in nature and mature CRN proteins also feature sizeable N-terminal regions that does not appear to affect function or localisation for CRN20_624, this is not a likely scenario.

Taken together, our work suggests distinct differences in cell death mediated by diverse CRN effector activities. These findings are thus consistent and build on previous work, which showed differential effects of CRN over-expression on *P. capsici* virulence (Stam *et al*., 2013b). This study further supports the emerging view that through yet unknown mechanisms this ancient class of effector proteins act on processes required for plant immunity. With an increasing number of nuclear host defence signalling components identified in plants together with pathogen effectors

that target the nucleus, there is a critical need to understand the nuclear processes that drive plant immunity and ETS. Our results strongly suggest that exploring the functions of CRN effectors, including those that induce cell death, will uncover immunity-associated nuclear processes in the host. Given the enormous diversity of nuclear effectors now identified in the oomycetes, these proteins form a rich source of molecular probes suited to study nuclear biology. CRN effectors and other nuclear effectors will thus emerge as valuable tools to unravel nuclear processes involved in plant immunity.

Acknowledgements

The Authors are grateful to the referees for their constructive comments. We would like to thank Prof. Paul Birch for providing Dexamethasone inducible Avr3a and R3a binary vectors. We are grateful to Dr. Markus Posch for his technical assistance and expertise offered during OMX microscopy experiments. The use of the OMX microscope was funded by an Medical Research Council Next Generation Optical Microscopy Award (Ref: MR/K015869/1). The Huitema lab is funded by the Biotechnology and Biological Sciences Research Council, the European Research Council and the Royal Society of Edinburgh.

Supplementary data:

Supplementary videos can be found on the CD-ROM attached to this thesis, or accessed online via

http://figshare.com/articles/Characterisation_of_cell_death_inducing_Phytophthora_capsici_CRN_effectors_suggests_diverse_activities_in_the_host_nucleus/787690

Supplementary Video 1-4.

Time-lapse video of cells expressing CRNs or EV control. *N. benthamiana* plants were infiltrated with CRN 20_624 at a final OD of 0.05 and video images captured 48 hours post-infiltration using transmitted light detection. Videos show vesicle movement within the cytoplasm during CRN expression. Video was taken using a 40x water dipping lens and a 3.2x zoom (Scale bar = 20 µm). Video 1: CRN20_624, Video 2: CRN79_188, Video 3 CRN83_152, Video 4 pb7WGF2-Empty vector control.

Chapter 4 . Confirmation of a conserved CRN-target interaction

This chapter is being prepared for submission as:

R Stam , GB Motion, PC Boevink and E Huitema (2013) A conserved oomycete CRN effector targets and modulates tomato TCP14-2. For submission to PNAS.

GBM contributed to developing the chromatin fractionation assay, PCB contributed vectors and insights for microscopy, EH contributed to data analysis

Abstract

CRNs proteins form a large and diverse group of effector proteins in *Phytophthora* spp. They are translocated into the host cell and thought to perturb many different nuclear processes, however confirmation of direct interaction partners is missing.

Genome-wide interaction studies in *Arabidopsis thaliana* revealed transcription factor TCP14 as a potential virulence target for effectors from multiple species. Here we show that a conserved CRN effector from *P. capsici* directly binds to tomato transcription factor TCP14-2. Binding of the CRN to the TF causes dissociation of the TF from the DNA as seen by altered nuclear localisation and disappearance of the protein from a chromatin associated protein fraction. We confirm that TCP14-2 has a role in enhancing resistance to *P. capsici* and that CRN12_997 is able to overcome this resistance.

This is the first demonstration of a direct CRN effector target and CRN mode of action *in planta*.

Introduction

Filamentous plant pathogens, including oomycetes, are ranked amongst the greatest threats to plants, animals and ecosystems (Fisher *et al*., 2012). Amongst the oomycetes, *Phytophthora infestans* and *P. sojae* form major threats to potato and soybean production respectively (Tyler, 2007; Fry, 2008). Recent years has seen the emergence of a wide range of *Phytophthora* species which collectively, not only affect an increasing range of crops but also devastate trees and shrubs, damaging important ecosystems and woodlands (Rizzo *et al*., 2002; Brasier *et al*., 2005). *P. capsici* has now been reported on dozens of valuable crops, including cucumber and tomato (Hausbeck and Lamour, 2004; Granke *et al*., 2012). Given that *Phytophthora* progresses through multiple disease cycles within a growing season, epidemics often become explosive under optimal conditions. There is a critical need to understand (conserved) *Phytophthora* virulence strategies.

Phytophthora spp are hemi-biotrophic pathogens. Infection features an early biotrophic stage, during which host tissue appears healthy, followed by a necrotrophic phase marked by cell death and tissue collapse. Infection is coupled to massive transcriptional changes in both host and pathogen (Jupe *et al*., 2013). Understanding the drivers of these changes will help to understand virulence and defence strategies in general.

Given that plants are exposed to diverse microbial communities, they must fend off potential pathogens during their lifecycle. Besides preformed barriers, contemporary models describe a plant immune system that can be activated upon perception of Pathogen Associated Molecular Patterns (PAMPs) by Pattern Recognition Receptors (PRRs). Ligand binding and perception leads to activation of complex signalling cascades, cellular defences and transcriptional reprogramming, important events leading to Pattern Triggered Immunity (PTI) and resistance to most microbes (Nicaise *et al*., 2009).

Plant pathogenic microbes are specialised organisms that have acquired and evolved the ability to suppress host immunity. Genome sequencing, functional genomics and

detailed biochemical analyses have helped identify pathogen encoded secreted proteins (effectors) that are delivered inside host tissues to perturb host processes and enable Effector-Triggered Susceptibility (Jones and Dangl, 2006; Hogenhout *et al*., 2009).

With numerous candidate effector proteins identified and described in most sequenced pathogens or pests, effectors are generally divided in two major subgroups based on their site of action (Oliva *et al*., 2010; Koeck *et al*., 2011). Intracellular effectors are delivered into the host cell to modulate cell processes (Birch *et al*., 2009; Howden and Huitema, 2012), whereas apoplastic effectors remain in the intracellular space and inhibit the activity of lytic enzymes, help detoxify or degrade preformed (chemical) barriers and prevent perception (Misas-Villamil and van der Hoorn, 2008; Bozkurt *et al*., 2011, 2012).

Intracellular oomycete effectors are modular proteins featuring a signal peptide followed by conserved N-terminal protein regions carrying motif(s) specifying translocation. RxLR effectors carry an Arg-x-Leu-Arg motif, whereas CRNs carry an LFLAK-motif (Leu-Phe-Leu-Ala-Lys) in their N-terminus (Schornack *et al*., 2009, 2010). CRNs are thought to be more ancient than RxLR effectors because, they are found in all plant pathogenic oomycetes sequenced to date (Tyler *et al*., 2006; Gaulin *et al*., 2008; Haas *et al*., 2009; Levesque *et al*., 2010; Links *et al*., 2011; Lamour *et al*., 2012a), whereas RXLRs are only found within the Peronosporales lineage. Similarly, CRN N-terminal regions, along with some of their C-terminal counterparts, are highly conserved amongst plant pathogenic oomycetes, suggesting distinct but important roles in oomycete biology. In addition to conserved CRN effector domains, comparisons between oomycete CRN effector domain inventories have also revealed dramatic expansion in the *Phytophthora* lineage. With a diverse and expanded C-terminal domain repertoire present in sequenced *Phytophthora* genomes, diversification occurred relatively late in oomycete evolution and has been suggested to be linked to incorporation of a necrotrophic phase in the life cycle (Stam *et al*., 2013b).

Although CRN effectors are commonly found in plant pathogenic oomycetes, little is known about their contribution towards virulence. Localisation of CRN C-termini in plants revealed that a diverse array of effector domains from a wide range of oomycetes, accumulate in nuclei. Some CRN domains cause cell death and chlorosis phenotypes in plants, suggesting perturbation of cellular processes by the effector activities carried by CRN C-termini (Liu *et al*., 2011; Shen *et al*., 2013; Stam *et al*., 2013a, 2013b). More detailed analyses revealed that the accumulation of the *P. infestans* CRN8 effector domain in the nucleus is required for cell death. Subsequently, CRN8, was shown to possess kinase activity *in planta*; confirming the presence of functions that could contribute to the infection process (van Damme *et al*., 2012).

To understand *Phytophthora* virulence strategies, or more specifically, understand the role(s) of effectors towards parasitism, the identification of their host targets represents the most critical step. Consequently, recent efforts have focussed on target identification and subsequent studies on the host processes affected, which in some cases have unveiled molecular events underpinning immunity and susceptibility in new detail.

A matrix two-hybrid screen using effector proteins from oomycete *Hyaloperonospora arabidopsidis* and *Pseudomonas syringae*, against a large protein set from *Arabidopsis thaliana* demonstrated that effector arsenals encoded by diverse pathogens, share common host targets. Furthermore, common host targets often formed important 'hubs' in the Arabidopsis immune network, suggesting that pathogens shaped their effector repertoires to target important regulators and suppress immunity during infection (Arabidopsis-Interactome-Mapping-Consortium, 2011; Mukhtar et al., 2011). One such example is the Arabidopsis transcription factor TCP14 (for TEOSINTE BRANCHED1, CYCLOIDEA, PROLIFERATING CELL). TCP transcription factors form a large family of transcription factors with a DNA binding basic helix loop helix domain, dubbed the TCP domain (Kosugi and Ohashi, 1997).

TCP14 plays various roles in plant growth and development (Cubas *et al*., 1999; Kieffer *et al*., 2011; Steiner *et al*., 2012a, 2012b) although more recently, other TPC-family members were implicated in plant immunity. Phytoplasma Aster Yellows, strain Witches' Broom (AY-WB), effector SAP11 destabalises CINCINNATA (CIN)-related TCPs. This destabilisation of CIN-TCPs leads to reduced JA response and enhanced reproduction of its insect vector Macrosteles quadrilineatus, thus benefiting the spread of the phytoplasma (Sugio *et al*., 2011). Chandran *et al.* (Chandran *et al*., 2009) suggest that TCPs might play a role during infection of Powdery Mildew Golovinomyces orontii. Finally, AtTCP14 was identified as a major hub targeted by *H. arabidopsidis* and Ps. syringae effectors (Arabidopsis-Interactome-Mapping-Consortium, 2011; Mukhtar *et al*., 2011), suggesting that diverse pathogens have independently evolved the ability to target important host proteins to suppress immunity.

Here we show that *Phytophthora capsici* CRN12_997 interacts with tomato transcription factor SlTCP14-2. Previously, it was shown that three HaRXLCRN effectors, harbouring both an RxLR and LFLAK motif in their N-termini, interact with the *A. thaliana* transcription factor AtTCP14 in yeast. We expanded on this observation and showed that a conserved *P. capsici* CRN effector interacts and affects the function of SlTCP14-2. Over-expression of SlTCP14-2 enhances immunity to *P. capsici*, a phenotype that can be reversed upon co-over-expression of CRN12_997 but not by the related effector CRN125_11. Consistent with a function that alters SlTCP14-2 function, CRN12_997 binds its target inside plant cells and causes SlTCP14-2 re-localisation in the nucleoplasm and nucleolus, which ultimately leads to degradation of TCP14-2. These results indicate that a specific effector-target interaction is present in two divergent oomycetes, suggesting that conservation of ancient host-target interactions underpin common virulence strategies in pathogens.

Methods

Homologies and alignments

HpaRXCRN sequences were obtained from work published by Mukthar *et al.* (Mukhtar *et al*., 2011). Tomato homologues for AtTCP14-4 and possible *P capsici* homologues were identified using BLASTn and selecting Reciprocal Best Blast Hits. Genes were amplified from cDNA made from *P. capsici*-infected tomato tissue. The domain structure of Hpa effectors was analysed using the methods described previously (Stam *et al*., 2013b) to confirm that the domain structure of Hpa and Pc effectors was identical. Subsequently all other CRNs with similar domain structure were extracted from Haas *et al* (2009). Sequences were truncated after the DWL domain and aligned using MUSCLE (Edgar, 2004). A maximum likelihood tree was created with PhyML and visualised with TreeDyn, using the phylogeny.lirmm.fr webserver. A conserved motif was drawn using jalview (Waterhouse *et al*., 2009). TCPs were aligned using MUSCLE.

Tomato TCP expression data was obtained from Microarray data generated from a *Phytophthora capsici*-tomato time course infection experiment using a custom Agilent 60-mer oligonucleotide microarray from predicted *P. capsici* (LT1534 v11.0)(Lamour *et al*., 2012a) and *Solanum lycopersicum* (ITAG 2.3) sequences (Tomato-Genome-Consortium and consortium, 2012; Jupe *et al*., 2013; Stam *et al*., 2013b).

Transient expression and localisation

For co-localisation, GFP-fusions of CRN C-termini were constructed using the pB7WGF2 vector and RFP-fusions were constructed for TCP genes using pGWB461. The constructs were transformed into *Agrobacterium tumefaciens* strain AGL1. Transformants were grown on LB medium containing Rifampicin and Spectinomycin to maintain the plasmids. For each construct, a single colony was grown overnight in liquid culture and resuspended in infiltration buffer (10 mM MgCl, 150 µM Acetosyringone) to an optical density at 600 nm (OD600) of 0.1 for confocal microscopy or 0.5 for co-immunoprecipitation and disease complementation assays.

The buffer was mixed 1:1 with buffer containing *Agrobacterium* carrying the TBSV silencing suppressor P19 and infiltrated into four to five week old *N. benthamiana* leaves. For Split YFP, CRN and TCP constructs were made using pCL112 and pCL113 vectors (Bos *et al*., 2010) and transiently expressed by AGL1 infiltration at an OD600 of 0.01. Plants were grown in a glasshouse under 16 hours light and temperatures of 26 °C by day and 22 °C by night

Confocal Microscopy

N. benthamiana leaves transiently expressing the construct of interest were harvested for microscopy 2 days after infiltration. To maintain cell viability and improve optical properties after detachment, the leaves were infiltrated with water before mounting on a microscope slide. Leaf samples were imaged using a Leica SP2 confocal microscope. Peak excitation/emission wavelengths were 488/509 nm for GFP, 561/607 nm for tagRFP and 514/527 nm for YFP.

Co-IP and western blot

Plant tissues were harvested at 3 dpi. Protein extractions were done using GTEN buffer (10% Glycerol, 25 mM Tris, 1 mM EDTA, 150 mM NaCl) supplemented with 2% PVPP, 10 mM DTT and 1X Complete protease inhibitor cocktail (Thermo Scientific). MG132 treatment was done by infiltrating 10 nM aqueous solution of MG132 into the leaves 4 hours prior harvesting. Samples were pulled down using antiFLAG M2 agarose (Sigma) or strepII-tag magnetic beads (Schmidt *et al*., 1996) (IBA GmbH) and run on 4-20% TGX PAGE gels (Biorad) before transfer to PVDF membranes using a Biorad Transblot system. Blots were blocked for 30 minutes with 5% milk in TBS-T (0.1% tween), probed with mouse anti-FLAG antibodies (Santa Cruz Biotech)(1:4000), StrepII-HRP antibody (Genscript)(1:5000) or mouse anti GFP antibody (Santa Cruz) (1:5000) in 5% milk in TBS-T. FLAG and GFP blots were secondarily probed with anti Mouse-HRP antibodies (1:20.000). All blots were washed 3-4 times in TBS-T for 5 minutes before incubation with Millipore Luminata Forte substrate. Blots were imaged on a Syngene G:BOX XT4 Imager. Average intensities of protein bands were measured in ImageJ.

Chromatin fractionation

Tagged candidate proteins were overexpressed in *N. benthamiana* as described above. Leaves were harvested and ground under liquid nitrogen 3 days post infiltration. Ground leaf tissue was suspended in 10 ml ice cold Buffer A (10 mM PIPES pH6.8, 10 mM KCl, 1.5 mM $MgCl_2$, 340 mM Sucrose, 10% glycerol, 0.5% Triton X-100, (1 mM DTT) and 1X SIGMAFAST protease inhibitor cocktail (Sigma)) and filtered through Miracloth (Calbiochem). A 6 ml aliquot of this whole-cell extract was taken and centrifuged at 3000g for 10 minutes at 4 °C. 500 µl of supernatant was suspended in loading buffer as soluble (S1) fraction. 1 ml of TCA-A (10 ml acetone, 2 ml TCA, 8 µl β-mercaptoethanol) was used to resuspend the pellet, containing chromatin bound proteins (P1). After brief vortexing, these samples were stored for 1 hour at -20 °C. Samples were centrifuged at 16000g for 30 minutes at 4 °C and the resulting pellets were washed 3 times with acetone/β-mercaptoethanol (10 ml acetone with 0.1% β-mercaptoethanol) before resuspending in SDS loading buffer.

Disease complementation assays

Leaves were harvested 3 days after infiltration and collected in 1.5 cm deep collection trays containing wet tissue paper. *P. capsici* strain LT1534 was inoculated as 10 µL droplets of zoospore solution (500,000 spores per mL). The trays were stored in an incubator under 16 hours light and at 26 °C by day and 22 °C by night. Lesion diameters were measured 2 days post inoculation as previously described (Rodriguez *et al*., 2013; Stam *et al*., 2013b)

Results

CRN effectors may target the nuclear host transcription factor TCP14

Previously, we reported that the CRN effector repertoire is widespread amongst plant pathogenic oomycetes and that a subset of these CRN effector domains is present in most sequenced genomes (Stam *et al*., 2013b). This observation raises the possibility that these conserved effectors share targets in diverse hosts. Recently, a large-scale yeast two-hybrid matrix led to the identification of the Arabidopsis TCP14 transcription factor as a candidate target for three *Hyaloperonospora arabidopsidis*

DXX domain containing effectors. The DXX C-terminal domain is among the most ancient domains as it is found in 8 out of 10 other examined Oomycetes and predates the emergence of the peronosporales lineage. We have identified and characterised the *P. capsici* CRN repertoire (Stam *et al*., 2013b). Amongst our set of 84 predicted full-length CRN proteins, two effectors featuring a DHB-DXX-DHA domain configuration were identified (Figure 4.1A). Pairwise comparisons between both PcCRN12_997 and PcCRN125_11 and their possible *H. arabidopsidis* counterparts (HaRxLCRN4, 14 and 17), revealed 41% sequence identity in alignments between DXX domains.

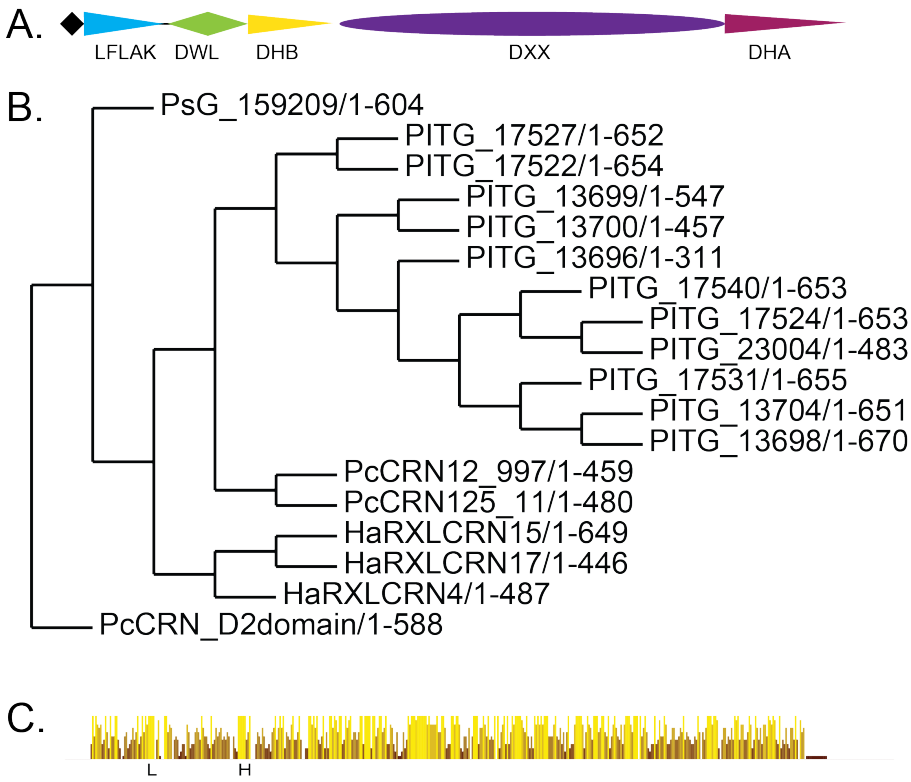

Figure 4.1 Overview of DHB-DXX-DHA containing CRNs

A) Diagram showing domain structure for the CRN effectors used in this study. These CRNs contain a signal peptide (black diamond), two highly conserved N-terminal domains and three C-terminal domains. B) Phylogenetic reconstruction of DHB-DXX-DHA domain containing CRNs, based on maximum likelihood clustering of the C-terminal domains using 100 bootstraps. C) Conservation motif for DHB-DXX-DHA domain containing Hpa and PcCRNs. Bright yellow bars show highly conserved regions (80% similarity – 100% identical), darker bars are more divergent. LFLAK and HVLVVVP domain are indicated with L and H respectively.

To assess relationships between CRN DXX domains in different species, we made a phylogenetic reconstruction of the C-terminal domains. This shows that CRN coding genes group together in species-specific clusters (Figure 4.1B) and confirms that these genes arose before speciation in the peronosporales. If CRN-target interactions are both ancestral and preserved, this could suggest that *P. capsici* CRN12_997 or CRN125_11 binds AtTCP14 orthologs during infection of its hosts.

Given that AtTCP14 (AT3G47620.1) may constitute a hub in the plant immune signalling network, targeted by pathogen effectors, we asked whether this protein has orthologs in tomato. Blast analyses identified two putative tomato orthologs of AtTCP14, which we named SlTCP14-1 and SlTCP14-2. Both share high sequence similarity with AtTCP14, though both proteins are more similar to each other than to AtTCP14 (Figure 4.2). Both tomato TCP proteins contain the highly conserved Helix-loop-Helix motif, including the conserved Cysteine at the start of the first helix, that characterise class I TCP proteins (Viola *et al*., 2013), like AtTCP14 (Figure 4.2A). To learn more about SlTCP14 gene expression, we examined microarray data from a *P. capsici* infection time course on tomato (Jupe *et al.* 2013). These data show that both SlTCP14-1 and SlTCP14-2 are expressed in tomato but down regulated in the early infection time points (Figure 4.2B). Intriguingly, these changes of gene expression coincide with the expression of DXX-domain containing CRNs as reported previously (Jupe *et al*., 2013; Stam *et al*., 2013b). These results suggest that SlTCP14-1 and SlTCP14-2 may form important host targets whose expression is repressed during the interaction with *P. capsici*.

BiFC shows specific YFP reconstitution phenotypes with CRN12_997 and SlTCP14-2

Given the presence of orthologous sequences for both *H. arabidopsidis* effectors and their putative target in *P. capsici* and tomato respectively, we aimed to test whether CRN12_997, CRN125_11 and both SlTCP14 proteins can interact *in vivo*. Bimolecular Fluorescence Complementation (BiFC) experiments, in which we co-expressed candidates fused to the N-terminal half of YFP (pCL112::CRN) and YFP C-terminus (pCL113::TCP) led to the specific accumulation of YFP signal in nucleoli for

Figure 4.2 TCP transcription factors and expression patterns

A) MUSCLE alignment of AtTCP14 and two tomato homologues. Levels of similarity are shown in purple (dark = high similarity). Underlined are the conserved basic region, boxed the helices of the Helix Loop Helix motif. Conserved functional Cysteine is marked with * B) Microarray expression data for tomato TCP14 candidates.

CRN12_997 and SlTCP14-2. We found low levels of YFP signal in the nucleoplasm for other CRN-TCP combinations (Figure 4.4). Given hat we found YFP signal in multiple treatments, we assessed the level of specificity between CRN12_997/CRN125_11-SlTCP14 combinations. For this purpose, we counted the number of fluorescent nuclei in all our treatments (Figure 4.4). These analyses revealed that in addition to specific localisation in the nucleolus, CRN12_997 and SlTCP14-2 co-expression led to a higher number of fluorescent nuclei (with YFP signal in the nucleolus) when compared to other combinations (Figure 4.4E).

To test whether differences in signal intensities were due to stability or levels of fusion proteins, we performed western blots (Figure 4.3). Although we found great differences in protein abundance levels between the two CRN fusions, these do not correlate with the differences in YFP signal between BiFC treatments. Taken together these observations thus show that there is strong reconstitution of YFP fluorescence specifically with CRN12_997 and SlTCP14-2 treatments, suggestive of an interaction between these proteins *in vivo*.

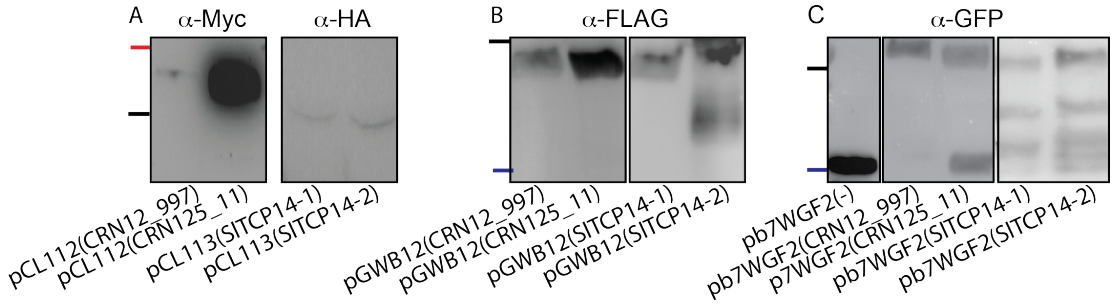

Figure 4.3 Confirmation of stable expression of fusion proteins

A) Fusion proteins for BiFC microscopy. B) FLAG-tagged proteins for phenotyping and co-immunoprecipitation. C) GFP-tagged proteins used for phenotyping and co-immunoprecipitations. Red, Black and Blue lines indicate 70, 50 and 25 kDa, respectively.

CRN12_997 and SlTCP14-2 are both present in a protein complex

To confirm our BiFC results we performed co-immunoprecipiation experiments using FLAG-tagged SlTCP14-2 and strepII-tagged GFP-CRN fusion proteins. SlTCP14-2 was co-expressed with CRN12_997 and CRN125_11 fusions in N. benthamiana after which complexes were purified from total leaf extracts by using Mag-strep and FLAG M2 magnetic beads. Immunoprecipitation of CRN12_997, CRN125_11 and free EGFP, using strepII specific magnetic beads in the presence of SLTCP14-2, led to a specific TCP signal for CRN12_997 only, suggesting an interaction between the CRN12-997 and SlTCP14-2 (Figure 4.5). Conversely, precipitation of TCP14-2 in the presence of CRN12_997, resulted in the specific detection of CRN12_997 in eluted samples (Figure 4.6), confirming this interaction. From this, we conclude that consistent with our BiFC results, CRN12_997 binds SlTCP14-2.

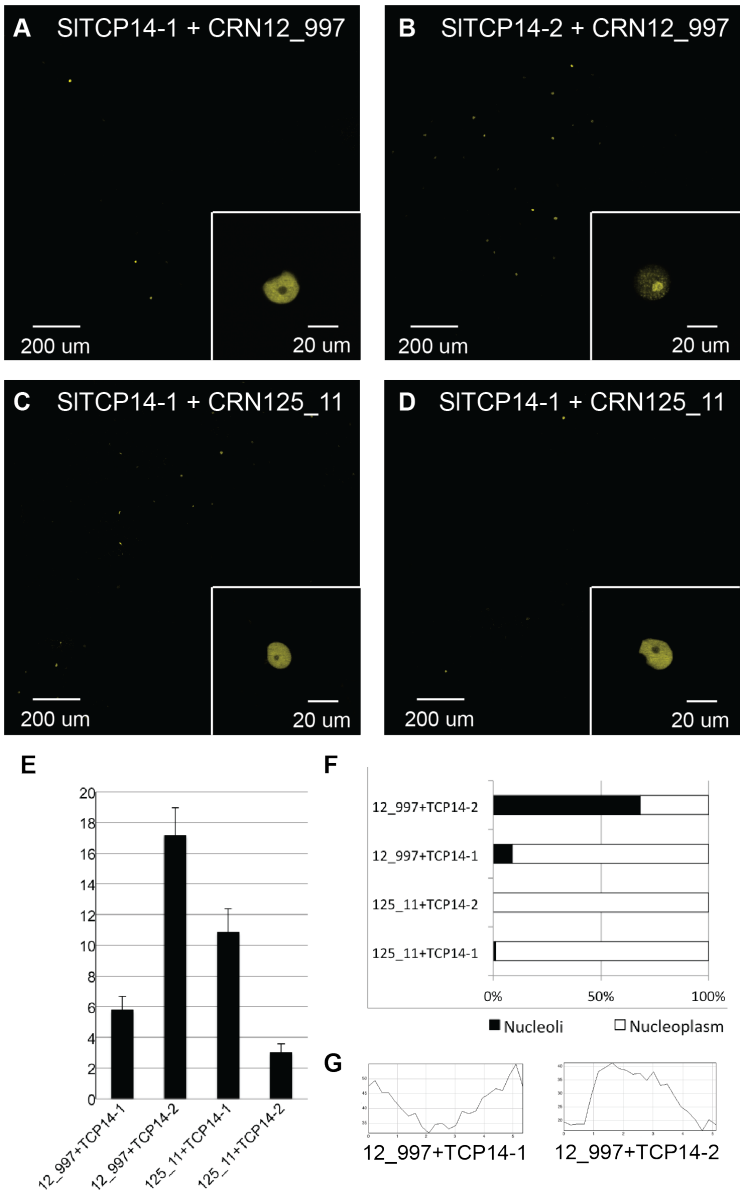

Figure 4.4 Split YFP confirms interaction of SlTCP14-2 and CRN12_997.

A-D) Reconstituted YFP fluorescence is observed in all CRN/TCP combinations, however the number of fluorescent nuclei is significantly higher for CRN12_997+SlTCP14-2 and with this combination reconstitution of fluorescence is observed in the nucleolus (insets). E) Amount of fluorescent nuclei per single slice image. F) Percentage of nuclei with fluorescence observed in the nucleolus. G) Fluorescence intensity profiles for insets of image A and B resp. showing relative higher fluorescence in the nucleolus of inset B.

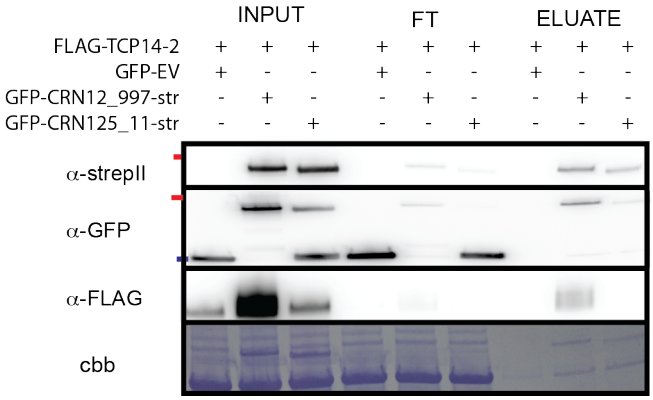

Figure 4.5 Specific interaction between CRN12_997 and SlTCP14-2.

StrepII- and GFP-tagged CRN proteins are present in all input samples and also visible after IP. FLAG-SlTCP14-2 is visible in the input samples and can only be observed in the eluate when CRN12_997 is co-expressed.Red lines indicate 50 kDa, Blue line 25 kDa.

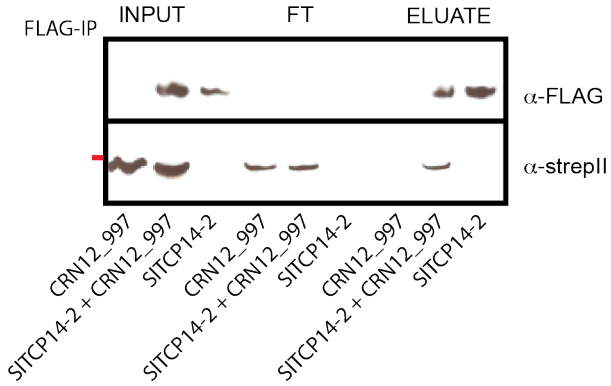

Figure 4.6 Reversed Co-IP of CRN12_997 and TCP14-2

FLAG-IP of FLAG tagged TCP14-2 co-immunoprecipitates Three samples were processed using FLAG antibody beads. CRN12_997 alone, SlTCP14-2 alone and CRN12_997 and SlTCP14-2 together. Flag tagged SlTCP14-2 is visible in the eluate and CRN12_997 co-immunooprecipiates when co-expressed, but does not aspecifically bind to the beads when expressed alone.

SlTCP14-2 contributes to immunity to *P. capsici*

Given that SlTCP14-2 and its *Arabidopsis* ortholog are targeted by CRN12_997 and effectors from both *H. arabidopsidis* and *Ps. syringae* respectively, we asked whether SlTCP14-2 contributes to immunity as was suggested in *Arabidopsis* (Mukhtar *et al.*, 2011). To test for a direct role in immunity, we overexpressed SlTCP14-2 in *N. benthamiana* and infected infiltrated leaf panels with *P. capsici* zoospores as described previously (Stam *et al.*, 2013b). Over-expression of SlTCP14-2 was found to

significantly reduce the growth rate of *P. capsici* in *N. benthamiana* when compared to empty vector controls (Figure 4.7A). This phenotype was specific to SlTCP14-2 as expression of its close tomato homolog, SlTCP14-1, in *N. benthamiana*, did not significantly affect *P. capsici* growth when compared to the empty vector (EGFP) (Figure 4.7A). Furthermore, expression of SlTCP14-2 inhibited *P. capsici* sporulation as sporangia were found to emerge only around SlTCP14-2 three days post infection and in sites expressing EGFP (Figure 4.7C).

CRN12_997 counteracts TCP14-2 induced growth inhibition

Previously, we have shown that when over-expressed *in planta*, CRN12_997 does not significantly enhance *P. capsici* growth. Given that SlTCP14-2 over-expression enhances immunity to *P. capsici*, we hypothesised that endogenous CRN12_997 is normally sufficient to suppress immunity, but high levels of SlTCP14-2 renders endogenous CRN12_997 incapable of suppressing immunity. If true, ectopic expression of CRN12_997 should boost *P. capsici* growth in the presence of high SlTCP14-2 levels.

To test this hypothesis, we co-infiltrated SlTCP14-2 with CRN12_997, CRN125_11 and empty vector combinations, followed by *P. capsici* infection assays. These experiments showed that CRN12_997 over-expression reconstitutes growth. Significant growth enhancement (ANOVA, $p<0.01$) was specific to co-expression of CRN12_997 with SlTCP14-2 as CRN125_11 co-expression was found not to enhance growth in these assays when compared to the control (Figure 4.7B). Importantly and as expected, we found that in the presence of CRN12_997, spore formation is also reconstituted despite over-expression of SlTCP14-2 at three days after infection (Figure 4.7D). To show that these effects are due to the presence of fusion proteins rather then large differences in levels or stability, all constructs were expressed in *N. benthamiana* on multiple occasions and found to be stable when expressed individually (Figure 4.3, Figure 4.5).

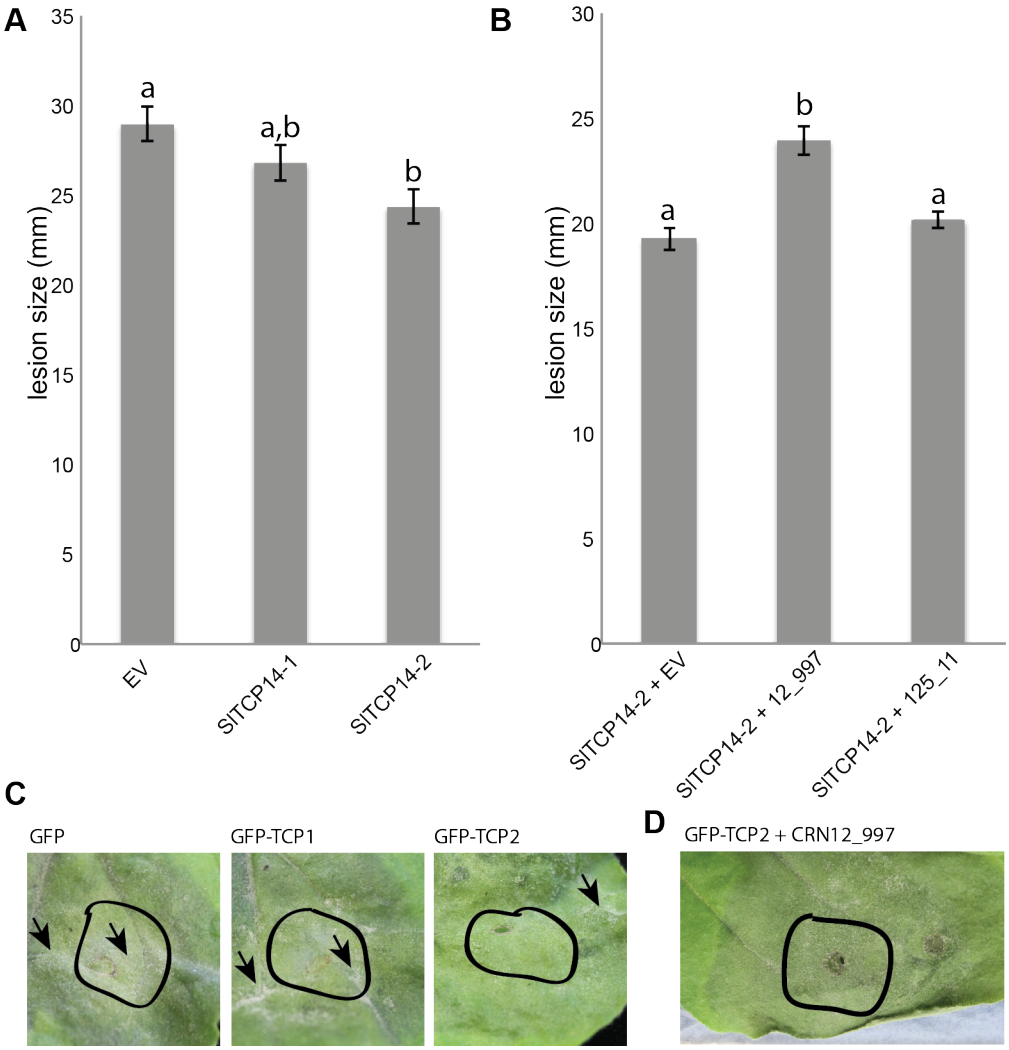

Figure 4.7 Sl-TCP14-2 reduces *P. capsici* virulence, CRN12_997 counteracts

A) Over-expression of SlTCP14-2 in *N. benthamiana* shows a significant reduction in growth compared to over-expression of free GFP (Anova $p<0.01$) SlTCP14-1 shows an intermediate growth reduction. B) Co-expression of SlTCP14-2 with CRN12_997, but not with CRN125_11 partially restores growth retention. C) Expression of SlTCP14-2 delays spore formation, no sporangia (arrowheads) can be observed within the infiltrated site (black line) three days post infection. D) After co-expression of CRN12_997 with SlTCP14-2 sporangia can be observed at 3 dpi

SlTCP14-2 and CRN12_997 co-expression alters localisation of SlTCP14-2

Given that CRN12_997 and SlTCP14-2 localise and interact in the nucleus, we asked whether on the subnuclear level, CRN12_997 and SlTCP14-2 co-localise. To co-localise CRN12_997 and SlTCP14-2, we co-expressed both proteins, fused to EGFP and tagRFP respectively, in *N. benthamiana* and assessed localisation. Expression of SlTCP14-2 together with EGFP (negative control) showed a speckled sub-nuclear

distribution pattern for SlTCP14-2 two days after agroinfiltration (Figure 4.8A-C). Interestingly, co-expression of CRN12_997 with SlTCP14-2 abolished the characteristic speckled subnuclear localisation pattern normally seen for SlTCP14 (Figure 4.8D-F). Co-expression of CRN125_11 contrasted these results as there we no changes in SlTCP14-2 localisation in our experiments (Figure 4.8G-I). Overexpression of CRN125_11 shows background fluorescence in the cytosol, due to cleavage of GFP from the fusion protein, however western blot analysis shows that a significant uncleaved fraction is also present (Figure 4.5). These results suggest that CRN12_997 may interfere with TCP function by altering its subnuclear localisation.

CRN12_997 dissociates TCP14-2 from DNA

TCPs and other transcription factors bind to DNA, where they regulate the expression of their target genes. Given our observations we hypothesised that CRN12_997 interferes with SlTCP14-2 DNA binding properties.

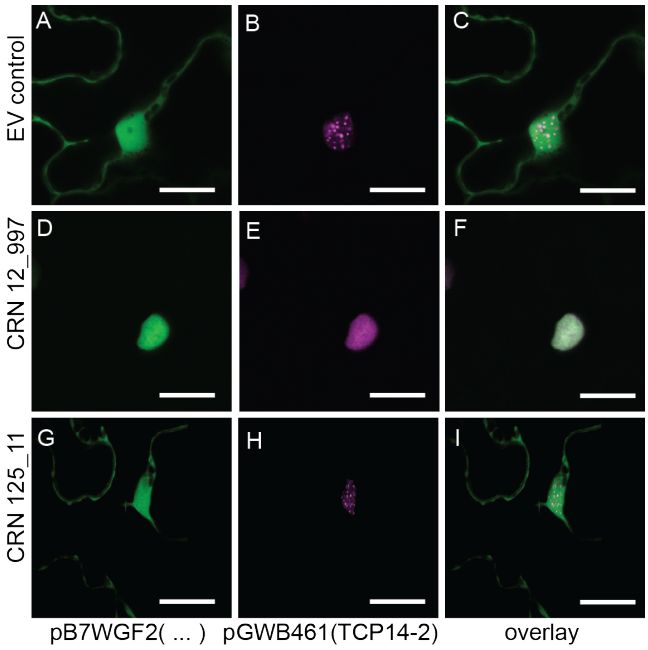

Figure 4.8 Co-expression of CRN12_997 and SlTCP14-2 alters TCP localisation

Over expressed RFP-tagged SlTCP14-2 in *N. benthamiana* plants shows a specific speckled phenotype when co-expressed with an eGFP control (A-C) or non-binding GFPtagged effector CRN125_11 (G-I). Co-expression with GFP tagged CRN12_997 abolishes this pattern. Panels show GFP channel (A,D,G), RFP channel, (B,E,H) or overlay images (C,E,I). Scale bar is 10 um

To test this hypothesis, we over-expressed both constructs in plants and used a chromatin-based fraction separation method. This allows us to separately image a soluble protein fraction and a DNA-associated protein fraction (Figure 4.9). Chromatin fractionation shows that under control circumstances SlTCP14-2 can be seen in the chromatin bound fraction. CRN12_997 can mainly be found in this fraction and CRN125_11 stays mainly in the soluble fraction.

When co-expressed with CRN12_997, TCP14-2 cannot be seen in the chromatin bound fraction any more, suggesting dissociation from the DNA. Unfortunately we cannot see TCP14-2 in the soluble fraction under these circumstances, possibly due to turnover during our fractionation assay.

Viola *et al*. (Viola *et al*., 2013) reported that oxidation alters DNA binding properties of Class II TCPs; TCPs were less likely to associate with DNA under oxidative situations and addition of deoxidising reagents like DTT abolished this effect. We redid our experiment with high DTT concentrations. Under these negative control conditions both CRNs can be found in both fractions and SlTCP14-2 stays in the chromatin bound fraction when co-expressed with CRN12_997 (Figure 4.9), showing that the dissociation of TCP14-2 by CRN12_997 can be prevented if oxidation is inhibited.

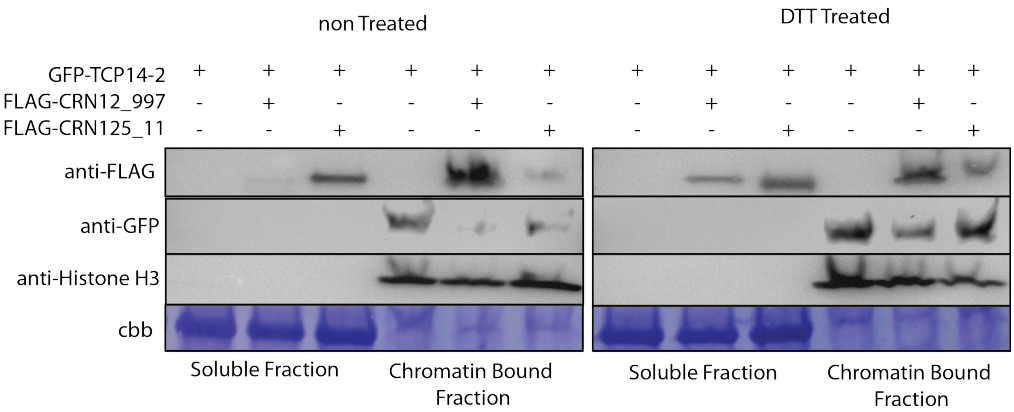

Figure 4.9 CRN12_997 dissociates SlTCP14-2 from the DNA-bound fraction.

In non treated samples, FLAG-tagged CRN12_997 can be seen mainly in the chromatin bound fraction and CRN125_11 mainly in the soluble fraction. SlTCP14-2 can be seen in the chromatin bound fraction when co-expressed with GFP, but is strongly recuded when co-expressed with CRN12_997 and not CRN125_11. DTT treatment prevents oxidation and prevents dissociation of TCPs from the DNA. It also causes more CRN12_997 to be seen in the soluble fraction.

Dissociation of TCP14-2 from DNA ultimately leads to degradation of the protein

Our fractionation assays suggest that SlTCP14-2 is not stable when it is not associated with chromatin, since we cannot detect SlTCP14-2 in the soluble fraction after the assay. To assess whether the dissociation from the chromatin-bound fraction leads to proteasomal degradation, we co-expressed CRN-SlTCP14 combinations and assessed TCP14 steady state levels in total cell extract.

Treatment with proteasome inhibitor MG132 four hours prior to extraction reveals that SlTCP14-2 is indeed subject to proteasomal degradation. Levels of SlTCP14-2 are twice as high in the presence of MG132 than without, confirming that dissociation of SlTCP14-2 by CRN12_997 ultimately leads to degradation of the TF, thus abolishing its role in defence.

Discussion

CRN effectors form a highly diverse class of proteins, however in contrast to other cytoplasmic effectors their C-termini are conserved. Phylogenetic reconstruction shows that some domains predate the split of the peronosporales lineage in the oomycetes (Haas *et al*., 2009; Schornack *et al*., 2010; Thines and Kamoun, 2010; Stam *et al*., 2013b).

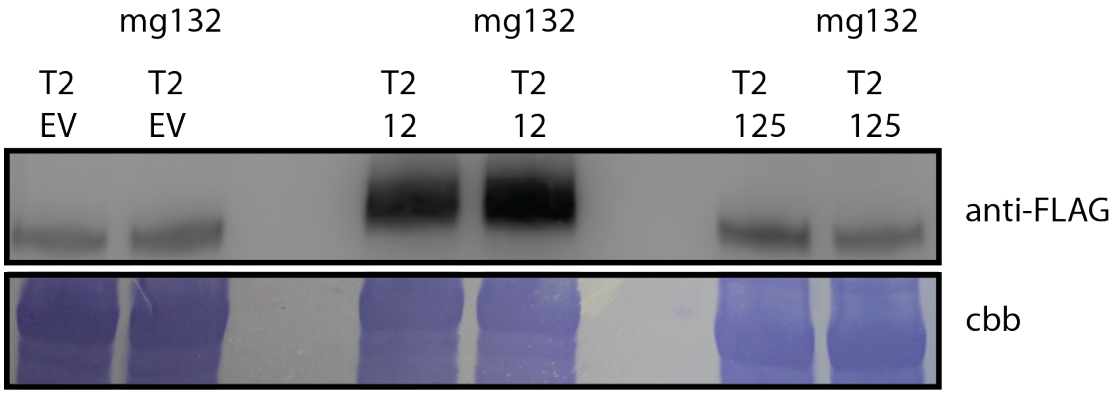

Figure 4.10 TCP14-2 degradation by the proteasome

Flag-tagged TCP14-2 (T2) levels are not affected in pairwise comparisons between water and MG132 protease inhibitor infiltrations when co-infiltrated with EV control or CRN125_11 (125), however intensity differences can be observed when co-expressed with CRN12_997 (12), suggesting that in presence of CRN12_997 TCP14-2 is degraded by the proteasome.

We used this information to gain evidence of CRN-protein interactions, leading to the identification of CRN-AtTCP14 interactions in the literature (Mukhtar *et al*., 2011). In this paper we show the first confirmation of a CRN-plant target interaction *in vivo* with a clear role in immunity.

For a number of oomycete and fungal effectors it has been shown that highly conserved effectors from different species target the same proteins, however in some cases diversifying selection creates host specificity (de Jonge *et al*., 2010; Anderson *et al*., 2012). In addition, it has been shown that also unrelated proteins are capable or targeting the same defence related proteins, as is the case for certain effectors from nematodes, oomycetes and bacteria. These targets form essential hubs in many regulatory processes (Song *et al*., 2009; Mukhtar *et al*., 2011; Lozano-Torres *et al*., 2012).

We have identified highly conserved DHB-DXX-DHA-domain containing CRNs that share homology between *H. arabidopsidis* and *P. capsici.* Phylogenetic reconstruction shows that the Crn genes cluster together based on species, suggesting an ancient common ancestor and important, conserved virulence function.

The *H. arabidopsidis* effectors were hypothesised to target a TCP transcription factor, AtTCP14, which has been characterised as belonging to the hub-proteins that form the most connected nodes in the plant-interactome network, so-called hub50 proteins. Additionally, plants without AtTCP14 show reduced resistance to *H. arabidopsidis* (Mukhtar *et al*., 2011), however a direct observation of an effector targeting the hub had not been shown.

We found two gene homologues for both effector and target genes in our *P. capsici*-tomato pathosystem and used BiFC to define which combination of genes is interacting. This method revealed the interaction of CRN12_997 with StTCP14-2, which could be confirmed with Co-IP. Our data further show that over-expression of the host target TCP14-2 significantly delays infection and sporulation.

Together these findings confirm the hypotheses that pathogens evolved effectors to target key hubs in their host and that these interactions are crucial throughout

evolution. We know that upon *P. capsici* infection large transcriptional changes take place in tomato, both on early infection as well as in later at the switch to necrotrophy (Jupe *et al*., 2013). Targetting of key plant hubs by pathogen effectors tells us that these changes are not merely the plants response, but also actively pursued by the pathogen. Consequently, this emphasises the need to move to a systems biology approach in plant-pathology to fully comprehend the complex interaction changes upon infection (Pritchard and Birch, 2011).

Co-localisation and chromatin fractionation of *N. benthamiana* over-expressing both CRN and target, shows that CRN12_997 interferes with TCP14-2 localisation. Unchallenged SlTCP14-2 localises in nuclear speckles, which are generally assumed to be particles that have a role processing and splicing of pre-mRNA in both mammals and plants. A number of TF has been confirmed to localise to these speckles (Spector and Lamond, 2011; Reddy *et al*., 2012). Co-expressed with CRN12_997, but not with CRN125_11, localisation diffuses and SlTCP14-2 dissociates from the chromatin-bound fraction of our protein extract. A small number of DNA binding domains has been predicted in effectors of bacteria (Boch and Bonas, 2010) and one fungal pathogen possibly binds DNA (Wang *et al*., 2007). However this is, to our knowledge, the first time that effectors from plant pathogens are shown to interfere with DNA binding properties of its target. The altered DNA binding properties of hub50 TFs are likely to be the cause for a whole range of transcriptional changes observed in tomato upon infection and major cause for enhanced virulence of the pathogen.

Acknowledgements

The authors would like to thank all Huitema lab members and prof Paul Birch for discussions of the manuscript. The Huitema lab is funded by the Biotechnology and Biological Sciences Research Council, the European Research Council and the Royal Society of Edinburgh

Chapter 5 . *De novo* identification of CRN effector targets

R Stam, AJM Howden, E Rijke and E. Huitema Unpublished work

AJMH contributed to preparation of mass spec samples; ER contributed to sample preparation and (sub)cloning of putative targets; EH contributed to data analysis

Abstract

Large numbers of CRN effectors are secreted by *P. capsici* upon infection of a host plant. CRNs are a large class of translocated nuclear effectors. Sequence diversity within the class suggests diverse roles for CRNs during infection. Previous work has shown that overexpression of different CRN effectors *in planta* has different effects: A small subset of predicted CRN proteins directly enhances virulence while others induce a hypersentitive response; the majority show no strong effect. Three necrosis-inducing CRN effectors show very different kinetics and subnuclear localisation. So far targets for CRN effectors are largely unknown.

We use both Yeast 2 Hybrid and co-immunoprecipitation-based approaches to identify new targets for CRN effectors. Our results demonstrate four CRN effectors have quite distinct putative targets: transcription factor Ethylene Response Factor 1 (ERF1), core histone H4 (His4), Glyceraldehyde 3'-phosphate dehydrogenase (GAPDH) and Mediator of RNA polymerase II, Fibrillarin 2 (FIB2). Interestingly, all these targets can be linked to transcriptional reprogramming of host cells, suggesting a common characteristic of CRN effectors during infection.

Introduction

Filamentous and bacterial pathogens secrete large numbers of effector molecules upon infection of their host (Stavrinides *et al*., 2008; Hogenhout *et al*., 2009; Stergiopoulos and de Wit, 2009; Oliva *et al*., 2010). These effectors come in many varieties. Generally effectors are secreted into the host cell to either prevent PTI or ETI, or to modify the host cell machinery to enable infection (Ellis *et al*., 2009). Effectors are thought to be partly responsible for the massive transcriptional changes seen upon infection (Jupe *et al*., 2013).

Notable examples of effector classes are TAL effectors from Xanthomonas, for their specific DNA-binding properties that have made them valuable for biotechnology applications (Kay and Bonas, 2009), and cytoplasmic RxLR effectors from Oomycete species, as these are highly abundant and form arguably the best studied effector class in filamentous pathogens (Morgan and Kamoun, 2007; Birch *et al*., 2008, 2009).

For large numbers of effectors, virulence activity has been shown. However, to unravel function and mode of action in the cell it is important to identify the host proteins targeted by effectors. Only a limited number of target proteins and effector functions have been identified.

Most knowledge on effector function emanates from bacterial effectors. Bacteria carry typically 20-30 secreted effectors on their genomes and a number of enzyme activities have been shown for them including: protease activity, E3 ligase activity, ADP-ribosyl transferase activity, and phosphothreonine lyase activity (Hann *et al*., 2010). Avr-PtoB, for example, has E3 ligase activity that ubiquitinates and leads to degradation of Fen, a tomato Pto-like receptor (Rosebrock *et al*., 2007).

In fungi, *Cladosporium fulvum* effector Epc6 masks chitin oligosaccharides to bind and block the chitin receptor LysM (de Jonge *et al*., 2010). *C. fulvum* Avr2 targets a tomato protease Rcr3, a gene under diversifying selection, which is required for resistance mediated by R-gene Cf2 (Rooney *et al*., 2005; Shabab *et al*., 2008). Interestingly, oomycete *P. infestans* effectors EPIC1 and EPIC2B and nematode *Globodera rostochiensis* Gr-VAP1 also target Rcr3. However, in the case of *P. infestans* this does not lead to Cf2-mediated resistance (Song *et al*., 2009; Lozano-

Torres *et al*., 2012). *P infestans* secretes another effector Avr-blb2, which targets another cysteine protease, C14 (Bozkurt *et al*., 2011).

AvrPiz-t from *Magnapother oryzae* targets a RING E3 Ubiquitin ligase, APIP6, and by doing so suppresses PTI in rice (Li *et al*., 2009). Another E3 Ligase, CMPG1 is targeted by Arv3a from *P infestans* which is involved in R3a-mediated defence responses (Bos *et al*., 2010). *P. infestans* Avr2 targets BLS1, which activates the R2-mediated defence response (Saunders *et al*., 2012a).

Most effector interactions that have been characterised localise outside the plant cell nucleus. Avr3a/R3a relocates to endosomal compartments (Engelhardt *et al*., 2012), Rcr3, C14 and the effectors that target it are secreted into the apoplast and localise around haustoria and Avr2 accumulates at the haustoria of infecting *P. infestans* when expressed in the plant cell (Rooney *et al*., 2005; Song *et al*., 2009; Saunders *et al*., 2012a). However, recently it has become evident that the nucleus plays a key role in immunity (Deslandes and Rivas, 2011). 66% of RxLR effectors in *Hyaloperonopsora arabidopsidis*, an oomycte pathogen of *Arabidopsis thaliana*, localise to the nucleus (Caillaud *et al*., 2012a) and similar observations have been made in *P. infestans* (Boevink *et al*., 2011). Therefore it is likely that many of them are targeting nuclear processes.

CRN effectors form a second large and diverse class of intracellular effectors in oomycetes (Haas *et al*., 2009; Schornack *et al*., 2010). Interestingly, the CRNs are also the only large class of effectors that exclusively localise to the nucleus (Chapter 2). Unfortunately, not much is known about the mode of action of CRN proteins. PiCRN8 has a kinase function when over-expressed *in planta*. To be fully functional it forms a dimer *in planta*. Interestingly mutations in the kinase domain still lead to induction of necrosis (van Damme *et al*., 2012). PcCRN12_997 does not show an enhanced virulence when over-expressed *in planta*, but reconstitutes growth when co-over-expressed with tomato (*Solanum lycopersicum)* TCP14-2 (Chapters 2 and 4), a TF of which a homolog in *Arabidopsis thaliana* is known to be involved in defence response (Mukhtar *et al*., 2011). Co-expression of SlTCP14-2 with CRN12_997 in *N. benthamiana* results in relocalisation of SlTCP14-2 due to dissociation of a chromatin

bound protein fraction (Chapter 4). In this chapter we will try to identify additional host target molecules for a selection of CRN effectors. Initially we will focus on three necrosis inducing CRNS (Chapters 2 and 3) and three CRNs that do not cause HR, including CRN12_997.

The two most used methods to detect protein-protein interactions are Yeast 2 Hybrid (Y2H) and Co-immunoprecipitation combined with Mass Spectrometry. In a Y2H experiment a single protein is expressed in yeast (the bait) and screened against a whole library of possible interactors (the prey). Bait and prey are coupled to different reporter genes and by using selection media and other reporter assays, putative protein-protein interactions can be identified.

Co-immunoprecipitation (Co-IP) relies on over-expression of a tagged effector protein *in planta*. Proteins are extracted and the effector is purified using immunoprecipitation. This purified extract should contain the effector protein and any protein that binds to it. To identify the co-immunoprecipitated proteins, the sample is submitted for mass spectrometry (Have *et al*., 2013).

Both approaches have been successful for plant-pathogen interactions. A combination of Y2H and Co-IP confirmed the interaction between Avr2 and BSL1 (Saunders *et al*., 2012a). Co-IP has also been used to identify putative interactors with BAX INHIBITOR-1, a protein involved in cell death regulation in *Nicotiana benthamiana*, in order to find out more about regulatory mechanisms *in planta* during infection (Weis *et al*., 2013).

Materials and methods

Y2H assay

Proquest Yeast 2 Hybrid assays were performed according to the manufacturers' manual (Invitrogen, USA). pENTR1A plasmids containing CRN C-termini were recombined with destination vector pDEST32 (Invitrogen, USA) using GATEWAY technology to create our bait plasmids. A prey library, containing potato cDNA was kindly provided by Miles Armstrong. To confirm interactions we grew the putative

interactor clones on triple drop out media lacking histidine or uracil and performed an X-gal assay according to the Proquest manual. Putative interactors (growing on at least triple drop-out medium (–LTH, up to 25 mM 3AT)) were isolated; plasmids were extracted and transformed in E. coli to allow isolation, propagation and sequencing of prey plasmids. Selected candidate plasmids were co-transformed back into yeast together with the original bait plasmid to confirm the interactions. To try to confirm weaker interactors we also used oNPG (Engelhardt, pers comm.) and CRPG (Proquest2hybrid manual, Invitrogen) quantitative interaction assays.

(Co)-Immunoprecipitation

StrepII-tagged CRN entry clones were recombined in the pB7WGF2 destination vector, a C-terminal GFP tagging vector suitable for protein expression *in planta* using *Agrobacterium tumefaciens*. Leaf tissue was harvested 3 days post infiltration with *Agrobacterium* using a GTEN extraction buffer as described in Chapter 2.

To test for expression and stability, we performed western blot analysis. 12 µL of leaf extract was loaded on SDS gels and blotted on PVDF membrane. The membranes were incubated overnight with antiGFP antibody (1:5000) followed by anti-Mouse-HRP (1:40.000, Santa Cruz Biotech, USA) in 5% milk. Bands were visualised using Milipore Forte Chemiluminescent substrate and detected using a Biorad Geldoc imager or Syngene G:BOX4. Coomassie briliant blue staining was done using Thermo Scientific imperial blue protein stain.

Mass Spectrometry

Co-immunoprecipitation was done using Chromotek GFP trap M, magnetic beads coated with anti GFP antibody. Immunoprecipitation was done according to the manufacturers guidelines and boiling magnetic beads for 5 minutes at 95 degrees released the proteins from the beads. Three biological reps were made for each CRN candidate.

Eluates were loaded onto biorad precast SDS-PAGE gels and run approximately 3 cm into the gel. Lanes were cut into two fractions. Each fraction was individually prepared for Mass Spec analysis. Gel pieces were washed with 100mM

NH_4HCO_3:100%ACN (10 min), aggregated in 100% ACN and again washed with 100mM NH_4HCO_3:100%ACN. After drying, pieces were incubated in 10mM DTT (45 min), before treatment with 5mM iodoacetamide (30 min in the dark). After washing with 100mM NH_4HCO_3:100%ACN (2x), pieces were digested overnight with 20 µL trypsin (0.1 g/ L in 50mM NH4HCO3). After digestion, pieces were washed in 0.05% TFA /50% ACN, sonicated (15 min) (3x) and cleaned (C18 column, ACE hplc), before loading on the mass spectrophotometer.

Protein identification

To identify *N. benthamiana* and *P. capsici* proteins in our sample, mass spectrometry data files were analysed with Maxquant (Cox and Mann, 2008), using the default settings for FTMS and TOF De-isotoping. Filtering of labelled peptides was disabled. FDR was set to <1%. A *N. benthamana* predicted protein database was kindly provided by J. Win and loaded to Andromeda configuration.

Perseus

Mass Spectrometry results were read in Perseus (http://www.perseus-framework.org/) and the data were treated as follows: 1) Pre-processing: detected contaminants were removed, all samples with single or no unique peptides were ignored, LQF intensities were log-transformed and all lanes for the replicates were grouped together. Missing values were replaced by random normal distributed values. 2) Data processing: a two-sample t-test was done with a threshold of 0.05 and S0 of 1.0. For analysis these data were plotted in a volcano-plot.

Results

Yeast 2 Hybrid screening

Yeast 2 hybrid assays identify ERF1 as possible target for CRN20_624

The three necrosis-inducing CRNs described in Chapter 2 and 3 were subjected to Y2H screens to identify putative targets. We performed a screen against a library created from cDNA of potato infected with *P. infestans*. We hypothesised that because CRN domains are conserved between *P. infestans* and *P. capsici* they are

likely to target conserved host proteins, which we would be able to identify using this library.

All constructs were tested for auto-activation with the vectors before proceeding (Figure 5.1). CRN20_624 and CRN79_188 did not show any auto-activation. CRN83_152 showed auto-activation and was not taken forward. The screen yielded 20 positive colonies for CRN20_624 of which 10 were selected, grown and the plasmids were extracted and sent for sequencing. Five of the 10 sequenced constructs corresponded with 83% similarity to tomato Ethylene Response Factor 1, an ortholog of A. thaliana ERF1 (

Table 5.1).

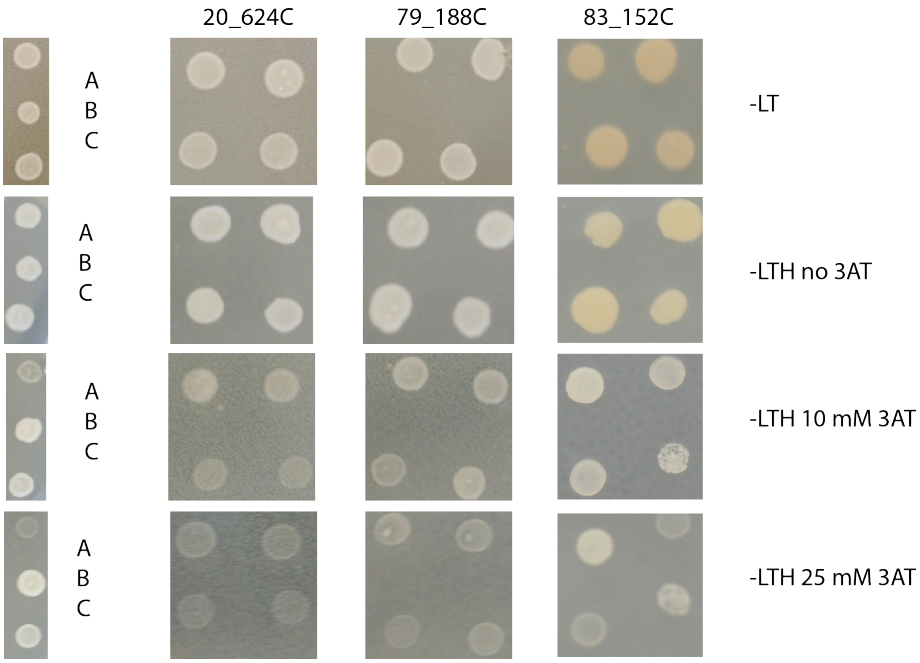

Figure 5.1 Auto Activation assays for CRN Ctermini

Three CRN C termini were recombined in Bait vector pDEST32 and transformed together with empty prey vector pDEST22 and spotted on drop out medium to test for auto activation. Panels on the left show non interacting , weak interacting and strongly interacting control samples (A,B,C respectively), as provided by Invitrogen. All samples grow well on –LT medium and –LTH medium lacking the 3AT inducer agent, confirming viable transformants. 20_624C and 79_188C show less or no growth on –LTH medium with added 3AT, resembling No interaction control A). 83_152 shows signs of weak auto activation for some of the spotted colonies.

We retransformed StERF1 into yeast and co-transformed with CRN20_624 to

confirm the interaction. Growth could be observed in triple dropout medium lacking Leucine, Tryptophan and Histidine, but was not evident on dropout medium lacking Leucine, Tryptophan and Uracil, the latter being a stronger reporter than Histidine (Figure 5.2A). Additional reporter assays did not confirm the interaction. In an X-gal assay co-transformants did not show a blue colour and in the more sensitive CRPG assay no red colour was observed, whereas control reactions showed that both assays are working well (Figure 5.2B,C).

10 colonies were selected for CRN79_188, however only 5 colonies returned valid sequences. Surprisingly, two colonies again returned ERF1. Other colonies contained, Rubisco, an ABC transporter and a porin molecule. This screen was, therefore, not followed up

Table 5.1 Putative targets for 20_624 C-terminus Y2H

Colony	Hit Gene name	Source	% similarity
1	N/A	Y2H Vector	99
2	Unknown	Tomato	83
3	TSA3	Camilla	65
4	ERF1	Tomato	83
5	ERF1	Tomato	83
6	Unknown	unknown	63
7	ERF1	Tomato	83
8	ERF1	Tomato	83
9	Cell wall Protein	unknown	50
10	ERF1	Tomato	83

Table 5.2 Putative targets for CRN79_188 C-terminus Y2H

Colony	Hit Gene name	Source	% similarity
1	ribulose-1,5-bisphosphate carboxylase	Tomato	95
2	ABC transporter	Tomato	97
3	Porin	Tomato	96
6	ERF1	Tomato	83
7	ERF1	Tomato	83

Unable to confirm ERF as target; not detectable in planta

StERF1 might form a very weak interaction with CRN20_624 that cannot be confirmed using re-transformation in yeast. To find out whether interaction does happen and can be confirmed *in planta* we cloned tomato SlERF1, the nearest homolog of StERF1 to test for interaction with CRN20_624, reasoning that since tomato is a natural host of *P. capsici* the interaction between these two proteins might be stronger. Unfortunately we were unable to detect either GFP- or FLAG-tagged SlERF1 on a western blot. Confocal microscopy showed that indeed the tERF1 signal is very low. The expected nuclear signal is barely stronger than background auto-fluorescence (Figure 5.2D).

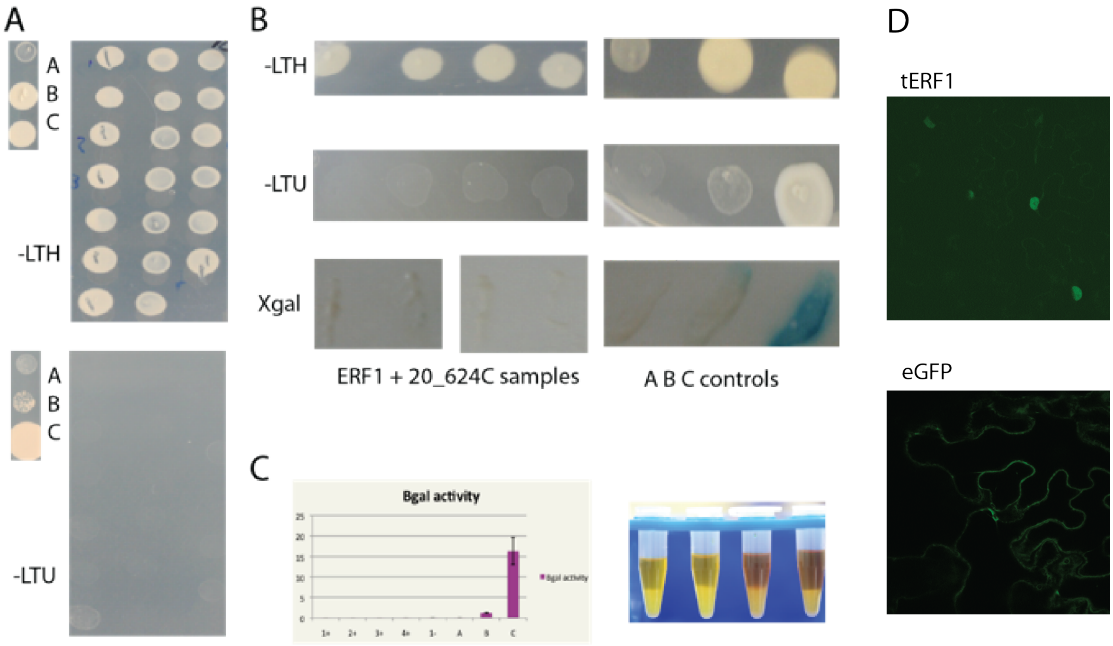

Figure 5.2 Yeast 2 Hybrid assays of CRN20_624 and microscopy of target tERF1

A) Yeast 2 Hybrid library screening using CRN20_624 yielded 20 colonies that were able to grow in –LTH medium, but not on stringent –LTU medium. Left panels show negative (A), weak interacting (B) and strongly interacting controls (C). B) Retransformation of identified interactor ERF1 with 20_624C showed similar results. Growth is observed on –LTH but not –LTU medium. Activity cannot be confirmed using a filter lift Xgal assay, ABC controls behave as expected. C) Relative B-gal activity calculated with an CPRG assay. Activity can be seen for the positive controls (BC), but not in the four ERF1/20_624C samples (1+ to 4+). ERF1 only sample (1-) and non interacting control A are included. D) Confocal microscopy image shows very weak tERF1 signals compared to background fluorescence, suggesting low expression or an unstable protein.

Immunoprecipitation and Mass Spectrometry

CRN effectors are successfully over-expressed in planta

To directly identify new CRN target genes *in planta*, we over-expressed GFP-tagged CRN effectors CRN12_997, CRN20_624, CRN32_256, CRN79_188 and CRN83_152 in *N. benthamiana*, using a 35S driven, GFP-tagging vector as described previously (Chapter 2, 3 and 4). Proteins were extracted using a GTEN buffer and Co-IP was performed using GFP-trap magnetic particles (Chromotek). Expression of the proteins was confirmed using western blotting (Figure 5.3). GFP-sized fragments are visible too, possibly due to cleavage of GFP, *in planta*, during the IP procedure or prolonged boiling required for elution from GFP-antibody beads. For mass spectrometry analysis, the samples were run 3 cm into SDS-PAGE gels and divided in half before digestion with trypsin and submission for Mass Spectrometry.

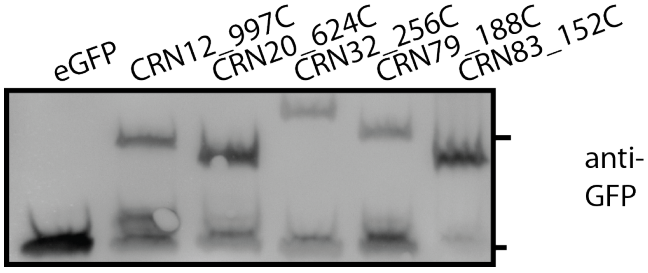

Figure 5.3 GRP-tagged CRN C-termini

Western blot showing GFP-tagged CRN C-termini after o-IP of samples submitted for mass spectrometry. All CRNs are visible at their expected molecular weights. Black lines on the side indicate 50 and 25 kDa.

Identification of co-immunoprecipitating proteins

Using Maxquant software and a *N. benthamaniana* predicted protein database we were able to identify between 240 and 550 co-immunoprecipitating proteins as sum of three biological reps for our CRN samples and free GFP controls. On average 12% can readily be determined as contaminants, like keratin (Table 5.3). Few samples had no unique peptide hit for the protein. Unfortunately, we found large numbers of peptides in free GFP control samples, indicating high 'stickiness' of the beads. The number of peptide hits unique to CRN samples and not present in GFP controls therefore is relatively low and ranges from 0 for CRN20_624 and CRN32_256 to 57 for CRN12_997.

Table 5.3 Overview of GFP Co-IP results

CRN name	Protein hits	Contaminants	No unique peptides	Not in GFP ctrl
12_997	549	40	2	57
20_624	241	36	12	0
32_256	239	34	6	0
79_188	391	54	16	31
83_152	333	35	12	8

Perseus analysis reveals putative targets for 3 CRN proteins

Cox and Mann (2011) have described how detection of protein-protein interactions is not only done by determining presence/absence in experimental and control samples. In fact protein-protein interactions can be identified by quantification of peptide levels and comparison to their levels in negative control samples: this eliminates low abundance false negatives and allows for the assignment of quality parameters.

To quantify the peptide intensities and test for enrichment compared to an EV control we analysed the data using Perseus. Perseus uses peptide quantities in three control and test samples and looks for a significant enrichment between them using a t-test ($p<0.05$). Data can subsequently be represented using "volcano-plots," These plots show the logarithmic ratio of protein intensities against the negative logarithmic p-value of a t-test. The curve indicates the region of significant interactors with a false discovery rate of 5% (Figure 5.4). CRN12_997 had 6 putative targets identified, CRN79_188 8 and CRN83_152 had 1 putative target (Table 5.4). The putative targets for CRN12_997 are annotated as two ribosomal proteins, H/ACA ribonucleoprotein complex subunit 4 and FIB2 mediator of RNA polymerase II (FIB2), a proteasome subunit and cell division cycle protein. The previously identified target TCP14-2 was not detected. For CRN79_188 three other ribosomal proteins were identified and other target candidates were annotated as a coatamer subunit, polyubiquitin, chloroplastic stem-loop binding protein and Glyceraldehyde-3-phosphate-dehydrogenase (GAPDH). For CRN83_152 the only identified putative target is Histone H4 (His4).

Selection for confirmation

The use of GFP-trap magnetic beads is known to result in false positives due to the elution by boiling. In addition the threshold values set in Perseus allow for high FDR. All putative candidates therefore need to be thoroughly checked and need confirmation *in vivo*.

Table 5.4 Putative CRN effector targets, Co-IP

CRN	Protein ID	Protein annotation	Pept	t-test Diff
12_997		CRN12_997	21	12.59082699
	NICBE_034751.1	30S ribosomal protein S9	7	5.370757103
	NICBE_038627.1	FIB2, Mediator of RNA polymerase II	9	4.92777284
	NICBE_080914.1	50S ribosomal protein L1	10	5.141908328
	NICBE_128167.1	H/ACA ribonucleoprotein complex subunit 4	10	4.514613469
	NICBE_143569.1	Cell division cycle protein 48 homolog	15	5.508037567
	NICBE_166405.1	26S proteasome non-ATPase	19	4.318505605
79_188		CRN79_188	32	13.71351178
	NICBE_050150.1	Coatomer subunit alpha-1	10	4.135152499
	NICBE_190604.1	Polyubiquitin 1	5	5.817478816
	NICBE_133253.1	40S ribosomal protein S14-2	4	4.562128067
	NICBE_151761.1	Glyceraldehyde-3-phosphate dehydrogenase	9	5.856728236
	NICBE_192613.1	30S ribosomal protein S13	8	5.63960584
	NICBE_300205.1	Chloroplast stem-loop binding protein	16	4.407911936
	NICBE_303719.1	30S ribosomal protein S10	4	4.220425288
	NICBE_339058.1	30S ribosomal protein S4	3	4.051137288
83_152		CRN83_152	21	13.23844465
	NICBE_414518.1	Histone H4	7	6.133881251

Based on their annotation, localisation (if known) and possible involvement in pathogenicity inferred from literature we selected one gene for CRN12_997; FIB2, and one gene for CRN79_188; GAPDH, to take forward for confirmation screening. FIB2 in *Arabidopsis* (AT4G25630) is a key regulatory protein involved in processing pre-ribosomal RNA located in the nucleolus. From other work presented in this thesis, we know that this is where CRN12_997 interacts with another target TCP14 (Chapter 4). Furthermore, AtTCP14 has been

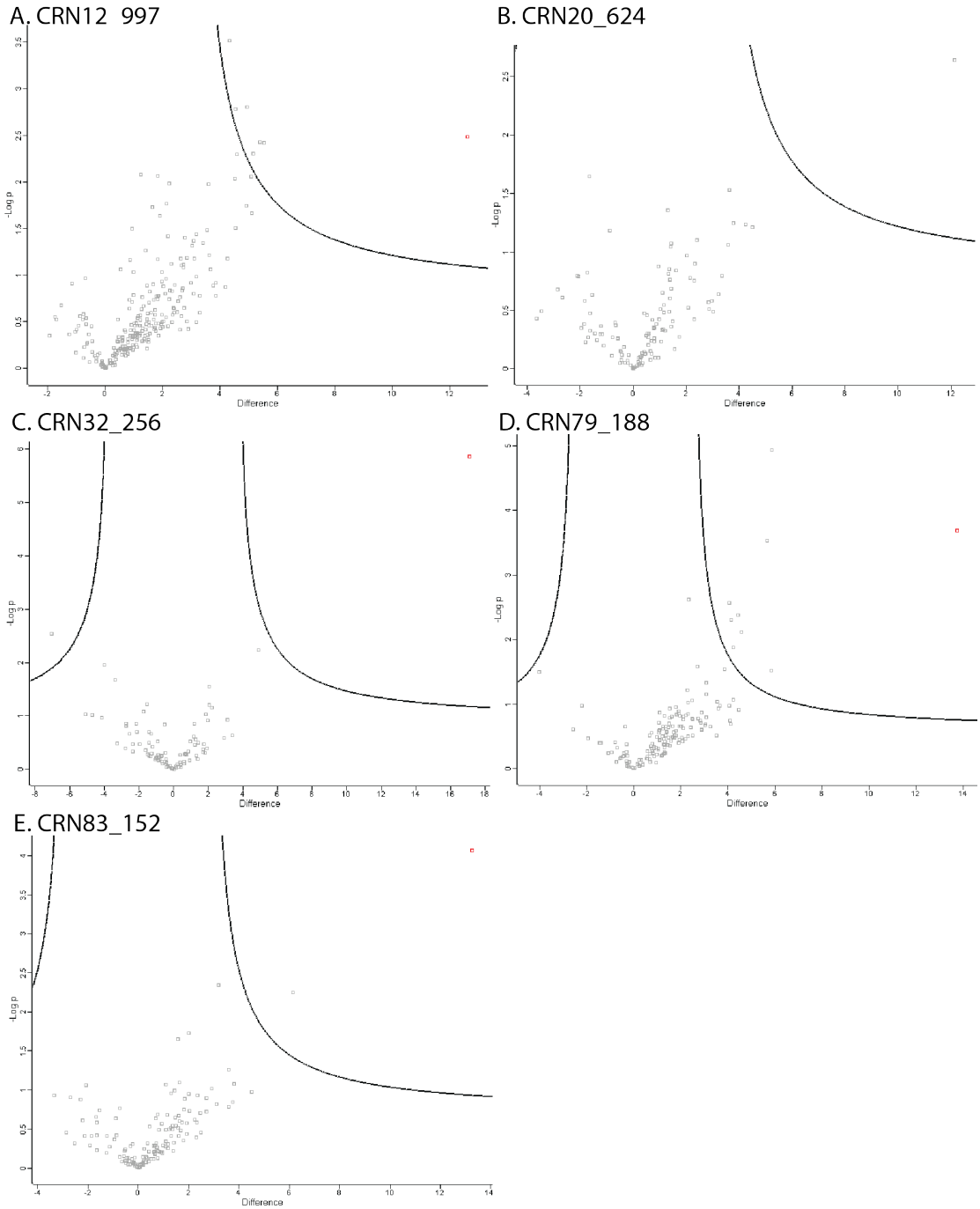

Figure 5.4 Volcano plots showing putative targets for 3 CRN proteins

Volcano-plots generated with Perseus identify putative targets for CRN proteins. For each protein the log of the CRN/EV-ratio is plotted against the negative log of the p-value from the t-test. This way the most likely interactors are plotted in the upper right corner. Grey dots are all co-immunoprecipitated proteins, the red dot is the immunoprecipitated CRN protein and curved lines show threshold values. All proteins above the line can be found in . FDR = 0.05, S0 = 2

reported to interact with FIB1, a homolog of FIB2, in *Arabidopsis* (Mukhtar *et al*., 2011). GAPDH is a known to play a role in the breakdown of glucose, but has been shown to re-localise to the nucleus in *Arabidopsis* under stress conditions and during apoptosis (Hara *et al*., 2005; Vescovi *et al*., 2013).

CRN12_997 co-localises with FIB2.

To be able to interact, CRN effectors need to co-localise with their putative targets *in planta*. We performed co-localisation studies for CRN12_997 and FIB2. When the two are co-expressed we see a brighter ring surrounding the nucleolus for CRN12_997. This perinucleolar accumulation cannot be observed when co-expressed with non-interactor GAPDH (Figure 5.5). When we previously overexpressed CRN12_997 alone (Chapters 2 and 4), we did not see accumulation around the nucleolus, however when co-expressed with SlTCP14-2 we saw relocalisation to the nucleolus (Chapter 4). Additionally, we have previously used AtFIB1 as nucleolar marker and when co-expressed with CRN20_624, another CRN predominantly localising to the nucleoplasm, we didn't see accumulation around the nucleolus (Chapter 2). This suggests that the relocalisation is specific for this interaction, though follow-up experiments with appropriate controls are required.

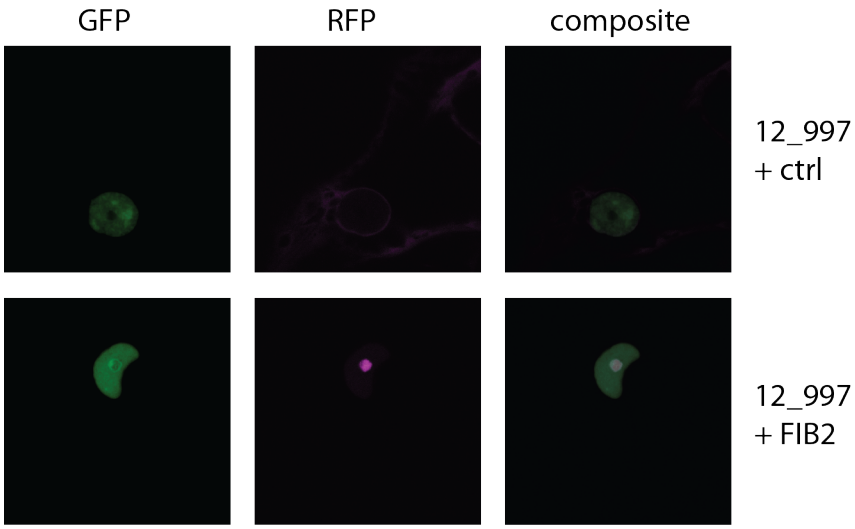

Figure 5.5 Perinucleolar localisation of CRN12_997

When expressed with a negative control (non-interactor FIB2), GFP-tagged CRN12_997 does not accumulate around the nucleolus. When co-expressed with FIB2 perinucleolar accumulation is visible.

Transgenic resources

To investigate the effect of CRN effectors we attempted to create stable transgenic *N. benthamiana* plants for three of the *Crn* genes used above. CRN12_997, CRN20_624 and CRN79_188. Additionally we included the N-terminus of CRN20_624. To make the expression of the transgene simple to measure, we used the GFP-tagged pB7WFG2 constructs described before.

Unfortunately, but not unsurprisingly, neither CRN20_624 nor CRN79_188 yielded viable stable transformants. Transformed plantlets did not grow or root and died shortly after transformation. CRN12_997 and CRN20_624N plants appeared to grow slightly better, but they never grew bigger than 7 cm. Examination by confocal microscopy revealed that expression of CRN20_624N-terminus could not be observed. Microscopy of CRN12_997 plants revealed a low level fluorescence only in a small number of guard cells.

Discussion

Interpretation of Y2H results

False results or weak interactions

A number of factors can contribute to the fact that we cannot confirm the interaction between CRN20_624 and StERF1 in yeast using strong reporter genes. First, it might be that SlERF1 is not a real interactor. False positive interactions are common in yeast 2 hybrid assays. This is why we approach these results with care. On the other hand, the interaction might be very weak or transient of nature. The likelihood of ERF1 being a false positive may seem increased by the fact that a CRN79_188 library screen also detects ERF1. On the other hand, CRN20_624 and CRN79_188 are both expressed at similar time points and both induce cell death (Chapter 1), albeit with different intensities (Chapter 3) and ERF1 plays important roles in defence responses.

ERF1 and its role in defence response

ERF TFs form a large family involved in stress responses and some of them have been

reported to be involved in resistance (Xu *et al*., 2011). OsERF922 in rice, negatively regulates resistance to Magnaporthe oryzae (Liu *et al*., 2012) and phosphorylation of ERF6 in *Arabidopsis* by MPK3/MPK6 activates PDF1.1 and PDF1.2, two genes involved in defence signalling (Meng *et al*., 2013).

ERF1 plays a role in one of the two branches of the JA-related defence pathway, it is related to numerous abiotic stress responses and its activation also leads to PDF-related defence signalling (Cheng *et al*., 2013). Interestingly, the ERF1-branch of JA signalling is generally associated with necrotic pathogens (Pieterse *et al*., 2012). As CRN20_624 is generally expressed during later stages of expression, this could indicate it has an active role in the switch to necrotrophy during *P. capsici* infection. New approaches are needed to confirm CRN20_624 and tERF1 intercation. Using other, possible stabilising tags during over-expression *in planta*, might be sufficient to pursue Co-IP.

Interpretation of Mass Spec results

Interactors for CRN20_624 and CRN32_256

Mass spectrometry identified relatively low numbers of specific interactors. CRN20_624 and CRN32_256 did not yield any candidates. There are a number of possible reasons for this: 1) both CRNs target unstable proteins that are degraded during the IP process of extraction; many proteins have a very short lifetime. Rapid turnover of the target would prevent detection by mass spectrometry. 2) the targets cannot be extracted using our extraction methods; for our protocol we use total leaf extract. During the extraction we might not achieve complete nuclear lysis or the physiological properties of the target protein may mean that it does not readily dissolve in the GTEN buffer, e.g. the protein may be hydrophobic, insoluble or bound to large DNA or membrane complexes. 3) neither of the CRNs have protein targets. There is evidence that effectors might not solely have evolved to target protein processes. A number of RxLR effectors in *Phytophthora* species have predicted DNA binding sites (Edgar Huitema, Graham Motion, personal communication). CRN effectors have not been predicted to be DNA-binding, but particularly given their

presence in the nucleus, this cannot be ruled out.

The CRN12_997 target complex?

Surprisingly CRN12_997 does not yield any mass spectrometry data for its confirmed target TCP14-2. A possible explanation may be the instability and relative low abundance of native TCP14-2. A second possibility is that CRN12_997 does not bind to TCP14-2 in *N. benthamiana* but has specifically evolved to bind in tomato (*S. lycopersicum*). *P. capsici* contains another closely homologous CRN, CRN125_11, that has been shown not to bind SlTCP14-2. It is possible that homologous CRNs, like CRN125_11, target TCP14 in *N. benthamiana*. We found that CRN12_997 possibly binds FIB2. This protein has been shown to localise to the nucleolus (as does CRN12_997), and it plays a role in viral infection.

AtTCP14 has been classified as a Hub-50 protein; in *Arabidopsis* it forms a central hub with over 50 interacting proteins (Mukhtar *et al*., 2011). Interestingly, FIB1, a near-identical homolog of FIB2 is amongst the interacting proteins. This finding supports the hypothesis that CRN12_997 disrupts transcription of defence related proteins by interfering with a TCP-FIB complex.

CRN79_188 and Glyceraldehyde 3'-phosphate dehydrogenase

GAPDH is predominantly described as a glycolytic enzyme and a marker for constitutive gene expression, and in fact has been used as such in recent plant pathology studies (Kaschani *et al*., 2010). Constitutive expression of GAPDH during plant infection, however, has been questioned (Kwon *et al*., 2009; Scholtz and Visser, 2013). GAPDH is widely studied in the context of Post Translational Modifications (PTMs) as many Redox PMTs, including nitrosylation inhibit the glycolytic activity (Zaffagnini *et al*., 2013). GAPDH is involved in apoptosis in humans and in *A. thaliana* it relocates to the nucleus as a response to oxidative stress (Hara *et al*., 2005; Vescovi *et al*., 2013). In fact, GAPDH is able to suppress reactive oxygen species-mediated cell death induced by BAX1 (Baek *et al*., 2004). In mammalian cells Japanese encephalitis virus infection increases the GADPH level in the cell nucleus early in infection and leads to co-localisation of RNA dependent RNA-polymerase,

though no direct interaction could be observed (Yang *et al*., 2009). In tomato, tomato bushy stunt virus requires GADPH and exploits its RNA binding properties to complete its replication (Wang and Nagy, 2008). We do not know whether CRN79_188 prevents GAPDH from entering the nucleus or actually recruits it. Even though viral infection differs enormously from eukaryotic infection, the fact that viruses exploit GAPDH in the plant nucleus is intriguing and begs the question what role GAPDH plays in *P. capsici* infection.

CRN83_152 and Histone H4

CRN83_152 is the first filamentous pathogen effector reported to target chromatin-components. Chromatin is a compact structure of DNA wrapped around octamers of core histone proteins (H2A, H2B, H3, H4), linked by Histone H1. For transcription to take place, histones must be modified to allow transcription factors and polymerases access to the DNA. Effectors from bacteria actively target chromatin in the plant nucleus (Bierne and Cossart, 2012; Rivas, 2012). Effector OspF from Human pathogen *Shigella flexneri* prevents phosphorylation of H3, which in turn blocks a series of inflammatory responses (Arbibe *et al*., 2007). In plants, histone modifications lead to up- or downregulation of defence pathways against both biotrophs and necrotrophs (Ma *et al*., 2011; Lai and Mengiste, 2013). Agrobacterium VirE2 recruits VIP1 (VirE2 INTERACTING PROTEIN) that directly binds to H2A and is required for typical tumour formation (Li *et al*., 2005) and *Ps. syringae* produces an OspF-like effector, HopAI1, with similar function (Zhang *et al*., 2007)

Defence complexes

At first sight the CRN effectors described in this chapter seem to be involved in different aspects of defence processes, though there are apparent links. MED25, a component of the RNA polymerase II complex in *A. thaliana*, forms an integral hub in plant defence. It physically interacts with AP2/ERF transcription factors ERF1 and MYC2 and regulates JA-responsive gene expression (Çevik *et al*., 2012). This directly links putative targets for CRN12_997 and CRN20_624. Chromatin remodelling, as

possible result of CRN83_152 interaction, may also add complex perturbation. Further studies are needed to rule out experimental artefacts, though it is possible that a large number of CRNs act on the same defence response complexes by causing tiny perturbations to many components, or act on them at different stages during infection. If true, this will require more complex and comprehensive experiments in the future. As suggested by Pritchard and Birch (2011) a systems biology approach would be required to simultaneously assess the effects of multiple (smaller) external factors on the plant defence and transcriptional networks during infection.

Concluding remarks

In this chapter we have identified a number of interesting putative CRN targets. The next steps in research should involve confirmation of the interaction using Co-immunoprecipitation and follow up studies including additional co-localisation experiments to see the effect of effector-target interaction in *P. capsici* infection. These follow up studies might prove challenging as previous putative targets like SlERF1 could not easily be expressed *in planta*.

Acknowledgements

We would like to thank all members of the Dundee effector consortium, especially Miles Armstrong and Stefan Engelhardt for sharing expertise with Y2H. We further thank Sara ten Have and Kelly Hodge for mass spec analysis, Vasiliki Zacharaki for help with Perseus, Jennifer Stephens and Jimmy Dessoly for help with stable transformation. The Huitema lab is funded by the Biotechnology and Biological Sciences Research Council, the European Research Council and the Royal Society of Edinburgh

Chapter 6 . General discussion

Computational identification of effectors: successes and pitfalls

Other than their assumed presence, not much was known about CRN effectors in *P. capsici* at the start of this project. In Chapter 1 we have shown that computational analysis allowed accurate identification of potential *Crn* genes.

This computational approach to effector identification is becoming more common and greatly enhances the speed with which putative effectors can be identified. We used a simple approach with predefined and adjusted HMM. A similar approach has since been successful for identifying RxLR effectors in *Hyaloperonospora* (Goritschnig *et al*., 2012) and *Bremia* species (Stassen *et al*., 2012). More advanced methods are required when searching for completely unknown effectors. In general, predicted proteomes are analysed and one tries to obtain as much annotation data as possible, reasoning is that this will reveal if proteins: 1) have similarities to known effectors or 2) have unknown function and are therefore potentially effectors (Jonge, 2012). To narrow down the results, they are generally filtered by whether they appear to be small cysteine rich proteins (6 or more Cys, <200 aa) and putatively secreted proteins. The latter is done by prediction of signal peptides (Dyrløv Bendtsen *et al*., 2004), subcellular localisations (Horton *et al*., 2007) and by excluding putative membrane binding proteins (Kahsay *et al*., 2004). Saunders *et al* (2012) have used additional hierarchical clustering to sort the potentially large number of putative effectors into subclasses. Subsequently they used word seekers such as MEME (Bailey *et al*., 2009) to identify potential new motifs in these classes.

These methods have proven successful, though caution is needed. First, the methods are heavily biased towards small and cysteine rich proteins; a large number of effectors meet this criterion, though RxLR and CRN effectors can be large (>300 aa) and the same is true for some fungal effectors (Catanzariti *et al*., 2006). Secondly, as we showed in Chapter 2, the software can be wrong; NLS prediction software only predicts NLS in a small number of CRNs. It could be that these CRN indeed do not have a NLS and use other means to locate in the nucleus, though as prediction

software is predominantly based on prokaryotes and mammals, it could be that the models are not adequate. Furthermore, some highly expressed CRNs have no signal peptide predicted. This has previously been noted (Haas *et al*., 2009) for other *Phytophthora* spp. It is therefore of high importance that once effectors have been confirmed as secreted or when certain predictions have been confirmed, this data is used to update the prediction software.

It is important to note that computational analysis is open for multiple interpretations. When we analysed the *Saprolegnia parasitica* genome data we observed a small number of putative CRN coding sequences in the genome. However, Jiang *et al.* (2013) conclude in their recent work on the *S. parasitica* genome that no *Crn* genes are present. Differences in threshold values for predictions of the same gene sequence lead to different conclusions.

Comparative genomics and CRN evolution: duplications and variations

Besides effector identification, genome analysis can facilitate the investigation of evolutionary patterns. In Chapter 2 we have shown that CRN effectors occur in all oomycete species that we tested. We have shown that the expansion of CRN domains in oomycetes roughly maps on to the phylogenetic tree of the oomycetes, suggesting recent domain expansion in *Phytophthora* species. This observation is supported by results from Seidl *et al.* (2012) who studied genome evolution in stramenopiles and conclude that genome expansion led to duplication of multiple gene families including effector families in the peronosporales.

In a recent study Shen *et al.* (2013) confirm duplication and recombination events for *Crn* genes in *P. sojae*, suggesting a birth and death model. Unfortunately, their study uses arbitrarily defined orthologous gene groups (OGGs) and not the previously defined domains we used. Additional work is needed to link OGGs to these domains and see for which domains duplication and recombination are most frequent.

Surprisingly a study of chytrid fungi revealed putative CRN-like genes in *Batrachochytrium dendrobatidis* (Joneson *et al*., 2011), unfortunately the authors do not explicitly state their methods for CRN identification. We redid the analysis and

confirm that for some C-terminal domains, there is strong support (E-values < 1e-40), though LFLAK support values are just past the default threshold (E=1e-5). Surprisingly, these CRN-like sequences show high variability in recombination rates, have a high non-synonymous SNP ratio (Farrer *et al*., 2013) and are highly upregulated on host tissue (Rosenblum *et al*., 2012). As CRN-like sequences do not occur in species closely related to *B. dendrobatidis* it remains an open question whether these are true CRN effectors and if so, how they have been acquired. Methods like horizontal gene transfer have been proposed (Sun *et al*., 2011). No data exists showing functions of CRN-like proteins in *B. dendrobatidis.*

A number of studies argue that both CRN and RxLR effectors are more likely to be highly variable and allow for a higher mutation rate due to duplications and their specific location on the genome (Raffaele *et al*., 2010b; Raffaele and Kamoun, 2012). In *Plasmopara halstedii* SNPs have been identified in 7/15 CRNs identified in transcriptome data (As-sadi *et al*., 2011). In *P. capsici*, resequencing of 63 different strains revealed a relatively low number of SNPs in CRN effectors (Lamour *et al*., 2012a), suggesting conserved function, though both studies conclude that higher resolution SNP mapping needs to be done for confirmation.

A stronger focus on methods from population genetics will provide more comprehensive insight into effector variation. RNA sequencing of large numbers of strains on different host species will provide insight into host specific expression of effectors and inform on CRN redundancies.

CRN localisation: Tools to elucidate nuclear defence machinery

Another major observation in this thesis is that CRN effectors with very different domains all localise to the nucleus (Chapter 2). This is true for CRN C-termini with and without predicted NLS. In the past few years the nucleus has been recognised as an important organelle in plant-pathogen interactions. Some nuclear processes involved in pathogen defence responses have been described, but many nuclear processes are unknown (Deslandes and Rivas, 2011).

In Chapter 3 of this thesis we showed how overexpressed CRN effectors that at first sight have a similar effect on plants, appear to have distinct characteristics. This

confirms our hypothesis that CRNs with distinct C-terminal domains fulfil different roles during the infection process. It remains to be determined if several *P. capsici* CRNs with the same domain have the same function. They might have adapted to have similar functions in different host plants. Gene expression or proteome analysis carried out in different host plants would help to support this idea.

Due to their nuclear localisation and supposedly different targets CRNs can be used to study nuclear processes. The CRNs from Chapter 3 are excellent examples to investigate different cell death processes and by studying CRN12_997 we have showed how a member of the TCP family know to be involved in growth and development (Kieffer *et al*., 2011), is also involved in plant defence (Chapter 4).

Cell death: intended or by accident?

At the beginning of this project, nothing was known about the functions of CRN proteins. Since then, a small number of studies have been published that elucidate some CRN functions. Two *P. sojae* CRNs, PsCRN63 and PsCRN115, are highly expressed during infection and silenced *P. sojae* lines show reduced virulence on soybean. These CRNs show high sequence similarity: the C-termini of the proteins differ in only four amino acids. The effects of over-expression of these CRNs, however, are very different; PsCRN63 induces cell death, whereas PsCRN115 is able to suppress elicitin-induced cell death and even PsCRN63-induced cell death (Liu *et al*., 2011). These CRNs share their domain structure with CRN83_152 and PiCRN2 from *P. infestans*; both of them are cell death inducers.

Previously putative kinase activity was predicted for D2-domain containing CRNs (Haas *et al*., 2009). This kinase activity has been confirmed for *P. infestans* PiCRN8, which has a RD Serine/Threonine kinase domain. When over-expressed in plant CRN8 forms dimers and shows auto-phosphorylation. This phosphorylation is not required for cell death induction, as a dominant phospho-mutant is still able to induce cell death (van Damme *et al*., 2012).

PiCRN8 has the same domain as CRN79_188, which we know induces cell death. CRN1_719 also has a D2 domain. The latter shows specific nucleolar localisation, but does not induce cell death when over-expressed (Chapter 2).

These observations beg the question whether or not cell death induction is a function of the CRNs. Given their expression profiles, some might be involved in the switch to necrotrophy, however, many show early upregulation, which could suggest that cell death observed after overexpression is a defence response (HR) from the plant, that is repressed by other effectors during natural infection, as was illustrated by PsCRN63 and PcCRN115. Either way, further research is needed to identify the *in planta* interacting proteins and elucidate the pathways that lead to the cell death in order to answer this question.

CRN targets: what is really happening?

In Chapter 5 we describe a number of putative CRN targets. The targets for three necrosis inducing CRNs are all very different, which is congruent with their different subnuclear localisations. Although the targets have not been completely confirmed, all three are potentially interesting candidates. CRN83_152 may target the histone H4 subunit, CRN79_188 targets a GAPDH molecule and CRN20_624 appears to interact with an ERF1-like transcription factor. We have described a confirmed interaction of CRN12_997 and a TCP14 TF and a possible interaction of the same CRN with FIB2.

Bhattacharjee *et al.* (2013) have described how many R-gene dependent defence responses lead to transcriptional reprogramming in plants. Furthermore they describe a number of bacterial effectors that seem to modulate transcriptional networks directly. Even though Tsuda *et al.* (2009) suggests that robust transcriptional networks might not be ideal effector targets, our results also suggest that CRN effectors have a direct effect on transcriptional networks.

ERF1 and TCP14 are important transcriptional regulators. ERF1 has been shown to be involved in defence signalling and has the potential to function as a switch in defence pathways (Xu *et al*., 2011; Pieterse *et al*., 2012). TCP14 is an important transcriptional regulator which, as we have shown, has a major role in virulence (Chapter 4).

The binding of CRN83_152 with Histone H4 seems different from binding to transcription factors or regulatory enzymes, though there are some recent studies

that show histone involvement in transcriptional regulation. Besides targeting TFs to influence gene regulation, it has become evident that chromatin remodelling can influence gene expression by changing the accessibility of genes for the transcriptional machinery. Chromatin remodelling can be caused by specific enzymes or in an ATP-dependent way (Ho and Crabtree, 2010) and plays an important role in responses to abiotic and biotic stress in *Arabidopsis* (Berr *et al*., 2012). Ma *et al.* (2011) recently reviewed how infection by bacterial plant pathogens induced both types of remodelling events. Association of CRN83_152 with core histone H4 might suggest a role in one of these events.

GAPDH, a mainly metabolism related gene, has been linked to important transcriptional changes. In human cells GAPDH can activate transcription of a co-activator complex linked to Histone transcription (Zheng *et al*., 2003). Additionally it has been observed that GAPDH moves between the cytosol and nucleus and that under stress conditions S-Nitrosylated GAPDH binds to a ubiquitin ligase which then targets nuclear proteins for degradation, initiating the cell death cycle (Hara *et al*., 2005).

Further research should focus on confirmation of these different transcriptional modifications caused by CRNs in host plants. For confirmed interactions, resolving three-dimensional structures of the interaction will help to achieve a better mechanistic insight. For RxLR effectors, crystal structures have shed light on key residues needed for interaction and have shown potential oligomerisation (Boutemy *et al*., 2011), but such information is missing for CRNs so far. Understanding CRN structures will thus be crucial to understand CRN mode of action and the effects of the large array of possible nuclear PMTs caused by CRN effectors.

CRNs and RxLR: two of a kind?

With the identification of a number of potential CRN and RxLR targets we can ask how CRNs relate to RxLR effectors. As discussed in previous chapters, CRNs and RxLR may have a common ancestor, but have they evolved to target distinct processes or are they merely different effectors targeting the same?

The first obvious difference is the presence of apoplastic RxLRs: *P. infestans* Avrblb2

directly targets host protease C14 (Bozkurt *et al*., 2011). Cytoplasmic RxLRs like Avr2 which targets the BR pathway (Saunders *et al*., 2012a), Avr3a, which suppresses HR induced by elicitor INF1 and MAPK defence responses by interacting with CMPG1 (Armstrong *et al*., 2005; Bos *et al*., 2010) and IPI-O, which possibly targets lectin-like receptor kinase LecRK-I.9 (Bouwmeester *et al*., 2011) and many other RXLRs do not localise to the nucleus as fluorescent protein fusions, suggesting diversification between CRNs and RxLRs.

On the other hand, there are a large number of nuclear RxLRs in *Hyaloperonospora* (Caillaud *et al*., 2012b), however their targets have not yet been described. A recent publication shows interaction of PiRxLR03192 with two NAC TF. These TF are localised to the ER and co-expression with the RxLR prevents re-localisation to the nucleus. This results in altered defence responses and enhanced virulence (Mclellan *et al*., 2013). Direct interaction with TFs to prevent localisation and/or function could be a common feature for both effector types. Unfortunately, like TCP TFs, NAC TFs form a large and very diverse class of TFs involved in many different processes (Olsen *et al*., 2005) and considerable research will be required to identify the genes and processes that are controlled by these TFs and have an effect on virulence.

To understand effector diversification (in localisation and/or function), in depth research of their evolution is necessary. We reported that RxLR and CRN effectors possibly originate from a common ancestor (Chapter 2). Comparisons with other oomycete genomes may allow reconstruction of the likely evolutionary trajectory and may aid in understanding how and when some effectors differentiated during evolution. Due to the sheer number of RxLR and CRN effectors and high rates of domain shuffling, this will be a difficult task.

Hubs and systems biology: each their own or orchestrated harmony?

It is becoming evident that different pathogen effectors can bind to the same targets. In Chapter 1 we introduced pseudomonas effectors that target the same LRRs (Shan *et al*., 2008) and even effectors from both fungi and oomycetes that inhibit the same proteases in tomato (Rooney *et al*., 2005; Shabab *et al*., 2008). In

addition to this, effectors of one species can have either positive or negative effects on the infection efficiency of another species. Recently it has been shown that an aphid effector, MP10, which reduces fecundity in *Myces persicae* by triggering JA pathways also decreased susceptibility to *P. capsici*, possibly due to activation of defences. Thus a defence pathway, triggered by a single effector, can lead to enhanced resistance to multiple unrelated species (Rodriguez *et al.* 2013).

There are examples of crosstalk between JA, SA and ET pathways involved in defence that lead to antagonistic effects for different pathogens or pests (Pieterse *et al*., 2012). This crosstalk can be useful for the plants to fend off multiple pests, but can also be exploited. For example an exosaccharide from the necrotrophic fungus *Botrytis cinerea* triggers the (in this case ineffective) SA response pathway and thereby inhibits the effective JA response in its host tomato (El Oirdi *et al*., 2011).

Complex underlying networks do not end with hormone pathways. The notion of hubs of important defence regulating genes that are interacting with one another is a key concept that we introduced earlier. We described how in *Arabidopsis* a large number of putative effector targets themselves have over 50 interacting proteins in plants (Mukhtar *et al*., 2011). We can safely assume that also CRN12_997 will have an integral effect on a large number of signalling pathways and transcription machinery components by disturbing SlTCP14-2, the same will be true for other CRNs. This argues in favour of a more comprehensive systems biology approach to plant pathogen interactions. A state based model where perturbations are not described as a string of consecutive molecular actions but as a switch in healthy and diseased states, is likely to be a more accurate description of what is going on during infection (Pritchard and Birch, 2011). Knockdown mutants in *P. capsici* will be needed to confirm effects of individual CRNs, like CRN12_997, on changes in gene expression or proteome composition of the plant. This systems-biology approach to plant pathogen interactions will be challenging, but will give insights in the complex interplay between different transcriptional pathways. In fact, molecular plant pathology can be used as a tool to unravel these pathways, as changes upon infection might reveal more biologically relevant outcomes than traditionally used

transient over-expression or knockout host plants.

Concluding remarks

In this thesis I have shown that CRNs form an exciting class of nuclear effectors in *P. capsici*. With large amounts of variation within the family, they form an excellent subject to study the effects of nuclear modification of the host plant. I show that different C-terminal effector domains appear to exhibit different functions as can be shown by the host responses to individual overexpression. Advanced evolutionary studies, including parallel sequencing of multiple strains on different hosts to identify intra-species variation, might help explain the abundance and diversity of CRN effectors.

I have confirmed a transcription factor as target for CRN12_997 and provided initial results on other transcription-related proteins as putative targets for other targets, showing that CRNs have an important role in rewiring nuclear processes during infection. The nucleus is a tightly regulated organelle and until we unravel the signalling events involved in infection we can only speculate if CRNs act on many small independent processes involved in pathogenicity or all act on the same pathways, in slightly different ways. Future studies will need to place the findings of this study into the bigger picture. Systems biology approaches, including expression and proteomics studies combined with knock-down systems in *P. capsici* will allow investigation of the expected range of changes in the nucleus during infection. Additionally it will reveal if the observed differences after over-expression are an artefact of overabundance during transient over-expression or represent true functional phenotypes. The study of CRN effectors will be a useful tool to help understand changes in the host nucleus during infection.

References

Allen, R.L., Bittner-Eddy, P.D., Grenville-Briggs, L.J., Meitz, J.C., Rehmany, A.P., Rose, L.E., and Beynon, J.L. (2004). Host-parasite coevolutionary conflict between Arabidopsis and downy mildew. Science **306**: 1957–60.

Allen, R.L., Meitz, J.C., Baumber, R.E., Hall, S.A., Lee, S.C., Rose, L.E., and Beynon, J.L. (2008). Natural variation reveals key amino acids in a downy mildew effector that alters recognition specificity by an Arabidopsis resistance gene. Mol Plant Pathol **9**: 511–523.

Altschul, S.F., Gish, W., Miller, W., Myers, E.W., Lipman, D.J., W., M., E.W., M., and D.J., L. (1990). Basic local alignment search tool. J Mol Biol **215**: 403–410.

Anderson, R.G., Casady, M.S., Fee, R. a, Vaughan, M.M., Deb, D., Fedkenheuer, K., Huffaker, A., Schmelz, E. a, Tyler, B.M., and McDowell, J.M. (2012). Homologous RXLR effectors from Hyaloperonospora arabidopsidis and Phytophthora sojae suppress immunity in distantly related plants. Plant J. **72**: 882–893.

Arabidopsis-Interactome-Mapping-Consortium (2011). Evidence for network evolution in an Arabidopsis interactome map. Science **333**: 601–7.

Arbibe, L., Kim, D.W., Batsche, E., Pedron, T., Mateescu, B., Muchardt, C., Parsot, C., and Sansonetti, P.J. (2007). An injected bacterial effector targets chromatin access for transcription factor NF-kappaB to alter transcription of host genes involved in immune responses. Nat. Immunol. **8**: 47–56.

Armbrust, E. V et al. (2004). The genome of the diatom Thalassiosira pseudonana: ecology, evolution, and metabolism. Science **306**: 79–86.

Armstrong, M.R. et al. (2005). An ancestral oomycete locus contains late blight avirulence gene Avr3a, encoding a protein that is recognized in the host cytoplasm. Proc Natl Acad Sci USA **102**: 7766–7771.

As-sadi, F., Carrere, S., Gascuel, Q., Hourlier, T., Rengel, D., Le Paslier, M.-C., Bordat, A., Boniface, M.-C., Brunel, D., Gouzy, J., Godiard, L., and Vincourt, P. (2011). Transcriptomic analysis of the interaction between Helianthus annuus and its obligate parasite Plasmopara halstedii shows single nucleotide polymorphisms in CRN sequences. BMC Genomics **12**: 498.

Axtell, M.J. and Staskawicz, B.J. (2003). Initiation of RPS2-specified disease resistance in Arabidopsis is coupled to the AvrRpt2-directed elimination of RIN4. Cell **112**: 369–77.

Ayers, A.R., Ebel, J., Finelli, F., Berger, N., and Albersheim, P. (1976). Host-pathogen interactions IX. Quantitative Assays of Elicitor Activity and Characterization of the Elicitor Present in the Extracellular Medium of Cultures of Phytophthora megasperma var. sojae. Plant Physiol. **57**: 751–759.

Baek, D. et al. (2004). Bax-induced cell death of Arabidopsis is meditated through reactive oxygen-dependent and -independent processes. Plant Mol Biol **56**: 15–27.

Bailey, T.L., Boden, M., Buske, F. a, Frith, M., Grant, C.E., Clementi, L., Ren, J., Li, W.W., and Noble, W.S. (2009). MEME SUITE: tools for motif discovery and searching. Nucleic Acids Res. **37**: W202–8.

Baxter, L. et al. (2010). Signatures of Adaptation to Obligate Biotrophy in the Hyaloperonospora arabidopsidis Genome. Science **330**: 1549–1551.

Beakes, G., Glockling, S., and Sekimoto, S. (2012). The evolutionary phylogeny of the oomycete "fungi." Protoplasma **249**: 3–19.

Berr, A., Ménard, R., Heitz, T., and Shen, W.-H. (2012). Chromatin modification and remodelling: a regulatory landscape for the control of Arabidopsis defence responses upon pathogen attack. Cell. Microbiol. **14**: 829–39.

Bhattacharjee, S., Garner, C.M., and Gassmann, W. (2013). New clues in the nucleus : Transcriptional reprogramming in effector-triggered immunity. Front. Plant-Microbe Interact. **4**.

Bhattacharjee, S., Hiller, N.L., Liolios, K., Win, J., Kanneganti, T.D., Young, C., Kamoun, S., and Haldar, K. (2006). The malarial host-targeting signal is conserved in the Irish potato famine pathogen. PLoS Pathog. **2**: e50.

Bierne, H. and Cossart, P. (2012). When bacteria target the nucleus: the emerging family of

nucleomodulins. Cell. Microbiol. **14**: 622–633.

Van der Biezen, E.A. and Jones, J.D. (1998). Plant disease-resistance proteins and the gene-for-gene concept. Trends Biochem Sci **23**: 454–456.

Birch, P.R. et al. (2009). Towards understanding the virulence functions of RXLR effectors of the oomycete plant pathogen Phytophthora infestans. J Exp Bot **60**: 1133 – 40.

Birch, P.R., Boevink, P.C., Gilroy, E.M., Hein, I., Pritchard, L., and Whisson, S.C. (2008). Oomycete RXLR effectors: delivery, functional redundancy and durable disease resistance. Curr Opin Plant Biol **11**: 373–379.

Birch, P.R.J., Rehmany, A.P., Pritchard, L., Kamoun, S., and Beynon, J.L. (2006). Trafficking arms: oomycete effectors enter host plant cells. Trends Microbiol. **14**: 8–11.

Bishop, J.G., Ripoll, D.R., Bashir, S., Damasceno, C.M., Seeds, J.D., and Rose, J.K. (2004). Selection on Glycine beta-1,3-endoglucanase genes differentially inhibited by a Phytophthora glucanase inhibitor protein. Genetics **169**: 1009–1019.

Blair, J.E., Coffey, M.D., Park, S.-Y., Geiser, D.M., and Kang, S. (2008). A multi-locus phylogeny for Phytophthora utilizing markers derived from complete genome sequences. Fungal Genet. Biol. **45**: 266–277.

Boch, J. and Bonas, U. (2010). Xanthomonas AvrBs3 family-type III effectors: discovery and function. Annu. Rev. Phytopathol. **48**: 419–36.

Boevink, P.C., Birch, P.R.J., Whisson, S.C., and Walker, J.M. (2011). Imaging Fluorescently Tagged Phytophthora Effector Proteins Inside Infected Plant Tissue. In Plant Immunity, J.M. McDowell, ed (Humana Press), pp. 195–209.

Boller, T. and Felix, G. (2009). A renaissance of elicitors: perception of microbe-associated molecular patterns and danger signals by pattern-recognition receptors. Annu. Rev. Plant Biol. **60**: 379–406.

Boller, T. and He, S.Y. (2009). Innate immunity in plants: an arms race between pattern recognition receptors in plants and effectors in microbial pathogens. Science **324**: 742–4.

Bolton, M.D. et al. (2008). The novel Cladosporium fulvum lysin motif effector Ecp6 is a virulence factor with orthologues in other fungal species. Mol Microbiol **69**: 119–136.

Bos, J.I.B. et al. (2010). Phytophthora infestans effector AVR3a is essential for virulence and manipulates plant immunity by stabilizing host E3 ligase CMPG1. Proc. Natl. Acad. Sci. U. S. A. **107**: 9909–14.

Bos, J.I.B., Chaparro-Garcia, A., Quesada-Ocampo, L.M., McSpadden Gardener, B.B., and Kamoun, S. (2009). Distinct amino acids of the Phytophthora infestans effector AVR3a condition activation of R3a hypersensitivity and suppression of cell death. Mol Plant Microbe Interact **22**: 269–281.

Bos, J.I.B., Kanneganti, T.D., Young, C., Cakir, C., Huitema, E., Win, J., Armstrong, M.R., Birch, P.R., and Kamoun, S. (2006). The C-terminal half of Phytophthora infestans RXLR effector AVR3a is sufficient to trigger R3a-mediated hypersensitivity and suppress INF1-induced cell death in Nicotiana benthamiana. Plant J **48**: 165–176.

Boutemy, L.S., King, S.R.F., Win, J., Hughes, R.K., Clarke, T.A., Blumenschein, T.M.A., Kamoun, S., and Banfield, M.J. (2011). Structures of Phytophthora RXLR effector proteins: a conserved but adaptable fold underpins functional diversity. J. Biol. Chem. **286**: 35834–42.

Bouwmeester, K., de Sain, M., Weide, R., Gouget, A., Klamer, S., Canut, H., and Govers, F. (2011). The Lectin Receptor Kinase LecRK-I.9 Is a Novel Phytophthora Resistance Component and a Potential Host Target for a RXLR Effector. PLoS Pathog **7**: e1001327.

Bowers, J.H., Papavizas, G.C., and Johnston, S.A. (1990). Effect of soil temperature and soil-water matric potential on the survival of Phytophthora capsici in natural soil. Plant Dis. **v. 74(10)** .

Bowler, C. et al. (2008). The Phaeodactylum genome reveals the evolutionary history of diatom genomes. Nature **456**: 239–244.

Bozkurt, T.O., Schornack, S., Banfield, M.J., and Kamoun, S. (2012). Oomycetes, effectors, and all that jazz. Curr. Opin. Plant Biol. **15**: 9.

Bozkurt, T.O., Schornack, S., Win, J., Shindo, T., Ilyas, M., Oliva, R., Cano, L.M., Jones, A.M.E., Huitema, E., van der Hoorn, R.A.L., and Kamoun, S. (2011). Phytophthora infestans effector AVRblb2 prevents secretion of a plant immune protease at the haustorial interface. Proc. Natl. Acad. Sci. **108**: 20832–20837.

Brasier, C.M., Beales, P.A., Kirk, S.A., Denman, S., and Rose, J. (2005). Phytophthora kernoviae sp. nov., an invasive pathogen causing bleeding stem lesions on forest trees and foliar necrosis of ornamentals in the UK. Mycol. Res. **109**: 853–859.

Brown, J.K.M. and Hovmøller, M.S. (2002). Aerial dispersal of pathogens on the global and continental scales and its impact on plant disease. Science **297**: 537–41.

Bruin, G.C.A. and Edgington, L.V. (1981). Adaptive resistance in Peronosporales to metalaxyl. Can. J. Plant Pathol. **3**: 201–206.

Brunner, F., Rosahl, S., Lee, J., Rudd, J.J., Geiler, C., Kauppinen, S., Rasmussen, G., Scheel, D., and Nurnberger, T. (2002). Pep-13, a plant defense-inducing pathogen-associated pattern from Phytophthora transglutaminases. Embo J **21**: 6681–6688.

Van den Burg, H.A., Harrison, S.J., Joosten, M.H., Vervoort, J., and de Wit, P.J. (2006). Cladosporium fulvum Avr4 protects fungal cell walls against hydrolysis by plant chitinases accumulating during infection. Mol. Plant Microbe Interact. **19**: 1420–1430.

Caillaud, M.-C., Piquerez, S.J.M., Fabro, G., Steinbrenner, J., Ishaque, N., Beynon, J., and Jones, J.D.G. (2012a). Subcellular localization of the Hpa RxLR effector repertoire identifies a tonoplast-associated protein HaRxL17 that confers enhanced plant susceptibility. Plant J. **69**: 252–65.

Caillaud, M.-C., Wirthmueller, L., Fabro, G., Piquerez, S.J.M., Asai, S., Ishaque, N., and Jones, J.D.G. (2012b). Mechanisms of Nuclear Suppression of Host Immunity by Effectors from the Arabidopsis Downy Mildew Pathogen Hyaloperonospora arabidopsidis (Hpa). Cold Spring Harb. Symp. Quant. Biol.

Cao, J. et al. (2011). Whole-genome sequencing of multiple Arabidopsis thaliana populations. Nat. Genet. **43**: 956–63.

Catanzariti, A.M., Dodds, P.N., Lawrence, G.J., Ayliffe, M.A., and Ellis, J.G. (2006). Haustorially expressed secreted proteins from flax rust are highly enriched for avirulence elicitors. Plant Cell **18**: 243–256.

Çevik, V., Kidd, B.N., Zhang, P., Hill, C., Kiddle, S., Denby, K.J., Holub, E.B., Cahill, D.M., Manners, J.M., Schenk, P.M., Beynon, J., and Kazan, K. (2012). MEDIATOR25 acts as an integrative hub for the regulation of jasmonate-responsive gene expression in Arabidopsis. Plant Physiol. **160**: 541–55.

Chandran, D., Tai, Y.C., Hather, G., Dewdney, J., Denoux, C., Burgess, D.G., Ausubel, F.M., Speed, T.P., and Wildermuth, M.C. (2009). Temporal global expression data reveal known and novel salicylate-impacted processes and regulators mediating powdery mildew growth and reproduction on Arabidopsis. Plant Physiol **149**: 1435–1451.

Chaparro-Garcia, A., Wilkinson, R.C., Gimenez-Ibanez, S., Findlay, K., Coffey, M.D., Zipfel, C., Rathjen, J.P., Kamoun, S., and Schornack, S. (2011). The receptor-like kinase SERK3/BAK1 is required for basal resistance against the late blight pathogen phytophthora infestans in Nicotiana benthamiana. PLoS One **6**: e16608.

Cheng, M.-C., Liao, P.-M., Kuo, W.-W., and Lin, T.-P. (2013). The Arabidopsis ETHYLENE RESPONSE FACTOR1 Regulates Abiotic Stress-Responsive Gene Expression by Binding to Different cis-Acting Elements in Response to Different Stress Signals. Plant Physiol. **162**: 1566–82.

Cheung, F., Win, J., Lang, J.M., Hamilton, J., Vuong, H., Leach, J.E., Kamoun, S., Andre Levesque, C., Tisserat, N., and Buell, C.R. (2008). Analysis of the Pythium ultimum transcriptome using Sanger and Pyrosequencing approaches. BMC Genomics **9**: 542.

Chou, S., Krasileva, K. V, Holton, J.M., Steinbrenner, A.D., Alber, T., and Staskawicz, B.J. (2011). Hyaloperonospora arabidopsidis ATR1 effector is a repeat protein with distributed recognition surfaces. Proc. Natl. Acad. Sci. U. S. A. **108**: 13323–8.

Chuma, I., Isobe, C., Hotta, Y., Ibaragi, K., Futamata, N., Kusaba, M., Yoshida, K., Terauchi, R., Fujita, Y., Nakayashiki, H., Valent, B., and Tosa, Y. (2011). Multiple translocation of the AVR-Pita effector gene among chromosomes of the rice blast fungus Magnaporthe oryzae and related species. PLoS Pathog. **7**: e1002147.

Cokol, M., Nair, R., and Rost, B. (2000). Finding nuclear localization signals. EMBO Rep **1**: 411 – 5.

Cox, J. and Mann, M. (2008). MaxQuant enables high peptide identification rates, individualized p.p.b.-range mass accuracies and proteome-wide protein quantification. Nat. Biotechnol. **26**:

1367–72.

Cox, J. and Mann, M. (2011). Quantitative, high-resolution proteomics for data-driven systems biology. Annu. Rev. Biochem. **80**: 273–99.

Cubas, P., Lauter, N., Doebley, J., and Coen, E. (1999). The TCP domain: a motif found in proteins regulating plant growth and development. Plant J. **18**: 215–22.

Damasceno, C.M., Bishop, J.G., Ripoll, D.R., Win, J., Kamoun, S., and Rose, J.K. (2008). Structure of the glucanase inhibitor protein (GIP) family from phytophthora species suggests coevolution with plant endo-beta-1,3-glucanases. Mol Plant Microbe Interact **21**: 820–830.

Van Damme, M., Bozkurt, T.O., Cakir, C., Schornack, S., Sklenar, J., Jones, A.M.E., and Kamoun, S. (2012). The Irish Potato Famine Pathogen Phytophthora infestans Translocates the CRN8 Kinase into Host Plant Cells. PLoS Pathog **8**: e1002875.

Dangl, J.L. and Jones, J.D. (2001). Plant pathogens and integrated defence responses to infection. Nature **411**: 826–833.

Davidson, C.R., Carroll, R.B., Evans, T.A., Mulrooney, R.P., and Kim, S.H. (2002). First Report of Phytophthora capsici Infecting Lima Bean (Phaseolus lunatus) in the Mid-Atlantic Region. Plant Dis. **86**: 1049.

Deslandes, L. and Rivas, S. (2011). The plant cell nucleus: A true arena for the fight between plants and pathogens. Plant Signal. Behav. **6**: 42–48.

Diéguez-Uribeondo, J., García, M.A., Cerenius, L., Kozubíková, E., Ballesteros, I., Windels, C., Weiland, J., Kator, H., Söderhäll, K., and Martín, M.P. (2009). Phylogenetic relationships among plant and animal parasites, and saprotrophs in Aphanomyces (Oomycetes). Fungal Genet. Biol. **46**: 365–76.

Dodds, P.N., Rafiqi, M., Gan, P.H., Hardham, A.R., Jones, D.A., and Ellis, J.G. (2009). Effectors of biotrophic fungi and oomycetes: pathogenicity factors and triggers of host resistance. New Phytol.

Dong, S. et al. (2011). Phytophthora sojae avirulence effector Avr3b is a secreted NADH and ADP-ribose pyrophosphorylase that modulates plant immunity. PLoS Pathog. **7**: e1002353.

Dou, D., Kale, S.D., Wang, X., Jiang, R.H.Y., Bruce, N. a, Arredondo, F.D., Zhang, X., and Tyler, B.M. (2008). RXLR-mediated entry of Phytophthora sojae effector Avr1b into soybean cells does not require pathogen-encoded machinery. Plant Cell **20**: 1930–47.

Duplessis, S. et al. (2011). Obligate biotrophy features unraveled by the genomic analysis of rust fungi. Proc. Natl. Acad. Sci. U. S. A. **108**: 9166–71.

Dyrløv Bendtsen, J., Nielsen, H., von Heijne, G., Brunak, S., and Bendtsen, J.D. (2004). Improved Prediction of Signal Peptides: SignalP 3.0. J. Mol. Biol. **340**: 783–795.

Edgar, R.C. (2004). MUSCLE: multiple sequence alignment with high accuracy and high throughput. Nucleic Acids Res **32**: 1792–1797.

Eitas, T.K. and Dangl, J.L. (2010). NB-LRR proteins: pairs, pieces, perception, partners, and pathways. Curr. Opin. Plant Biol. **13**: 472–7.

Ellis, J., Catanzariti, A.M., and Dodds, P. (2006). The problem of how fungal and oomycete avirulence proteins enter plant cells. Trends Plant Sci **11**: 61–63.

Ellis, J.G. and Dodds, P.N. (2011). Showdown at the RXLR motif: Serious differences of opinion in how effector proteins from filamentous eukaryotic pathogens enter plant cells. Proc. Natl. Acad. Sci. U. S. A. **108**: 14381–2.

Ellis, J.G., Rafiqi, M., Gan, P., Chakrabarti, A., and Dodds, P.N. (2009). Recent progress in discovery and functional analysis of effector proteins of fungal and oomycete plant pathogens. Curr Opin Plant Biol.

Engelhardt, S., Boevink, P.C., Armstrong, M.R., Ramos, M.B., Hein, I., and Birch, P.R.J. (2012). Relocalization of late blight resistance protein R3a to endosomal compartments is associated with effector recognition and required for the immune response. Plant Cell **24**: 5142–58.

Erwin, D.C. and Ribeiro, O.K. (1996). Phytophthora Diseases Worldwide (APS Press: St. Paul, Minnesota).

Etalo, D.W., Stulemeijer, I.J.E., van Esse, P.H., de Vos, R.C.H., Bouwmeester, H.J., and Joosten, M.H. a. J. (2013). System-Wide Hypersensitive Response-Associated Transcriptome and Metabolome Reprogramming in Tomato. Plant Physiol. **31**.

Farrer, R. a., Henk, D. a., Garner, T.W.J., Balloux, F., Woodhams, D.C., and Fisher, M.C. (2013). Chromosomal Copy Number Variation, Selection and Uneven Rates of Recombination Reveal Cryptic Genome Diversity Linked to Pathogenicity. PLoS Genet. **9**: e1003703.

Felix, G., Duran, J.D., Volko, S., and Boller, T. (1999). Plants have a sensitive perception system for the most conserved domain of bacterial flagellin. Plant J. **18**: 265–276.

Felix, G., Regenass, M., and Boller, T. (1993). Specific perception of subnanomolar concentrations of chitin fragments by tomato cells: induction of extracellular alkalinization, changes in protein phosphorylation, and establishment of a refractory state. Plant J. **4**: 307–316.

Finn, R.D., Tate, J., Mistry, J., Coggill, P.C., Sammut, J.S., Hotz, H.R., Ceric, G., Forslund, K., Eddy, S.R., Sonnhammer, E.L., and Bateman, A. (2008). The PFAM protein familes database. Nucleic Acids Res.: D281 – D288.

Fisher, M.C., Henk, D.A., Briggs, C.J., Brownstein, J.S., Madoff, L.C., McCraw, S.L., and Gurr, S.J. (2012). Emerging fungal threats to animal, plant and ecosystem health. Nature **484**: 186–194.

Flor, H.H. (1971). Current status of the gene-for-gene concept. Annu Rev Phytopathol **9**: 275–296.

Flor, H.H. (1942). Inheritance of pathogenicity in Melampsora lini. Phytopathology **32**: 653–669.

Foster, S.J., Park, T.H., Pel, M., Brigneti, G., Sliwka, J., Jagger, L., van der Vossen, E., and Jones, J.D.G. (2009). Rpi-vnt1.1, a Tm-22 homolog from Solanum venturii, confers resistance to potato late blight. Mol Plant Microbe Interact **22**: 589–600.

Fournier, P.-E., El Karkouri, K., Leroy, Q., Robert, C., Giumelli, B., Renesto, P., Socolovschi, C., Parola, P., Audic, S., and Raoult, D. (2009). Analysis of the Rickettsia africae genome reveals that virulence acquisition in Rickettsia species may be explained by genome reduction. BMC Genomics **10**: 166.

Friesen, T.L., Faris, J.D., Solomon, P.S., and Oliver, R.P. (2008). Host-specific toxins: effectors of necrotrophic pathogenicity. Cell Microbiol **10**: 1421–1428.

Fry, W.E. (2008). Phytophthora infestans: the plant (and R gene) destroyer. Mol Plant Pathol **9**: 385–402.

Gaulin, E., Madoui, M.-A.A., Bottin, A., Jacquet, C., Mathe, C., Couloux, A., Wincker, P., Dumas, B., and Mathé, C. (2008). Transcriptome of Aphanomyces euteiches: new oomycete putative pathogenicity factors and metabolic pathways. PLoS One **3**: e1723.

Gevens, a J., Donahoo, R.S., Lamour, K.H., and Hausbeck, M.K. (2007). Characterization of Phytophthora capsici from Michigan Surface Irrigation Water. Phytopathology **97**: 421–8.

Gijzen, M. and Nurnberger, T. (2006). Nep1-like proteins from plant pathogens: recruitment and diversification of the NPP1 domain across taxa. Phytochemistry **67**: 1800–1807.

Gilroy, E.M. et al. (2011a). Presence/absence, differential expression and sequence polymorphisms between PiAVR2 and PiAVR2-like in Phytophthora infestans determine virulence on R2 plants. New Phytol. **191**: 763–776.

Gilroy, E.M., Taylor, R.M., Hein, I., Boevink, P., Sadanandom, A., and Birch, P.R.J. (2011b). CMPG1-dependent cell death follows perception of diverse pathogen elicitors at the host plasma membrane and is suppressed by Phytophthora infestans RXLR effector AVR3a. New Phytol. **190**: 653–66.

Gobena, D., Roig, J., Galmarini, C., Hulvey, J., and Lamour, K. (2012). Genetic diversity of Phytophthora capsici isolates from pepper and pumpkin in Argentina. Mycologia **104**: 102–7.

Gomez-Gomez, L. and Boller, T. (2002). Flagellin perception: a paradigm for innate immunity. Trends Plant Sci. **7**: 251–256.

Goodin, M.M., Chakrabarty, R., Banerjee, R., Yelton, S., and DeBolt, S. (2007). New Gateways to Discovery. Plant Physiol. **145**: 1100–1109.

Goritschnig, S., Krasileva, K. V, Dahlbeck, D., and Staskawicz, B.J. (2012). Computational Prediction and Molecular Characterization of an Oomycete Effector and the Cognate Arabidopsis Resistance Gene. PLoS Genet **8**: e1002502.

Granke, L.L. and Hausbeck, M.K. (2009). Effects of Temperature, Concentration, Age, and Algaecides on Phytophthora capsici Zoospore Infectivity. Plant Dis. **94**: 54–60.

Granke, L.L., Quesada-ocampo, L., Lamour, K., and Hausbeck, M.K. (2012). Advances in Research on Phytophthora capsici on Vegetable Crops in The United States. Plant Dis. **95**: 1588–1600.

Granke, L.L., Windstam, S.T., Hoch, H.C., Smart, C.D., and Hausbeck, M.K. (2009). Dispersal and

Movement Mechanisms of Phytophthora capsici Sporangia. Phytopathology **99**: 1258–1264.

Grant, S.R., Fisher, E.J., Chang, J.H., Mole, B.M., and Dangl, J.L. (2006). Subterfuge and manipulation: type III effector proteins of phytopathogenic bacteria. Annu. Rev. Microbiol. **60**: 425–449.

Grouffaud, S., van West, P., Avrova, A.O., Birch, P.R.J., and Whisson, S.C. (2008). Plasmodium falciparum and Hyaloperonospora parasitica effector translocation motifs are functional in Phytophthora infestans. Microbiology **154**: 3743–3751.

Gunderson, J.H., Elwood, H., Ingold, A., Kindle, K., and Sogin, M.L. (1987). Phylogenetic relationships between chlorophytes, chrysophytes, and oomycetes. Proc. Natl. Acad. Sci. USA **84**: 5823–5827.

Haas, B.J. et al. (2009). Genome sequence and analysis of the Irish potato famine pathogen Phytophthora infestans. Nature **461**: 393–8.

Hamilton, J.P. and Buell, C.R. (2012). Advances in plant genome sequencing. Plant J. **70**: 177–90.

Hann, D.R., Gimenez-Ibanez, S., and Rathjen, J.P. (2010). Bacterial virulence effectors and their activities. Curr. Opin. Plant Biol. **13**: 388–93.

Hara, M.R. et al. (2005). S-nitrosylated GAPDH initiates apoptotic cell death by nuclear translocation following Siah1 binding. Nat. Cell Biol. **7**: 665–74.

Hardham, A.R. (2005). Phytophthora cinnamomi. Mol. Plant Pathol. **6**: 589–604.

Hauck, P., Thilmony, R., and He, S.Y. (2003). A Pseudomonas syringae type III effector suppresses cell wall-based extracellular defense in susceptible Arabidopsis plants. Proc Natl Acad Sci U S A **100**: 8577–8582.

Hausbeck, M.K. and Lamour, K.H. (2004). Research Progress and Management Challenges Phytophthora capsici on Vegetable Crops : Plant Dis. **88**: 1292–1303.

Have, S., Boulon, S., Ahmad, Y., and Lamond, A.I. (2013). Mass spectrometry-based immuno-precipitation proteomics – The user ' s guide. Proteomics **11**: 1153–1159.

Haverkort, A.J., Struik, P.C., Visser, R.G.F., and Jacobsen, E. (2009). Applied Biotechnology to Combat Late Blight in Potato Caused by Phytophthora Infestans. Potato Res. **52**: 249–264.

Heese, A., Hann, D.R., Gimenez-Ibanez, S., Jones, A.M.E., He, K., Li, J., Schroeder, J.I., Peck, S.C., and Rathjen, J.P. (2007). The receptor-like kinase SERK3/BAK1 is a central regulator of innate immunity in plants. Proc. Natl. Acad. Sci. U. S. A. **104**: 12217–22.

Hein, I., Gilroy, E.M., Armstrong, M.R., and Birch, P.R.J. (2009). The zig-zag-zig in oomycete–plant interactions. Mol. Plant Pathol. **10**: 547–562.

Heller, A. and Thines, M. (2009). Evidence for the importance of enzymatic digestion of epidermal walls during subepidermal sporulation and pustule opening in white blister rusts (Albuginaceae). Mycol. Res. **113**: 657–67.

Ho, L. and Crabtree, G.R. (2010). Chromatin remodelling during development. Nature **463**: 474–84.

Hogenhout, S.A., Van der Hoorn, R. a L., Terauchi, R., and Kamoun, S. (2009). Emerging concepts in effector biology of plant-associated organisms. Mol. Plant. Microbe. Interact. **22**: 115–22.

Horton, P., Park, K.J., Obayashi, T., Fujita, N., Harada, H., Adams-Collier, C.J., and Nakai, K. (2007). WoLF PSORT: protein localization predictor. Nucleic Acids Res **35**: W585 – 7.

Howden, A.J.M. and Huitema, E. (2012). Effector-triggered post-translational modifications and their role in suppression of plant immunity. Front. Plant Sci. **3**.

Hulvey, J., Hurtado-Gonzalez, O., Aragón-Caballero, L., Gobena, D., Storey, D., Finley, L., and Lamour, K.H. (2011). Genetic Diversity of the Pepper Pathogen Phytophthora capsici on Farms in the Amazonian High Jungle of Peru. Am. J. Plant Sci. **02**: 461–466.

Hurtado-Gonzáles, O., Aragon-Caballero, L., Apaza-Tapia, W., Donahoo, R., and Lamour, K. (2008). Survival and spread of Phytophthora capsici in Coastal Peru. Phytopathology **98**: 688–94.

Jiang, R.H., Tripathy, S., Govers, F., and Tyler, B.M. (2008). RXLR effector reservoir in two Phytophthora species is dominated by a single rapidly evolving superfamily with more than 700 members. Proc Natl Acad Sci USA **105**: 4874–4879.

Jiang, R.H.Y. et al. (2013). Distinctive Expansion of Potential Virulence Genes in the Genome of the Oomycete Fish Pathogen Saprolegnia parasitica. PLoS Genet. **9**: e1003272.

Jones, J.D.G. and Dangl, J.L. (2006). The plant immune system. Nature **444**: 323–9.

Joneson, S., Stajich, J.E., Shiu, S.-H., and Rosenblum, E.B. (2011). Genomic transition to pathogenicity in chytrid fungi. PLoS Pathog. **7**: e1002338.

Jonge, R. de (2012). In silico identification and characterization of effector catalogs. In Plant Fungal

Pathogens, M.D. Bolton and B.P.H.J. Thomma, eds (Humana Press), pp. 415–425.

De Jonge, R., van Esse, H.P., Kombrink, A., Shinya, T., Desaki, Y., Bours, R., van der Krol, S., Shibuya, N., Joosten, M.H. a J., and Thomma, B.P.H.J. (2010). Conserved fungal LysM effector Ecp6 prevents chitin-triggered immunity in plants. Science **329**: 953–5.

Judelson, H.S. (2012). Dynamics and innovations within oomycete genomes: insights into biology, pathology, and evolution. Eukaryot. Cell **11**: 1304–12.

Judelson, H.S. et al. (2008). Gene expression profiling during asexual development of the late blight pathogen Phytophthora infestans reveals a highly dynamic transcriptome. Mol Plant Microbe Interact **21**: 433–447.

Jupe, F., Pritchard, L., Etherington, G., MacKenzie, K., Cock, P., Wright, F., Sharma, S.K., Bolser, D., Bryan, G., Jones, J., and Hein, I. (2012). Identification and localisation of the NB-LRR gene family within the potato genome. BMC Genomics **13**: 75.

Jupe, J., Stam, R., Howden, A.J.M., Morris, J.A., Zhang, R., Hedley, P.E., Huitema, E., and Remco, S. (2013). Phytophthora capsici-tomato interaction features dramatic shifts in gene expression associated with a hemi-biotrophic lifestyle. Genome Biol. **14**.

Kahsay, R.Y., Gao, G., and Liao, L. (2004). An improved hidden Markov model for transmembrane protein detection and topology prediction and its applications to complete genomes. Bioinformatics **21**: 1853–1858.

Kale, S.D. et al. (2010). External lipid PI3P mediates entry of eukaryotic pathogen effectors into plant and animal host cells. Cell **142**: 284–95.

Kamoun, S. (2007). Groovy times: filamentous pathogen effectors revealed. Curr Opin Plant Biol **10**: 358–365.

Karimi, M., Inzé, D., and Depicker, A. (2002). GATEWAY vectors for Agrobacterium-mediated plant transformation. TRENDS Plant S cience **7**: 193–195.

Kaschani, F., Shabab, M., Bozkurt, T., Shindo, T., Schornack, S., Gu, C., Ilyas, M., Win, J., Kamoun, S., and van der Hoorn, R.A.L. (2010). An effector-targeted protease contributes to defense against Phytophthora infestans and is under diversifying selection in natural hosts. Plant Physiol. **154**: 1794–804.

Kawamura, Y., Hase, S., Takenaka, S., Kanayama, Y., Yoshioka, H., Kamoun, S., and Takahashi, H. (2009). INF1 elicitin activates jasmonic acid- and ethylene-mediated signalling pathways and induces resistance to bacterial wilt disease in tomato. J. Phytopathol. **157**: 287–297.

Kay, S. and Bonas, U. (2009). How Xanthomonas type III effectors manipulate the host plant. Curr Opin Microbiol.

Kay, S., Hahn, S., Marois, E., Hause, G., and Bonas, U. (2007). A bacterial effector acts as a plant transcription factor and induces a cell size regulator. Science **318**: 648–651.

Kieffer, M., Master, V., Waites, R., and Davies, B. (2011). TCP14 and TCP15 affect internode length and leaf shape in Arabidopsis. Plant J. **68**: 147–58.

Kinkema, M., Fan, W., and Dong, X. (2000). Nuclear localization of NPR1 is required for activation of PR gene expression. Plant Cell **12**: 2339–2350.

Koeck, M., Hardham, A.R., and Dodds, P.N. (2011). The role of effectors of biotrophic and hemibiotrophic fungi in infection. Cell. Microbiol. **13**: 1849–57.

Kosugi, S. and Ohashi, Y. (1997). PCF1 and PCF2 specifically bind to cis elements in the rice proliferating cell nuclear antigen gene. Plant Cell **9**: 1607–19.

Kroon, L.P.N.M., Brouwer, H., de Cock, A.W. a M., and Govers, F. (2012). The genus phytophthora anno 2012. Phytopathology **102**: 348–64.

Kunjeti, S.G., Evans, T.A., Marsh, A.G., Gregory, N.F., Kunjeti, S., Meyers, B.C., Kalavacharla, V.S., and Donofrio, N.M. (2012). RNA-Seq reveals infection-related global gene changes in Phytophthora phaseoli, the causal agent of lima bean downy mildew. Mol. Plant Pathol. **13**: 454–66.

Kunze, G., Zipfel, C., Robatzek, S., Niehaus, K., Boller, T., and Felix, G. (2004). The N terminus of bacterial elongation factor Tu elicits innate immunity in Arabidopsis plants. Plant Cell **16**: 3496–507.

Kwon, M.J., Oh, E., Lee, S., Roh, M.R., Kim, S.E., Lee, Y., Choi, Y.-L., In, Y.-H., Park, T., Koh, S.S., and Shin, Y.K. (2009). Identification of novel reference genes using multiplatform expression data

and their validation for quantitative gene expression analysis. PLoS One **4**: e6162.

Lai, Z. and Mengiste, T. (2013). Genetic and cellular mechanisms regulating plant responses to necrotrophic pathogens. Curr. Opin. Plant Biol.

Lamour, K.H. et al. (2012a). Genome sequencing and mapping reveal loss of heterozygosity as a mechanism for rapid adaptation in the vegetable pathogen Phytophthora capsici. Mol. Plant-Microbe Interact.

Lamour, K.H. and Hausbeck, M.K. (2003). Susceptibility of Mefenoxam-Treated Cucurbits to Isolates of Phytophthora capsici Sensitive and Insensitive to Mefenoxam. Plant Dis. **87**: 920–922.

Lamour, K.H., Stam, R., Jupe, J., and Huitema, E. (2012b). The oomycete broad-host-range pathogen Phytophthora capsici. Mol. Plant Pathol. **13**: 329–337.

Lamour, K.H., Win, J., and Kamoun, S. (2007). Oomycete genomics: new insights and future directions. FEMS Microbiol Lett **274**: 1–8.

Latijnhouwers, M., de Wit, P.J.G.M., and Govers, F. (2003). Oomycetes and fungi: similar weaponry to attack plants. Trends Microbiol. **11**: 462–469.

Leonelli, L., Pelton, J., Schoeffler, A., Dahlbeck, D., Berger, J., Wemmer, D.E., and Staskawicz, B. (2011). Structural elucidation and functional characterization of the Hyaloperonospora arabidopsidis effector protein ATR13. PLoS Pathog. **7**: e1002428.

Leonian, L.H. (1922). Stem and fruit blight of peppers caused by Phytophthora capsici sp. nov. Phytopathology **12**: 401–408.

Lévesque, C.A. et al. (2010). Genome sequence of the necrotrophic plant pathogen Pythium ultimum reveals original pathogenicity mechanisms and effector repertoire. Genome Biol. **11**: R73.

Levy, A., Zheng, J.Y., and Lazarowitz, S.G. (2013). The tobamovirus Turnip Vein Clearing Virus 30-kilodalton movement protein localizes to novel nuclear filaments to enhance virus infection. J. Virol. **87**: 6428–40.

Li, J., Krichevsky, A., Vaidya, M., Tzfira, T., and Citovsky, V. (2005). Uncoupling of the functions of the Arabidopsis VIP1 protein in transient and stable plant genetic transformation by Agrobacterium. Proc. Natl. Acad. Sci. U. S. A. **102**: 5733–8.

Li, W. et al. (2009). The Magnaporthe oryzae avirulence gene AvrPiz-t encodes a predicted secreted protein that triggers the immunity in rice mediated by the blast resistance gene Piz-t. Mol Plant Microbe Interact **22**: 411–420.

Links, M.G., Holub, E., Jiang, R.H.Y., Sharpe, A.G., Hegedus, D., Beynon, E., Sillito, D., Clarke, W.E., Uzuhashi, S., and Borhan, M.H. (2011). De novo sequence assembly of Albugo candida reveals a small genome relative to other biotrophic oomycetes. BMC Genomics **12**: 503.

Liu, D., Chen, X., Liu, J., Ye, J., and Guo, Z. (2012). The rice ERF transcription factor OsERF922 negatively regulates resistance to Magnaporthe oryzae and salt tolerance. J. Exp. Bot. **63**: 3899–911.

Liu, J. and Coaker, G. (2008). Nuclear trafficking during plant innate immunity. Mol. Plant **1**: 411–22.

Liu, T., Ye, W., Ru, Y., Yang, X., Gu, B., Tao, K., Lu, S., Dong, S., Zheng, X., Shan, W., Wang, Y., and Dou, D. (2011). Two host cytoplasmic effectors are required for pathogenesis of Phytophthora sojae by suppression of host defenses. Plant Physiol. **155**: 490–501.

Loo, J. a. (2008). Ecological impacts of non-indigenous invasive fungi as forest pathogens. Biol. Invasions **11**: 81–96.

Lozano-Torres, J.L. et al. (2012). Dual disease resistance mediated by the immune receptor Cf-2 in tomato requires a common virulence target of a fungus and a nematode. Proc. Natl. Acad. Sci. U. S. A. **109**: 10119–24.

Ma, K.-W., Flores, C., and Ma, W. (2011). Chromatin configuration as a battlefield in plant-bacteria interactions. Plant Physiol. **157**: 535–43.

Macho, A.P., Guevara, C.M., Tornero, P., Ruiz-Albert, J., and Beuzón, C.R. (2010). The Pseudomonas syringae effector protein HopZ1a suppresses effector-triggered immunity. New Phytol. **187**: 1018–33.

Mackey, D., Holt, B.F., Wiig, A., and Dangl, J.L. (2002). RIN4 interacts with Pseudomonas syringae type III effector molecules and is required for RPM1-mediated resistance in Arabidopsis. Cell **108**: 743–754.

Martin, K., Kopperud, K., Chakrabarty, R., Banerjee, R., Brooks, R., and Goodin, M.M. (2009).

Transient expression in Nicotiana benthamiana fluorescent marker lines provides enhanced definition of protein localization, movement and interactions in planta. Plant J. **59**: 150–62.

Mclellan, H., Boevink, P.C., Armstrong, M.R., Pritchard, L., Gomez, S., Morales, J., Whisson, S.C., Beynon, J.L., and Birch, P.R.J. (2013). An RxLR Effector from Phytophthora infestans Prevents Re-localisation of Two Plant NAC Transcription Factors from the Endoplasmic Reticulum to the Nucleus. PLoS Pathog. **in press**.

Meng, X., Xu, J., He, Y., Yang, K.-Y., Mordorski, B., Liu, Y., and Zhang, S. (2013). Phosphorylation of an ERF Transcription Factor by Arabidopsis MPK3/MPK6 Regulates Plant Defense Gene Induction and Fungal Resistance. Plant Cell **25**: 1126–42.

Misas-Villamil, J.C. and van der Hoorn, R.A.L. (2008). Enzyme-inhibitor interactions at the plant-pathogen interface. Curr Opin Plant Biol **11**: 380–388.

Monaghan, J. and Zipfel, C. (2012). Plant pattern recognition receptor complexes at the plasma membrane. Curr. Opin. Plant Biol. **15**: 349–57.

Money, N.P., Davis, C.M., and Ravishankar, J.P. (2004). Biomechanical evidence for convergent evolution of the invasive growth process among fungi and oomycete water molds. Fungal Genet. Biol. **41**: 872–6.

Morgan, W. and Kamoun, S. (2007). RXLR effectors of plant pathogenic oomycetes. Curr. Opin. Microbiol. **10**: 332–8.

Moy, P., Qutob, D., Chapman, B.P., Atkinson, I., and Gijzen, M. (2004). Patterns of gene expression upon infection of soybean plants by Phytophthora sojae. Mol. Plant-Microbe Interact. **17**: 1051–1062.

Mukhtar, M.S. et al. (2011). Independently Evolved Virulence Effectors Converge onto Hubs in a Plant Immune System Network. Science **333**: 596–601.

Nguyen Ba, A., Pogoutse, A., Provart, N., and Moses, A. (2009). NLStradamus: a simple Hidden Markov Model for nuclear localization signal prediction. BMC Bioinformatics **10**: 202.

Nguyen, H.P., Chakravarthy, S., Velásquez, A.C., McLane, H.L., Zeng, L., Nakayashiki, H., Park, D.-H., Collmer, A., and Martin, G.B. (2010). Methods to study PAMP-triggered immunity using tomato and Nicotiana benthamiana. Mol. Plant. Microbe. Interact. **23**: 991–9.

Nicaise, V., Roux, M., and Zipfel, C. (2009). Recent advances in PAMP-triggered immunity against bacteria: pattern recognition receptors watch over and raise the alarm. Plant Physiol. **150**: 1638–47.

Oh, S.K. et al. (2009). In planta expression screens of Phytophthora infestans RXLR effectors reveal diverse phenotypes, including activation of the Solanum bulbocastanum disease resistance protein Rpi-blb2. Plant Cell **21**: 2928 – 47.

El Oirdi, M., El Rahman, T.A., Rigano, L., El Hadrami, A., Rodriguez, M.C., Daayf, F., Vojnov, A., and Bouarab, K. (2011). Botrytis cinerea manipulates the antagonistic effects between immune pathways to promote disease development in tomato. Plant Cell **23**: 2405–21.

Oliva, R. et al. (2010). Recent developments in effector biology of filamentous plant pathogens. Cell. Microbiol. **12**: 705–15.

Olsen, A.N., Ernst, H. a, Leggio, L. Lo, and Skriver, K. (2005). NAC transcription factors: structurally distinct, functionally diverse. Trends Plant Sci. **10**: 79–87.

Opperman, C.H. et al. (2008). Sequence and genetic map of Meloidogyne hapla: A compact nematode genome for plant parasitism. Proc. Natl. Acad. Sci. U. S. A. **105**: 14802–7.

Palmer, J.M. and Keller, N.P. (2010). Secondary metabolism in fungi: does chromosomal location matter? Curr. Opin. Microbiol. **13**: 431–6.

Pandey, S.P. and Somssich, I.E. (2009). The role of WRKY transcription factors in plant immunity. Plant Physiol. **150**: 1648–55.

Park, C.-J. and Ronald, P.C. (2012). Cleavage and nuclear localization of the rice XA21 immune receptor. Nat. Commun. **3**: 920.

Pieterse, C.M.J., Van der Does, D., Zamioudis, C., Leon-Reyes, A., and Van Wees, S.C.M. (2012). Hormonal modulation of plant immunity. Annu. Rev. Cell Dev. Biol. **28**: 489–521.

Ploetz, R. (2000). Panama Disease : A Classic and Destructive Disease of Banana. Plant Heal. Prog.: 1–7.

Posch, M., Khoudoli, G. a, Swift, S., King, E.M., Deluca, J.G., and Swedlow, J.R. (2010). Sds22

regulates aurora B activity and microtubule-kinetochore interactions at mitosis. J. Cell Biol. **191**: 61–74.

Pritchard, L. and Birch, P. (2011). A systems biology perspective on plant-microbe interactions: biochemical and structural targets of pathogen effectors. Plant Sci. **180**: 584–603.

Qiao, Y. et al. (2013). Oomycete pathogens encode RNA silencing suppressors. Nat. Genet. **45**: 330–3.

Raffaele, S. et al. (2010a). Genome Evolution Following Host Jumps in the Irish Potato Famine Pathogen Lineage. Science **330**: 1540–1543.

Raffaele, S. and Kamoun, S. (2012). Genome evolution in filamentous plant pathogens: why bigger can be better. Nat. Rev. Microbiol. **10**: 417–30.

Raffaele, S., Win, J., Cano, L.M., and Kamoun, S. (2010b). Structural and comparative genome analyses reveal the plastic secretome of the oomycete plant pathogen Phytophthora infestans. . BMC Genomics **11**: 637.

Rasmussen, M.W., Roux, M., Petersen, M., and Mundy, J. (2012). MAP Kinase Cascades in Arabidopsis Innate Immunity. Front. Plant Sci. **3**: 169.

Reddy, A.S.N., Day, I.S., Göhring, J., and Barta, A. (2012). Localization and dynamics of nuclear speckles in plants. Plant Physiol. **158**: 67–77.

Richards, T.A., Dacks, J.B., Jenkinson, J.M., Thornton, C.R., and Talbot, N.J. (2006). Evolution of filamentous plant pathogens: gene exchange across eukaryotic kingdoms. Curr. Biol. **16**: 1857–1864.

Rivas, S. (2012). Nuclear dynamics during plant innate immunity. Plant Physiol. **158**: 87–94.

Rizzo, D.M., Garbelotto, M., Davidson, J.M., Slaughter, G.W., and Koike, S.T. (2002). Phytophthora ramorum as the cause of extensive mortality of Quercus spp. and Lithocarpus densiflorus in California. Plant Dis. **86**: 205–214.

Rodriguez, P.A., Stam, R., Warbroek, T., and Bos, J.I. (2013). Mp10 and Mp42 from the aphid species Myzus persicae trigger plant defenses in Nicotiana benthamiana through different activities. Mol. Plant. Microbe. Interact. **in press**.

Rooney, H.C., Van't Klooster, J.W., van der Hoorn, R.A., Joosten, M.H., Jones, J.D., and de Wit, P.J. (2005). Cladosporium Avr2 inhibits tomato Rcr3 protease required for Cf-2-dependent disease resistance. Science **308**: 1783–1786.

Rose, J.K., Ham, K.S., Darvill, A.G., and Albersheim, P. (2002). Molecular cloning and characterization of glucanase inhibitor proteins: coevolution of a counterdefense mechanism by plant pathogens. Plant Cell **14**: 1329 – 45.

Rosebrock, T.R., Zeng, L., Brady, J.J., Abramovitch, R.B., Xiao, F., and Martin, G.B. (2007). A bacterial E3 ubiquitin ligase targets a host protein kinase to disrupt plant immunity. Nature **448**: 370–374.

Rosenblum, E.B., Poorten, T.J., Joneson, S., and Settles, M. (2012). Substrate-specific gene expression in Batrachochytrium dendrobatidis, the chytrid pathogen of amphibians. PLoS One **7**: e49924.

Rouxel, T. et al. (2011). Effector diversification within compartments of the Leptosphaeria maculans genome affected by Repeat-Induced Point mutations. Nat. Commun. **2**: 202.

Saunders, D.G.O., Breen, S., Win, J., Schornack, S., Hein, I., Bozkurt, T.O., Champouret, N., Vleeshouwers, V.G. a a, Birch, P.R.J., Gilroy, E.M., and Kamoun, S. (2012a). Host protein BSL1 associates with Phytophthora infestans RXLR effector AVR2 and the Solanum demissum Immune receptor R2 to mediate disease resistance. Plant Cell **24**: 3420–34.

Saunders, D.G.O., Win, J., Cano, L.M., Szabo, L.J., Kamoun, S., and Raffaele, S. (2012b). Using Hierarchical Clustering of Secreted Protein Families to Classify and Rank Candidate Effectors of Rust Fungi. PLoS One **7**: e29847.

Savory, E.A., Adhikari, B.N., Hamilton, J.P., Vaillancourt, B., Buell, C.R., and Day, B. (2012a). mRNA-Seq analysis of the Pseudoperonospora cubensis transcriptome during cucumber (Cucumis sativus L.) infection. PLoS One **7**: e35796.

Savory, E.A., Zou, C., Adhikari, B.N., Hamilton, J.P., Buell, C.R., Shiu, S.-H., and Day, B. (2012b). Alternative Splicing of a Multi-Drug Transporter from Pseudoperonospora cubensis Generates an RXLR Effector Protein That Elicits a Rapid Cell Death. PLoS One **7**: e34701.

Schirawski, J. et al. (2010). Pathogenicity determinants in smut fungi revealed by genome

comparison. Science **330**: 1546–8.

Schlarbaum, S., Hebard, F., Spaine, P.C., and Kamalay, J.C. (1997). Three American tragedies: chestnut blight, butternut canker, and Dutch elm disease. In Exotic pests of eastern forests conference proceedings, K.O. Britton, ed, pp. 45–54.

Schmidt, T.G., Koepke, J., Frank, R., and Skerra, A. (1996). Molecular interaction between the Strep-tag affinity peptide and its cognate target, streptavidin. J. Mol. Biol. **255**: 753–66.

Scholtz, J.J. and Visser, B. (2013). Reference gene selection for qPCR gene expression analysis of rust-infected wheat. Physiol. Mol. Plant Pathol. **81**: 22–25.

Schornack, S. et al. (2009). Ten things to know about oomycete effectors. Mol Plant Pathol **10**: 795–803.

Schornack, S., van Damme, M., Bozkurt, T.O., Cano, L.M., Smoker, M., Thines, M., Gaulin, E., Kamoun, S., and Huitema, E. (2010). Ancient class of translocated oomycete effectors targets the host nucleus. Proc. Natl. Acad. Sci. **107**: 17421–17426.

Scott, M.S., Boisvert, F.-M., McDowall, M.D., Lamond, A.I., and Barton, G.J. (2010). Characterization and prediction of protein nucleolar localization sequences. Nucleic Acids Res. **38**: 7388–7399.

Seidl, M.F., Van den Ackerveken, G., Govers, F., and Snel, B. (2012). Reconstruction of oomycete genome evolution identifies differences in evolutionary trajectories leading to present-day large gene families. Genome Biol. Evol. **4**: 199–211.

Shabab, M., Shindo, T., Gu, C., Kaschani, F., Pansuriya, T., Chintha, R., Harzen, A., Colby, T., Kamoun, S., and van der Hoorn, R.A. (2008). Fungal effector protein AVR2 targets diversifying defense-related cys proteases of tomato. Plant Cell **20**: 1169–1183.

Shan, L., He, P., Li, J., Heese, A., Peck, S.C., Nurnberger, T., Martin, G.B., and Sheen, J. (2008). Bacterial effectors target the common signaling partner BAK1 to disrupt multiple MAMP receptor-signaling complexes and impede plant immunity. Cell Host Microbe **4**: 17–27.

Shao, F. (2008). Biochemical functions of Yersinia type III effectors. Curr. Opin. Microbiol. **11**: 21–9.

Shen, D., Liu, T., Ye, W., Liu, L., Liu, P., Wu, Y., Wang, Y., and Dou, D. (2013). Gene Duplication and Fragment Recombination Drive Functional Diversification of a Superfamily of Cytoplasmic Effectors in Phytophthora sojae. PLoS One **8**: e70036.

Shen, Q.-H. and Schulze-Lefert, P. (2007). Rumble in the nuclear jungle: compartmentalization, trafficking, and nuclear action of plant immune receptors. EMBO J. **26**: 4293–301.

Simpson, A. and Roger, A. (2004). The real "kingdoms" of eukaryotes. Curr. Biol.: 693–696.

Song, J. et al. (2003). Gene RB cloned from Solanum bulbocastanum confers broad spectrum resistance to potato late blight. Proc. Natl. Acad. Sci. USA **100**: 9128–9133.

Song, J., Win, J., Tian, M., Schornack, S., Kaschani, F., Ilyas, M., van der Hoorn, R.A., and Kamoun, S. (2009). Apoplastic effectors secreted by two unrelated eukaryotic plant pathogens target the tomato defense protease Rcr3. Proc Natl Acad Sci USA **106**: 1654–1659.

Song, W.-Y., Wang, G.-L., Chen, L.-L., Kim, H.-S., Pi, L.-Y., Holsten, T., Gardner, J., Wang, B., Zhai, W.-X., Zhu, L.-H., Fauquet, C., and Ronald, P. (1995). A Receptor Kinase-Like Protein Encoded by the Rice Disease Resistance Gene, Xa21. Science **270**: 1804–1806.

Spanu, P.D. et al. (2010). Genome expansion and gene loss in powdery mildew fungi reveal tradeoffs in extreme parasitism. Science **330**: 1543–6.

Spector, D.L. and Lamond, A.I. (2011). Nuclear speckles. Cold Spring Harb. Perspect. Biol. **3**.

Stam, R., Howden, A.J.M., Delgado-Cerezo, M., M. M. Amaro, T.M., Motion, G.B., Pham, J., Huitema, E., Delgado Cerezo, M., and Amaro, T.M.M.M. (2013a). Characterization of cell death inducing Phytophthora capsici CRN effectors suggests diverse activities in the host nucleus. Front. Plant Sci. **4**: (387).

Stam, R., Jupe, J., Howden, A.J.M., Morris, J.A., Boevink, P.C., Hedley, P.E., and Huitema, E. (2013b). Identification and characterisation of CRN effectors in Phytophthora capsici shows modularity and functional diversity. PLoS One **8**: e59517.

Stassen, J.H.M. and Van den Ackerveken, G. (2011). How do oomycete effectors interfere with plant life? Curr. Opin. Plant Biol. **14**: 407–414.

Stassen, J.H.M., Seidl, M.F., Vergeer, P.W.J., Nijman, I.J., Snel, B., Cuppen, E., and Van den Ackerveken, G. (2012). Effector identification in the lettuce downy mildew Bremia lactucae by massively parallel transcriptome sequencing. Mol. Plant Pathol. **13**: 719–31.

Stavrinides, J., McCann, H.C., and Guttman, D.S. (2008). Host-pathogen interplay and the evolution of bacterial effectors. Cell Microbiol **10**: 285–292.

Steiner, E., Efroni, I., Gopalraj, M., Saathoff, K., Tseng, T.-S., Kieffer, M., Eshed, Y., Olszewski, N., and Weiss, D. (2012a). The Arabidopsis O-linked N-acetylglucosamine transferase SPINDLY interacts with class I TCPs to facilitate cytokinin responses in leaves and flowers. Plant Cell **24**: 96–108.

Steiner, E., Yanai, O., Efroni, I., Ori, N., Eshed, Y., and Weiss, D. (2012b). Class I TCPs modulate cytokinin-induced branching and meristematic activity in tomato. Plant Signal. Behav. **7**: 807–10.

Stergiopoulos, I. and de Wit, P.J. (2009). Fungal effector proteins. Annu Rev Phytopathol **47**: 233–263.

Sugio, A., Kingdom, H.N., MacLean, A.M., Grieve, V.M., and Hogenhout, S.A. (2011). Phytoplasma protein effector SAP11 enhances insect vector reproduction by manipulating plant development and defense hormone biosynthesis. Proc. Natl. Acad. Sci. U. S. A. **108**: E1254–63.

Sun, G., Yang, Z., Kosch, T., Summers, K., and Huang, J. (2011). Evidence for acquisition of virulence effectors in pathogenic chytrids. BMC Evol. Biol. **11**: 195.

Sun, W.X., Jia, Y.J., O'Neill, N.R., Feng, B.Z.H., and Zhang, X.G. (2008). Genetic diversity in Phytophthora capsici from eastern China. Can. J. Plant Pathol. **30**: 414–424.

Szczesny, R., Büttner, D., Escolar, L., Schulze, S., Seiferth, A., and Bonas, U. (2010). Suppression of the AvrBs1-specific hypersensitive response by the YopJ effector homolog AvrBsT from Xanthomonas depends on a SNF1-related kinase. New Phytol. **187**: 1058–74.

Thines, M., Choi, Y.-J., Kemen, E., Ploch, S., Holub, E.B., Shin, H.-D., and Jones, J.D.G. (2009). A new species of Albugo parasitic to Arabidopsis thaliana reveals new evolutionary patterns in white blister rusts (Albuginaceae). Persoonia **22**: 123–8.

Thines, M. and Kamoun, S. (2010). Oomycete-plant coevolution: recent advances and future prospects. Curr. Opin. Plant Biol. **13**: 427–433.

Thomma, B.P.H.J., Nürnberger, T., and Joosten, M.H. a J. (2011). Of PAMPs and effectors: the blurred PTI-ETI dichotomy. Plant Cell **23**: 4–15.

Tian, M., Benedetti, B., and Kamoun, S. (2005). A Second Kazal-like protease inhibitor from Phytophthora infestans inhibits and interacts with the apoplastic pathogenesis-related protease P69B of tomato. Plant Physiol **138**: 1785 – 93.

Tian, M., Huitema, E., da Cunha, L., Torto-Alalibo, T., and Kamoun, S. (2004). A Kazal-like extracellular serine protease inhibitor from Phytophthora infestans targets the tomato pathogenesis-related protease P69B. J Biol Chem **279**: 26370–26377.

Tian, M., Win, J., Song, J., van der Hoorn, R., van der Knaap, E., and Kamoun, S. (2007). A Phytophthora infestans cystatin-like protein targets a novel tomato papain-like apoplastic protease. Plant Physiol **143**: 364–377.

Tomato-Genome-Consortium and consortium, sol genomics (2012). The tomato genome sequence provides insights into fleshy fruit evolution. Nature **485**: 635–641.

Torto, T.A., Li, S., Styer, A., Huitema, E., Testa, A., Gow, N. a R., van West, P., and Kamoun, S. (2003). EST mining and functional expression assays identify extracellular effector proteins from the plant pathogen Phytophthora. Genome Res. **13**: 1675–85.

Truong, N. V., Liew, E.C.Y., and Burgess, L.W. (2010). Characterisation of Phytophthora capsici isolates from black pepper in Vietnam. Fungal Biol. **114**: 160–170.

Tsuda, K., Sato, M., Stoddard, T., Glazebrook, J., and Katagiri, F. (2009). Network properties of robust immunity in plants. PLoS Genet **5**: e1000772.

Tyler, B.M. et al. (2013). Microbe-Independent Entry of Oomycete RxLR Effectors and Fungal RxLR-Like Effectors Into Plant and Animal Cells Is Specific and Reproducible.

Tyler, B.M. et al. (2006). Phytophthora genome sequences uncover evolutionary origins and mechanisms of pathogenesis. Science **313**: 1261–6.

Tyler, B.M. (2007). Phytophthora sojae: root rot pathogen of soybean and model oomycete. Mol. Plant Pathol. **8**: 1–8.

Vercauteren, A., Boutet, X., D'hondt, L., Van Bockstaele, E., Maes, M., Leus, L., Chandelier, A., and Heungens, K. (2011). Aberrant genome size and instability of Phytophthora ramorum oospore progenies. Fungal Genet. Biol. **48**: 537–43.

Vescovi, M., Zaffagnini, M., Festa, M., Trost, P., Lo Schiavo, F., and Costa, A. (2013). Nuclear accumulation of cytosolic glyceraldehyde-3-phosphate dehydrogenase in cadmium-stressed Arabidopsis roots. Plant Physiol. **162**: 333–46.

Viola, I.L., Guttlein, L.N., and Gonzalez, D. (2013). Redox modulation of plant developmental regulators from the class I TCP transcription factor family. Plant Physiol.

Vleeshouwers, V.G. a a, Raffaele, S., Vossen, J.H., Champouret, N., Oliva, R., Segretin, M.E., Rietman, H., Cano, L.M., Lokossou, A., Kessel, G., Pel, M. a, and Kamoun, S. (2011). Understanding and exploiting late blight resistance in the age of effectors. Annu. Rev. Phytopathol. **49**: 507–31.

Van der Vossen, E., Sikkema, A., Hekkert, B.L., Gros, J., Stevens, P., Muskens, M., Wouters, D., Pereira, A., Stiekema, W., Allefs, S., and vd Vossen, E.A.G. (2003). An ancient R gene from the wild potato species Solanum bulbocastanum confers broad-spectrum resistance to Phytophthora infestans in cultivated potato and tomato. Plant J. **36**: 867–882.

Wang, C.I. et al. (2007). Crystal structures of flax rust avirulence proteins AvrL567-A and -D reveal details of the structural basis for flax disease resistance specificity. Plant Cell **19**: 2898–2912.

Wang, Q. et al. (2011). Transcriptional Programming and Functional Interactions within the Phytophthora sojae RXLR Effector Repertoire. Plant Cell Online **23**: 2064–2086.

Wang, R.Y.-L. and Nagy, P.D. (2008). Tomato bushy stunt virus co-opts the RNA-binding function of a host metabolic enzyme for viral genomic RNA synthesis. Cell Host Microbe **3**: 178–87.

Waterhouse, A.M., Procter, J.B., Martin, D.M.A., Clamp, M., and Barton, G.J. (2009). Jalview Version 2,Äîa multiple sequence alignment editor and analysis workbench. Bioinformatics **25**: 1189–1191.

Wawra, S. et al. (2012). Host-targeting protein 1 (SpHtp1) from the oomycete Saprolegnia parasitica translocates specifically into fish cells in a tyrosine-O-sulphate-dependent manner. Proc. Natl. Acad. Sci. U. S. A. **109**: 2096–101.

Wawra, S., Djamei, A., Albert, I., Nürnberger, T., Kahmann, R., and West, P. Van (2013). In Vitro Translocation Experiments with RxLR-Reporter Fusion Proteins of Avr1b from Phytophthora sojae and AVR3a from Phytophthora infestans Fail to Demonstrate Specific Autonomous Uptake in Plant and Animal Cells. Mol. Plant-Microbe Interact. **26**: 528–536.

Weis, C., Pfeilmeier, S., Glawischnig, E., Isono, E., Pachl, F., Hahne, H., Kuster, B., Eichmann, R., and Hückelhoven, R. (2013). Co-immunoprecipitation-based identification of putative BAX INHIBITOR-1-interacting proteins involved in cell death regulation and plant-powdery mildew interactions. Mol. Plant Pathol.: 1–12.

Whisson, S.C. et al. (2007). A translocation signal for delivery of oomycete effector proteins into host plant cells. Nature **450**: 115–118.

Wilton, M. and Desveaux, D. (2010). Lessons learned from type III effector transgenic plants. Plant Signal. Behav. **5**: 746–8.

Win, J., Kanneganti, T.D., Torto-Alalibo, T., and Kamoun, S. (2006). Computational and comparative analyses of 150 full-length cDNA sequences from the oomycete plant pathogen Phytophthora infestans. Fungal Genet. Biol. **43**: 20–33.

Win, J., Krasileva, K. V, Kamoun, S., Shirasu, K., Staskawicz, B.J., and Banfield, M.J. (2012). Sequence divergent RXLR effectors share a structural fold conserved across plant pathogenic oomycete species. PLoS Pathog. **8**: e1002400.

Win, J., Morgan, W., Bos, J., Krasileva, K. V, Cano, L.M., Chaparro-Garcia, A., Ammar, R., Staskawicz, B.J., and Kamoun, S. (2007). Adaptive evolution has targeted the C-terminal domain of the RXLR effectors of plant pathogenic oomycetes. Plant Cell **19**: 2349 – 69.

De Wit, P.J., Mehrabi, R., Van den Burg, H.A., and Stergiopoulos, I. (2009). Fungal effector proteins: past, present and future. Mol Plant Pathol **10**: 735–747.

Xu, Z.-S., Chen, M., Li, L.-C., and Ma, Y.-Z. (2011). Functions and application of the AP2/ERF transcription factor family in crop improvement. J. Integr. Plant Biol. **53**: 570–85.

Yaeno, T., Li, H., Chaparro-Garcia, A., Schornack, S., Koshiba, S., Watanabe, S., Kigawa, T., Kamoun, S., and Shirasu, K. (2011). Phosphatidylinositol monophosphate-binding interface in the oomycete RXLR effector AVR3a is required for its stability in host cells to modulate plant immunity. Proc. Natl. Acad. Sci. U. S. A. **108**: 14682–7.

Yang, S.-H., Liu, M.-L., Tien, C.-F., Chou, S.-J., and Chang, R.-Y. (2009). Glyceraldehyde-3-phosphate dehydrogenase (GAPDH) interaction with 3' ends of Japanese encephalitis virus RNA and colocalization with the viral NS5 protein. J. Biomed. Sci. **16**: 40.

Yeam, I., Nguyen, H.P., and Martin, G.B. (2010). Phosphorylation of the Pseudomonas syringae effector AvrPto is required for FLS2/BAK1-independent virulence activity and recognition by tobacco. Plant J. **61**: 16–24.

Zadoks, J.C. (2008). The Potato Murrain on the European Continent and the Revolutions of 1848.

Zaffagnini, M., Morisse, S., Bedhomme, M., Marchand, C.H., Festa, M., Rouhier, N., Lemaire, S.D., and Trost, P. (2013). Mechanisms of nitrosylation and denitrosylation of cytoplasmic glyceraldehyde-3-phosphate dehydrogenase from Arabidopsis thaliana. J. Biol. Chem.: M113.475467–.

Zhang, J. et al. (2007). A Pseudomonas syringae effector inactivates MAPKs to suppress PAMP-induced immunity in plants. Cell Host Microbe **1**: 175–85.

Zheng, L., Roeder, R.G., and Luo, Y. (2003). S phase activation of the histone H2B promoter by OCA-S, a coactivator complex that contains GAPDH as a key component. Cell **114**: 255–66.

Zhu, S., Li, Y., Vossen, J.H., Visser, R.F.G.F., and Jacobsen, E. (2012). Functional stacking of three resistance genes against Phytophthora infestans in potato. Transgenic Res. **21**: 89–99.

Zipfel, C. (2008). Pattern-recognition receptors in plant innate immunity. Curr. Opin. Immunol. **20**: 10–6.

Zipfel, C., Kunze, G., Chinchilla, D., Caniard, A., Jones, J.D.G., Boller, T., and Felix, G. (2006). Perception of the Bacterial PAMP EF-Tu by the Receptor EFR Restricts Agrobacterium-Mediated Transformation. Cell **125**: 749–760.

Zipfel, C., Robatzek, S., Navarro, L., Oakeley, E.J., Jones, J.D.G., Felix, G., and Boller, T. (2004). Bacterial disease resistance in Arabidopsis through flagellin perception. Nature **428**: 764–7.

List of publications

List of paper published during this PhD project.

As part of this thesis:

Stam, Remco, Andrew J.M. Howden, Magdalena Delgado Cerezo, Tiago M.M.M. Amaro, Graham B. Motion, Jasmine Pham and Edgar Huitema (2013). Characterisation of cell death inducing Phytophthora capsici CRN effectors suggests diverse activities in the host nucleus. Frontiers in Plant Science, 4.

Stam, Remco, Julietta Jupe, Andrew J. M. Howden, Jenny A Morris, Petra C Boevink, Pete E Hedley, and Edgar Huitema. 2013. "Identification and Characterisation of CRN Effectors in *Phytophthora Capsici* Shows Modularity and Functional Diversity." *PLoS ONE 8(3): e59517*

Not part of this thesis:

Rodriguez, Patricia A., **Remco Stam**, Tim Warbroek and Jorunn I Bos (2013). Mp10 and Mp42 from the aphid species Myzus persicae trigger plant defenses in Nicotiana benthamiana through different activities. Molecular plant-microbe interactions : MPMI, in press.

Jupe, Julietta, **Remco Stam**, Andrew J. M. Howden, Jenny A Morris, Runxuan Zhang, Pete E Hedley, and Edgar Huitema. 2013. "*Phytophthora Capsici*-tomato Interaction Features Dramatic Shifts in Gene Expression Associated with a Hemi-biotrophic Lifestyle." *Genome biology 14(R63)*

Lamour, Kurt H, Joann Mudge, Daniel Gobena, Oscar P Hurtado-Gonzales, Jeremy Schmutz, Alan Kuo, Neil A Miller, Brandon J Rice, Sylvain Raffaele, Liliana Cano, Arvind K Bharti, Ryan S Donahoo, Sabra L Finley, Edgar Huitema, Jon Hulvey, Darren Platt, Asaf Salamov, Alon Savidor, Rahul Sharma, **Remco Stam**, Dylan Storey, Marco Thines, Joe Win, Brian Haas, Darrell Dinwiddie, Jerry Jenkins, Jim Knight, Jason Affourtit, Clif S Han, Olga Chertkov, Erika A Lindquist, Chris Detter, Igor V Grigoriev, Sophien Kamoun, and Stephen F Kingsmore. 2012. "Genome Sequencing and Mapping Reveal Loss of Heterozygosity as a Mechanism for Rapid Adaptation in the Vegetable Pathogen *Phytophthora Capsici*." *Molecular Plant-Microbe Interactions 25(10):1350-60*

Lamour, Kurt H, **Remco Stam**, Julietta Jupe, and Edgar Huitema. 2012. "The Oomycete Broad-host-range Pathogen *Phytophthora Capsici*." *Molecular Plant Pathology 13(4): 329–37*